N66 23799
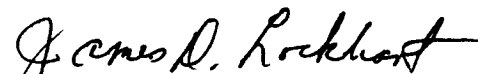
(ACCESSION NUMBER)   (THRU)

(PAGES)   (CODE)

(NASA CR OR TMX OR AD NUMBER)   (CATEGORY)

RF LIQUID-LEVEL

SENSING TECHNIQUE
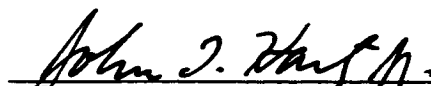
Contract NAS 8-11476

Prepared by: James D. Lockhart
Staff Engineer
NASA Planning and Advanced Development
Research and Development Division

Approved: John T. Hart, Jr.
Manager
NASA Planning and Advanced Development
Research and Development Division

LOCKHEED MISSILES & SPACE COMPANY

FOREWORD

LOCKHEED MISSILES & SPACE COMPANY

CONTENTS

LOCKHEED MISSILES & SPACE COMPANY

ILLUSTRATIONS

TABLES

LOCKHEED MISSILES & SPACE COMPANY

Section 1

INTRODUCTION

The investigation and development of an RF liquid-level sensing technique was divided into two parts, a laboratory investigation and an expanded development program. The objectives were to determine the feasibility of the resonant cavity technique through a series of practical tests and to obtain more refined design information that would provide a means for evaluating the technique.

The basic principle is that the dielectric property of a fluid contained in a tank (cavity) with conducting walls causes the resonant frequency to change in proportion to the amount of that fluid in the cavity. The cavity is excited by radio frequency (RF) electrical energy, and a change is detected in the resonant frequency when it is compared to that of the empty tank. By applying a scaling factor, the level or volume of the fluid in the tank is determined.

1.1 LABORATORY INVESTIGATION

During the laboratory investigation, tests were conducted with liquid hydrogen (LH_2), liquid oxygen (LOX), and liquid rocket fuel (RP-1) to determine the range and type of liquids that could be measured. Also, the technique was examined to determine whether or not mode jumping occurred and to take the required steps to prevent it. The basic theory (see Appendix A) and the contribution of the various components of a system were studied as a parallel effort throughout the program.

Additional studies include the determination of the limits and effect of tank geometry, operation under both static and dynamic conditions, and the response of a system for fill and drain applications. A series of seven LH_2 tests were conducted in a right cylinder tank, 24 in. in diameter and 24 in. high. This was followed by three LOX tests and a series of tests with RP-1. Accuracy for the various configurations and liquids were determined.

1-1

The laboratory investigation produced satisfactory results, and sufficient time was available to conduct (1) a series of experiments using unexpanded polystyrene beads to simulate a liquid, and (2) a few tests to simulate a zero g condition.

1.2 DEVELOPMENT PROGRAM

During the second part of the program, testing in large tanks was conducted with RP-1 and LH_2. An Agena tank was modified, and the spherical section was used for the RP-1 experiments. A 60-in.-diameter spherical cryogenic tank which was approximately the same configuration as the modified Agena tank was used for the LH_2. Approximately 15 RP-1 and 4 LH_2 tests were performed.

LOX experiments were performed in the 24-in. tank and consisted of 20 tests. One of these tests was conducted with liquid nitrogen to determine the extent of the effect of the paramagnetic property of LOX on the application of the technique.

Simulated zero g experiments, including approximately 25 configurations, were continued during the second part of the program. Also, effort was expended on the design of a system for installation on the Saturn S-IVB Battleship. The Agena tank used for the RP-1 experiments was reworked to provide a 3/13 scale model of the Saturn S-IVB.

Section 2
BACKGROUND

In conjunction with propellant-management-and-measuring-system studies conducted during the RIFT stage design (Contract NAS 8-3600), J. C. Miller of Lockheed Missiles & Space Company (LMSC) suggested that the determination of the amount of propellant on board might be ascertained by treating the supply tank as a resonant cavity. RF energy would be used to excite the tank, and the resonant frequency detected. The resonant frequency, a function of the dielectric constant of the material contained in the cavity, would change in accordance with the amount of propellant contained in the stage. This approach was first described to NASA/MSFC in the LMSC monthly progress report of January 1963 (Ref. 1). Additional information regarding the progress of the development was contained in the February and December 1963 progress reports (Refs. 2 and 3).

A preliminary study that produced encouraging results led to an analytical study (see Ref. 4) conducted by LMSC Electronic Science Laboratory personnel. Although not conclusive, the analytical study indicated that the RF resonant cavity principle was potentially sound. A proposal for a continuation of the investigation and development of the application was submitted and resulted in this contract.

A patent disclosure was prepared and assigned a LMSC document number (Ref. 5) on 7 March 1963. The patent application was forwarded via NASA/MSFC to the NASA Western Operation Office (Ref. 6).

Section 3
LABORATORY INVESTIGATION

The laboratory investigation was essentially divided into four tasks: (a) RF system and component design, (b) experiments with LH_2, (c) experiments with LOX, and (d) experiments with RP-1.

The RF system and component design was carried out in LMSC's Research and Development facilities, Building 151, Sunnyvale, California. A copper tank, 22 1/2 in. in diameter by 22 1/2 in. high, thin wall (.022-in. thick), was used to study probe designs and to verify component values for the RF system design. Beads of unexpanded polystyrene were used to simulate the liquids.

The cryogenic experiments (LH_2 and LOX) were conducted in the components test laboratory of LMSC's Santa Cruz Test Base. A heavy wall aluminum tank, 24 in. in diameter and 24 in. high, was used as the test vessel.

The RP-1 experiments were conducted at the NASA/Lockheed facilities in Hangar No. 1, Moffett Field. The test vessel used was the aluminum cryogenic tank described above.

One type of RF system was used for measuring the field characteristics of the tank. A sweep generator provided the RF energy to the tank, and a marker generator was used to superimpose a mark on the sweep trace on an oscilloscope at the resonant frequency. The frequency of the marker generator was used as the indication of the resonant frequency. A second type of RF system that was used was a self-excited oscillator in which the tank was the frequency determining element.

3.1 RF SYSTEMS

Figure 3-1 presents a block diagram of the RF resonant cavity liquid-level sensing system that employs the sweep technique. A Telonic sweep generator, set for a 50-MHz

3-1
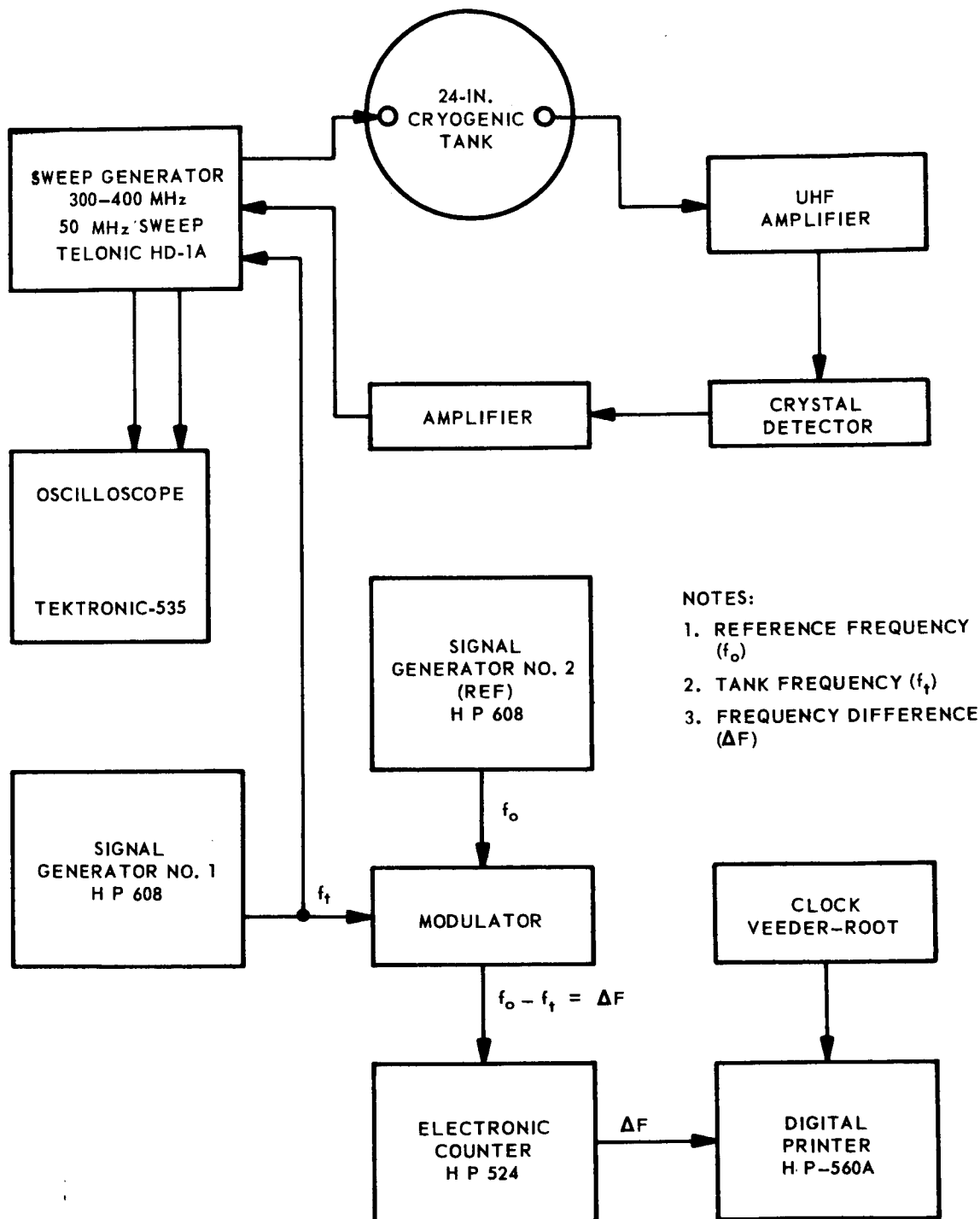
Fig. 3-1 RF Resonant Cavity Sweep System

sweep over the range of 300 to 400 MHz, was used. The generator signal fed to one of the two loop probes mounted in the top of the 24-in. cryogenic tank produced an output signal from the tank that was detected by the second loop probe. This signal was amplified and returned to the sweep generator to complete the circuit.

The composite sweep was displayed on an oscilloscope. A Hewlett-Packard 608 (HP 608) signal generator (No. 1) was connected to the modulator and also to the oscilloscope. The frequency was manually adjusted to position the marker (HP 608, No. 1) at the resonant frequency (f_t). The composite oscilloscope display (Fig. 3-2) represents the frequency sweep of the tank.

A second HP 608 signal generator (No. 2) was set near the empty tank resonant frequency (f_0) and the signal applied to the modulator. A filter was incorporated in the modulator that allowed only the difference frequency ($f_0 - f_t$) to pass to the electronic counter (HP 524). An elapsed time clock provided a reference for correlating the data. The difference frequency and the reference time were printed on paper tape for recording.

A block diagram of the RF resonant cavity liquid-level sensing technique operating as a self-oscillating system is shown in Fig. 3-3. The wide-band UHF amplifier provided a positive feedback across the tank, and the combination of amplifier and tank served as an RF oscillator. The remainder of the circuitry was the same as described for the sweep technique.

As the tank was filled in each system, the resonant frequency of the tank (f_t) decreased and $f_0 - f_t$ (Δf) increased. This change was a result of the change in the dielectric of the tank cavity.

One of the more serious limitations in determining the overall accuracy of the RF liquid-level system was the accuracy of available comparison instrumentation. Weighing and volume measuring was used for the RP-1 experiments. The large tare weight in proportion to the weight of LOX and especially LH_2, in addition to the complicated piping for filling and venting, eliminated weighing methods for determining the amount of liquid in the tank. Instrumentation for obtaining comparative liquid level was installed inside the tank.
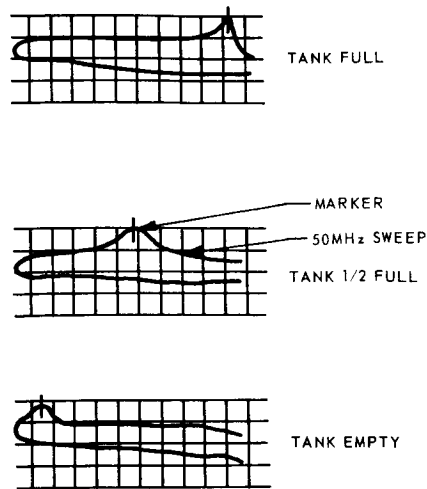
Fig. 3-2 Typical Oscilloscope Traces, Sweep System
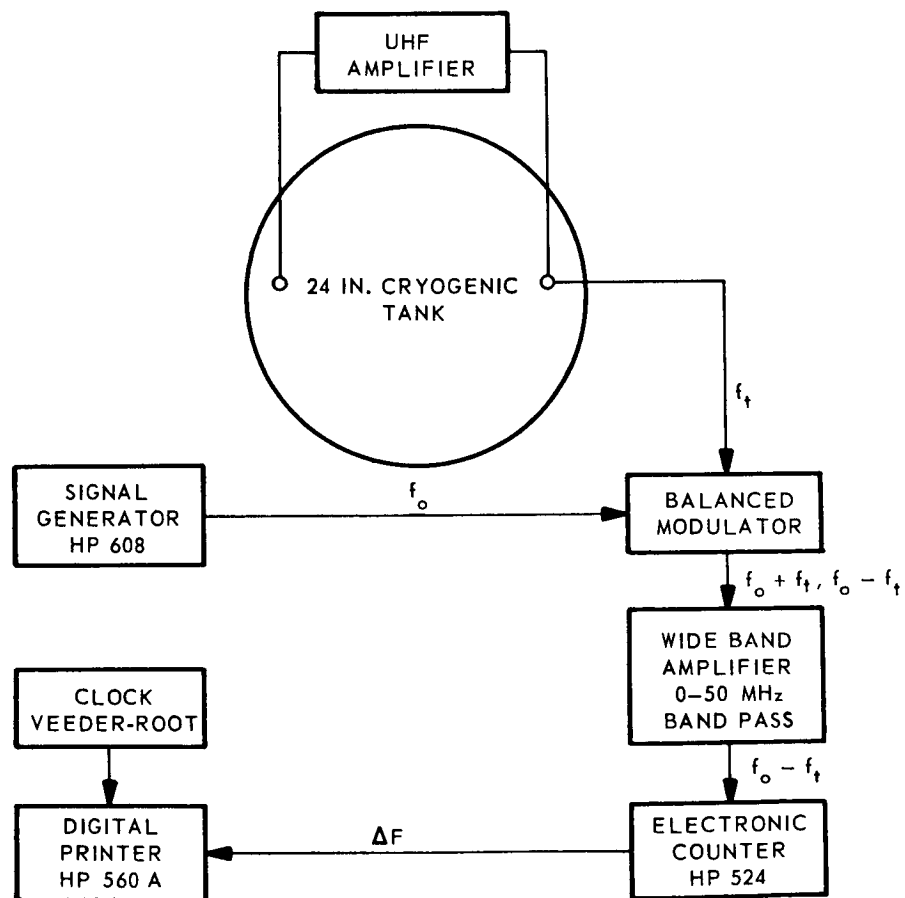
Fig. 3-3 RF Resonant Cavity Self-Oscillating System

3-4

Three sets of level detectors were installed for the LH_2. One set of four resistance temperature probes (RTB's) were mounted in such a manner that three discrete levels could be detected. Two of the four temperature probes were located at the same level for confidence readings. A series of 10 carbon resistors provided continuous level monitoring. Also, 12 independent (single-point) carbon resistors were installed. Typical response curves for the three types of level detectors are shown in Fig. 3-4. The change in output is shown as the detectors were uncovered during a LH_2 boiloff. It is believed that the lag of the RTB was due to the total mass of the RTB. The indication of a change by the carbon resistors was due to the surface disturbance caused by boiling.

The instrumentation was attached with epoxy, either directly to the tank wall (or the internal insulation) or mounted on a glass-epoxy board. This was satisfactory for the LH_2; however, because of the possibility of the board absorbing oxygen, the mounting was replaced by a Teflon tube for the LOX experiments. The carbon resistors were selected over thermocouples because of their higher output at the liquid-to-cold-gas range for LH_2. Some difficulty was experienced in setting the recorders for the carbon resistors at the warm tank condition; however, once the adjustments were properly scaled, excellent performance was attained. Only single-point carbon resistors were used for the LOX experiments. The results from these were far from ideal.

3.2 LIQUID HYDROGEN EXPERIMENTS

Seven separate LH_2 tests were conducted. These tests included experiments with and without internal insulation, with and without a baffle, and with different lengths of conducting fill lines. Figure 3-5, an internal view of the 24-in. cryogenic tank, shows the instrumentation rake, slosh baffle, and electrically grounded fill line. The RF loop probes were covered with foam insulation to reduce heat leaks and protect the RF connectors. (It was found during later tests that this was not necessary.) The RF resonant cavity system used throughout the LH_2 tests was the manual track system shown in Fig. 3-1.
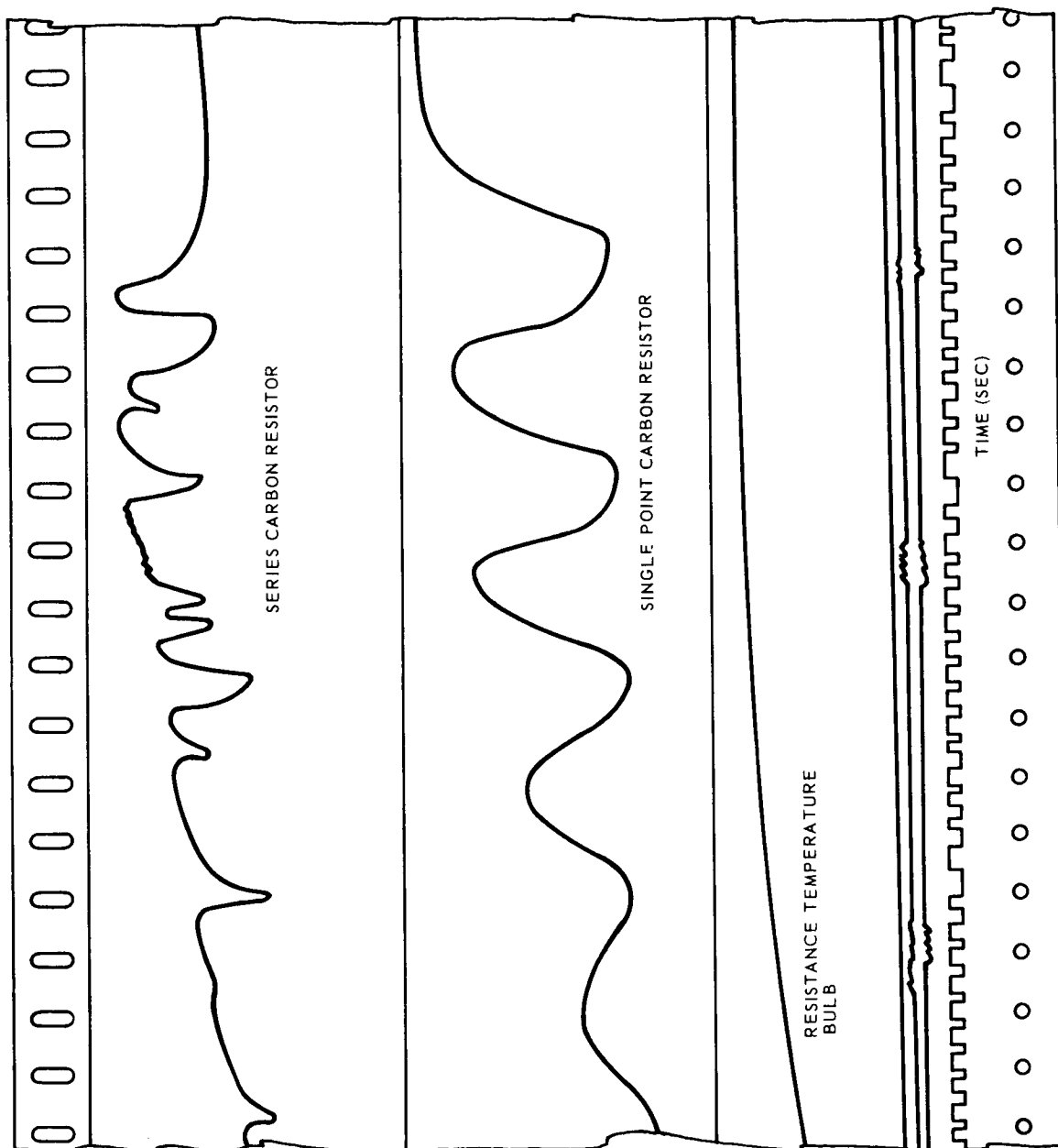
Fig. 3-4 Typical Response Curves, Comparative Level Instrumentation

The first test consisted of filling the tank at a uniform rate and allowing the LH_2 to boil off with direct venting of the gaseous hydrogen. The resistance temperature probes (RTB's) provided the only level comparing indications that were recorded for the test. Figure 3-6 is a plot of the data obtained during the run.

Table 3-1 is a tabulation of the test conditions for the seven experiments. A detailed report of the experiments was furnished in February 1965 in the enclosure to LMSC-A734537 (Ref. 7).

A plot of RF difference frequency versus liquid level for test 5 is presented in Fig. 3-7. The reverse curve at the start of the fill cycle is an indication of the sensitivity of the RF resonant cavity liquid-level sensing technique. The change in frequency, indicating a change of level, was attributed to the change of tank dimensions due to the chilling of the tank.

The results of the LH_2 experiments were encouraging. The RF system functioned with various internal tank configurations. The interal insulation caused only minor attenuation of the signal. The metallic fill line did not suppress the mode, and the system functioned with a rather complicated baffle. The results of the test pointed out the need for improved instrumentation for determining the liquid level so that the RF system could be calibrated.

3.3 LIQUID OXYGEN EXPERIMENTS

The LH_2 experiments were conducted at the Santa Cruz Test Base on 25-27 January 1965. The internal configuration 24-in. cryogenic tank is shown in Fig. 3-8. The fiberglass fill line was replaced with Teflon, and 12 individual level-sensing carbon resistors were mounted on a Teflon tube. The empty tank resonant frequency was 377 MHz, and the frequency decreased to approximately 314 MHz when the tank was full. The empty tank Q was about 300. Both the manual track system and the self-oscillating system were used for exciting the tank. A plot of difference frequency (Δf) versus liquid height for the experiments is shown in Fig. 3-9.

3-7
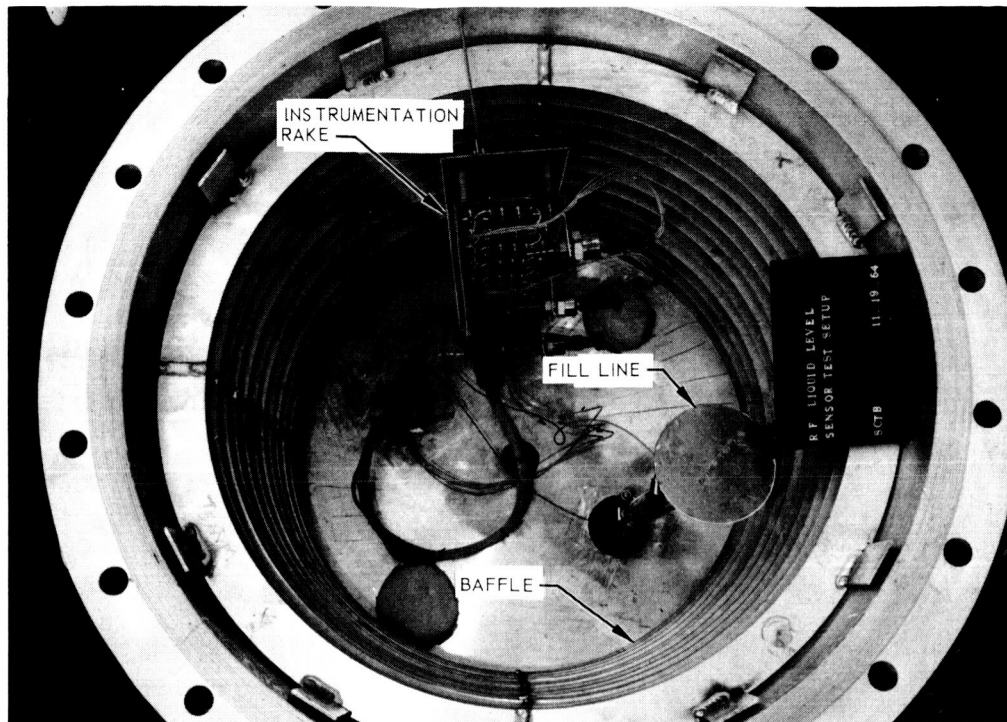
Fig. 3-5 Twenty-Four Inch Cryogenic Tank, With Baffle, Instrumentation
Rake, and Fill Line
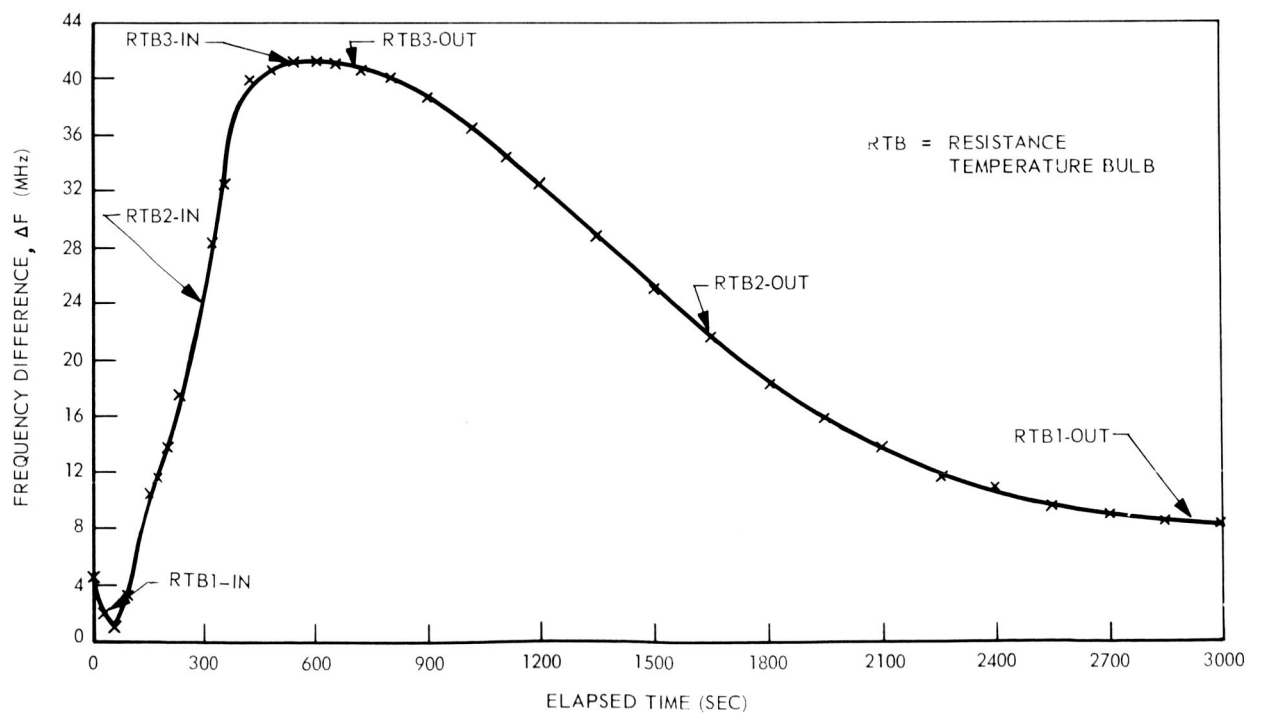
Fig. 3-6 Resonant Frequency Difference Vs. Time, LH$_2$ Run 1

3-8

Table 3-1

LIQUID HYDROGEN TEST CONDITIONS

Test No.	Insulation	Instrumentation			Fill Line		Slosh Baffle
		RTB	Carbon Resistors		Length (in.)	Material	
			Series	Parallel			
1	Internal, 1 in. thick	Yes	No	Yes (no data)	22	Fiber-glass	No
2	Internal, 1 in. thick	Yes	No	Yes (no data)	22	Fiber-glass	No
3	Internal, 1 in. thick	Yes	No	Yes	8 / 14	Fiber-glass / Copper	No / No
4	Internal, 1 in. thick	Yes	No	Yes	8 / 14	Fiber-glass / Copper	No
5	External, 2 1/2 in. Fiber-glass	Yes	Yes	Yes	8 / 14	Fiber-glass / Copper	No
6	External, 1 in. Fiber-glass	Yes	Yes	Yes	22	Fiber-glass	No
7	External, 1 in. Fiber-glass	Yes	Yes	Yes	8 / 14	Fiber-glass / Copper	Yes
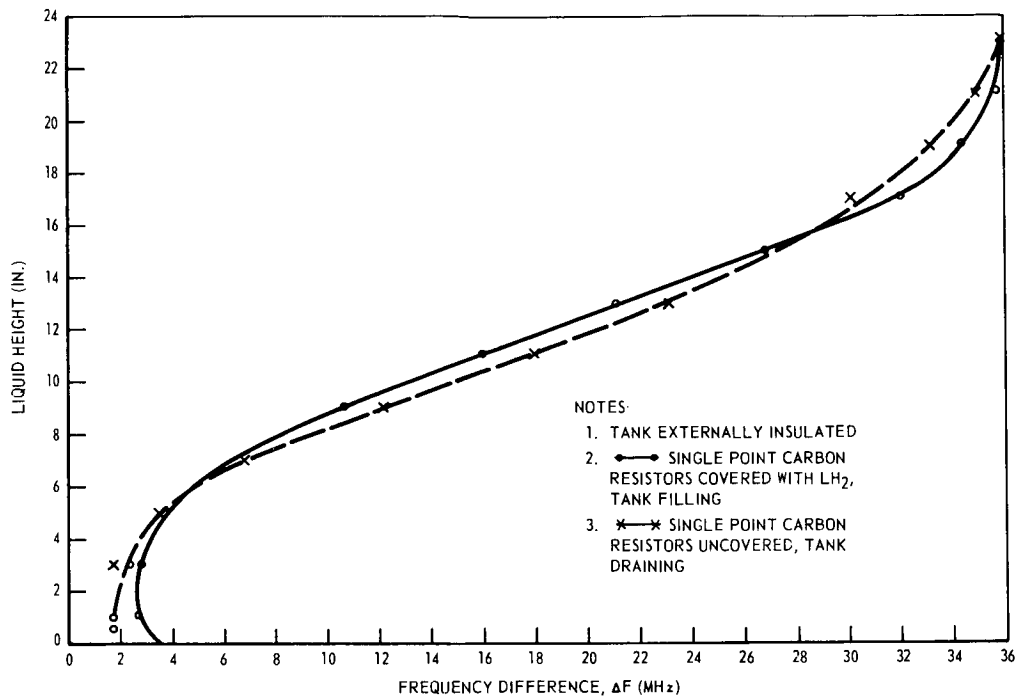
Fig. 3-7 Resonant Frequency Difference Vs. Liquid Level, LH_2 Run 5

The results of these tests were very similar to those obtained from the LH_2 experiments. The difference in the frequency range corresponds to the calculated values using the 1.5 value for the dielectric constant of LOX versus the 1.20 value for LH_2.

3.4 LIQUID ROCKET FUEL EXPERIMENTS

The RP-1 experiments were conducted at the NASA/Lockheed facilities in Hangar No. 1 at Moffett Field during the period of 14 December 1964 through 8 January 1965.

These experiments of the RF resonant cavity sensing technique with a third standard liquid propellent (RP-1) were made to determine surface effects on the accuracy of the RF system and to determine the overall system accuracy.

The resonant frequency characteristics of the 24-in. cryogenic tank were determined by a series of RP-1 fills. These tests were made with the internal fill line, instrumentation,
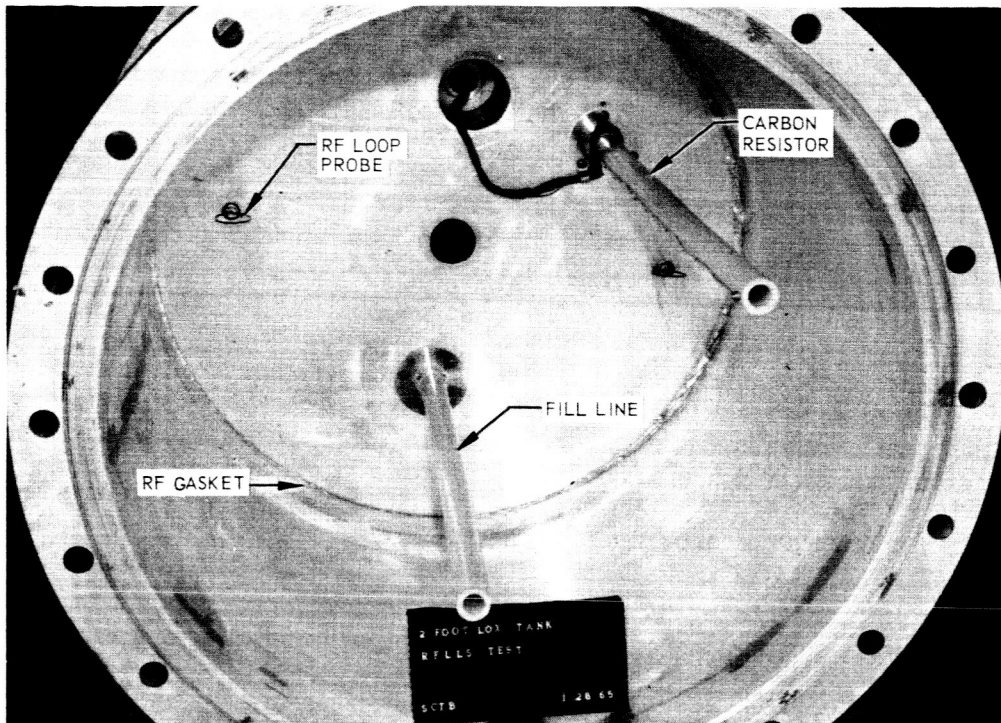
Fig. 3-8 Twenty-Four Inch Cryogenic Tank With Baffle, Rake, and
RF Loop Probes
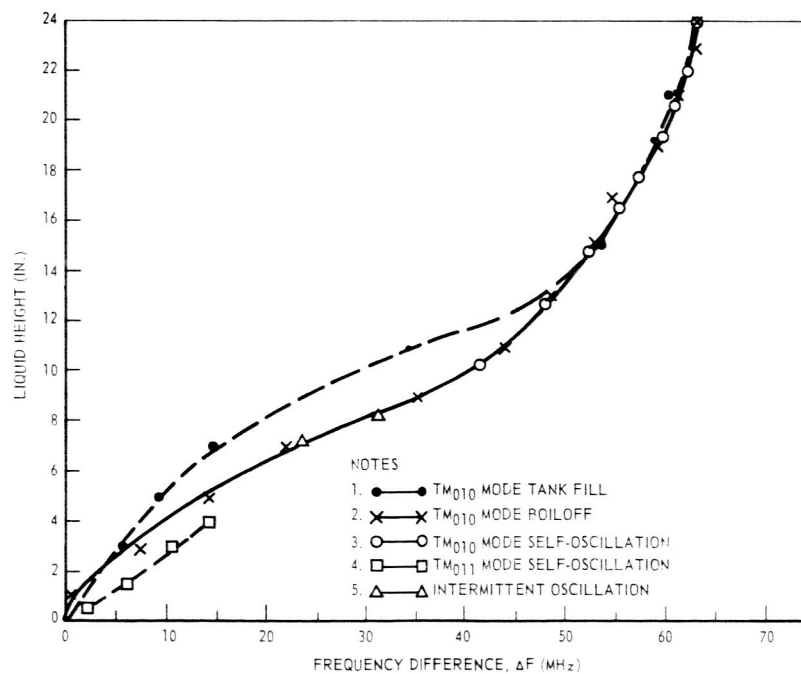
Fig. 3-9 Resonant Frequency Difference Vs. Liquid Level, LOX Runs

3-11

rake, and baffle removed. A plot of resonant frequencies versus RP-1 content is shown in Fig. 3-10; the resultant resonant frequency versus RP-1 content, with the slosh baffle installed in the tank, is also shown.

The RP-1 tests also included an accuracy and repeatibility experiment. A calibration run was made by carefully weighing the amount of RP-1 as it was added to or removed from the tank. Forty-two increments were used in obtaining the fill cycle. Without reference to the calibration curve, a separate complete fill and drain cycle was measured. The test was started with the tank approximately half full. The tank was then filled, emptied, and refilled to the starting point; each increment of RP-1 was weighed. The resulting curve is shown in Fig. 3-11, and the percent of error is shown in Fig. 3-12. It is believed that the error at 4 percent is a misreading and that the increase in the percent error at the 50- to 60-percent level was due to an accumulated error.

To determine the effect of changing surface conditions on the accuracy of the RF sensing system, the tank was tilted from its normal upright position with volumes of 25, 50 and 75 percent for angles from 4 to 59 deg from the horizontal position. The results of these tilt experiments, including one test with 50-percent volume with the baffle installed, are shown in Fig. 3-13.

3.5 MISCELLANEOUS BENCH TESTS

To facilitate the evaluation of the RF resonant cavity liquid-level sensing technique, a series of bench tests were conducted. A thin wall (.020 in.) copper tank 22 1/2 in. in diameter and 22 1/2 in. high (Fig. 3-14) was fabricated. Unexpanded polystyrene beads were used to simulate the liquids. A study of a few probe configurations and probe locations was made. The electrical characteristics of both the tank and the major components of the RF circuit were measured for the purpose of determining the requirements for the self-oscillating system. Also, a brief experiment was conducted to obtain an insight into the RF system performance under a zero g condition.
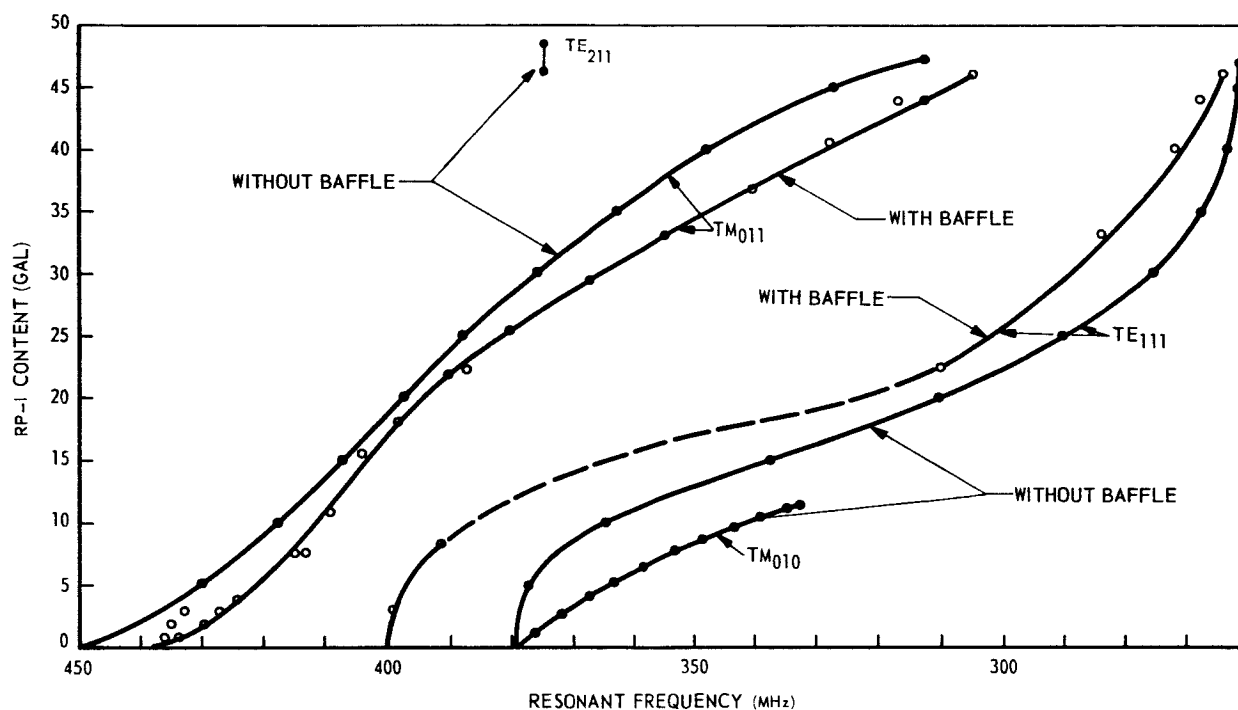
Fig. 3-10 Resonant Frequency Characteristics, RP-1
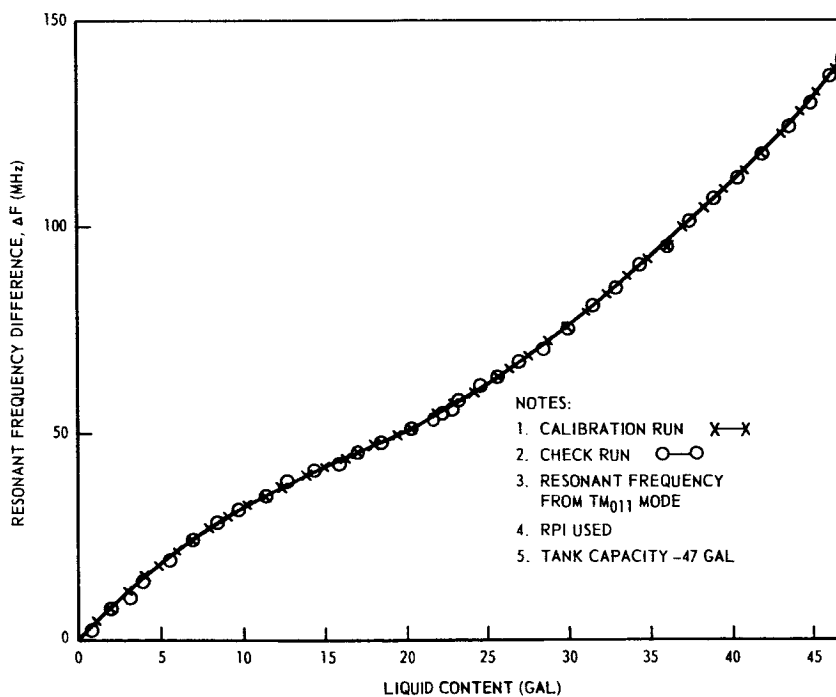
Fig. 3-11 Calibration Curve, Twenty-Four Inch Cryogenic Tank, RP-1

3-13
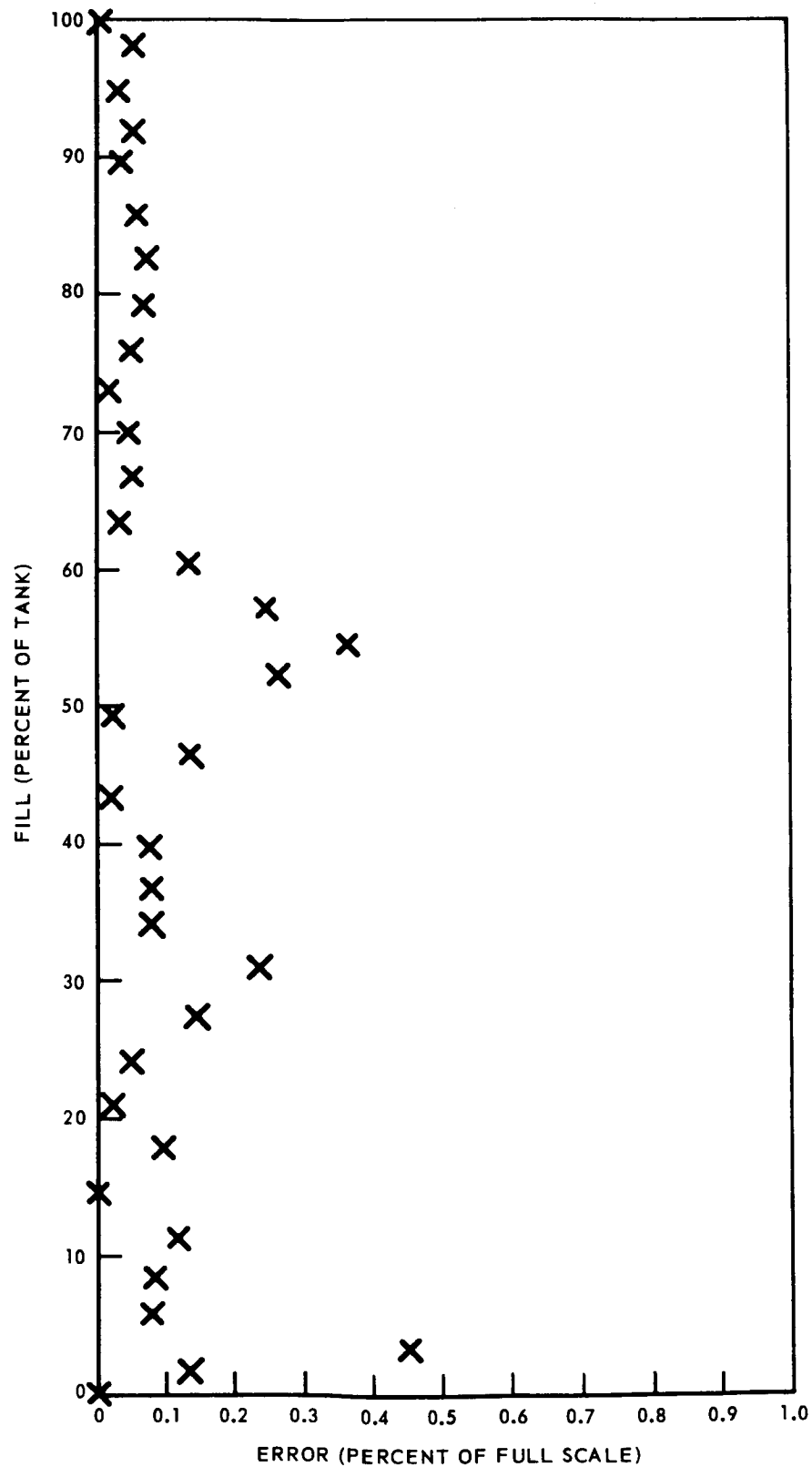
Fig. 3-12 RF System Accuracy
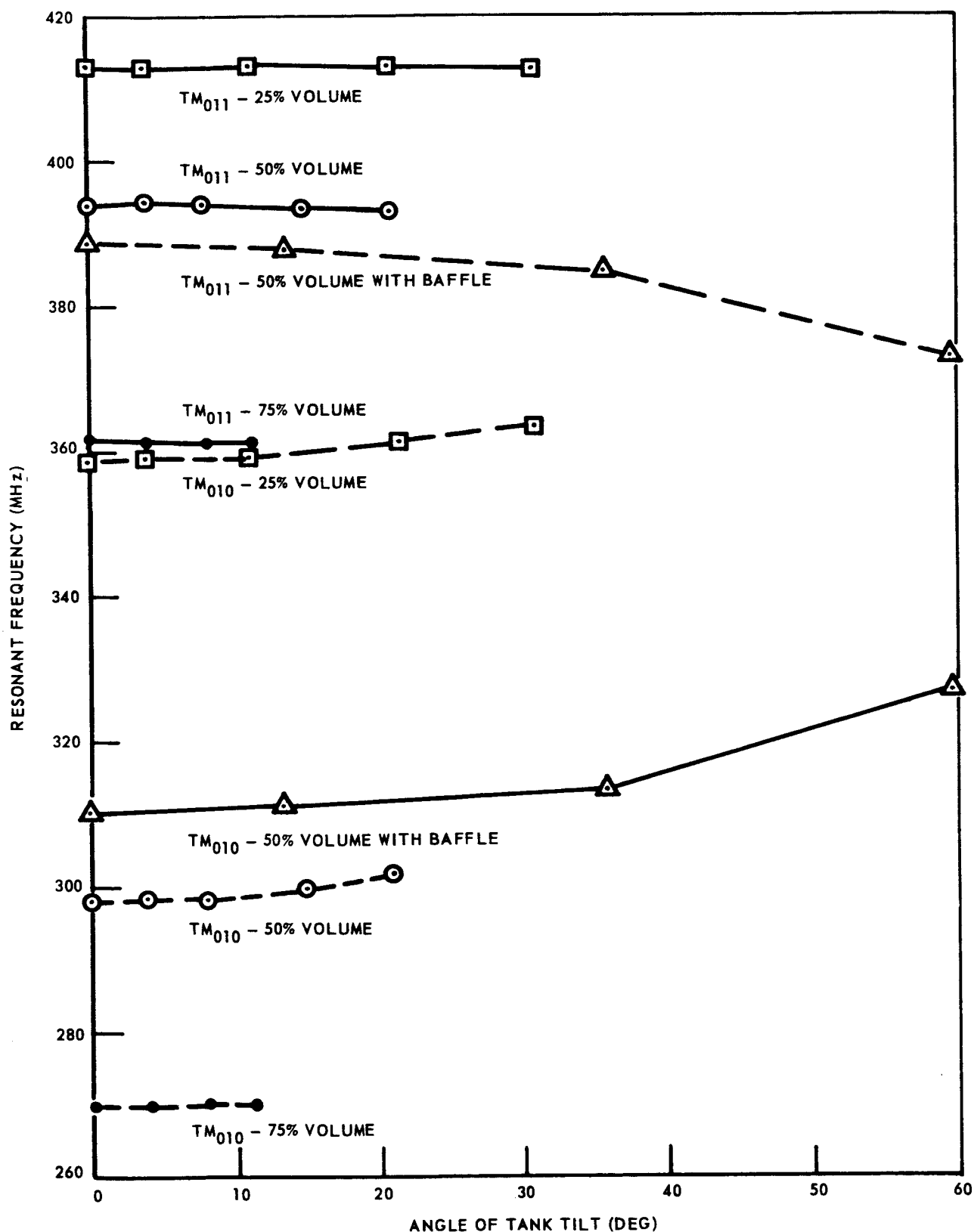
Fig. 3-13 Surface Effects

To simulate zero g conditions for LH_2, a void was created by placing a cardboard tube of 4-5/8 in. outer diameter in the copper tank. The outer portion of the tank was filled with polystyrene beads. The plot of resonant frequency versus content, with and without the void, is shown in Fig. 3-15.

Also a quantity of the polystyrene beads (3-1/2 quarts) was put into a plastic bag. The bag was then positioned at various locations in the tank. The results of this experiment are shown in Table 3-2.

Table 3-2

RESONANT FREQUENCY AS A FUNCTION OF
DIELECTRIC LOCATION

Position of Dielectric	Resonant Frequency (MHz)		
	TM_{011}	TE_{111}	TM_{010}
Uniformly on Bottom (Control)	471.6	403.7	395.2
Top Along Axis	469.0	398.0	386.0
Center Axis	472.6	394.7	386.2
Bottom Axis	465.0	400.0	385.0
Top, Parallel to Axis	469.5	402.0	392.0
Bottom, Parallel to Axis	471.5	399.0	392.5
	468.5	402.0	390.0

To sustain oscillation over the entire fill range of the tank, it is necessary to maintain a phase relationship between the cavity and the circuit. Impedance measurements of the tank and circuit were made to obtain additional design data. The results of this work are included in Ref. 7.
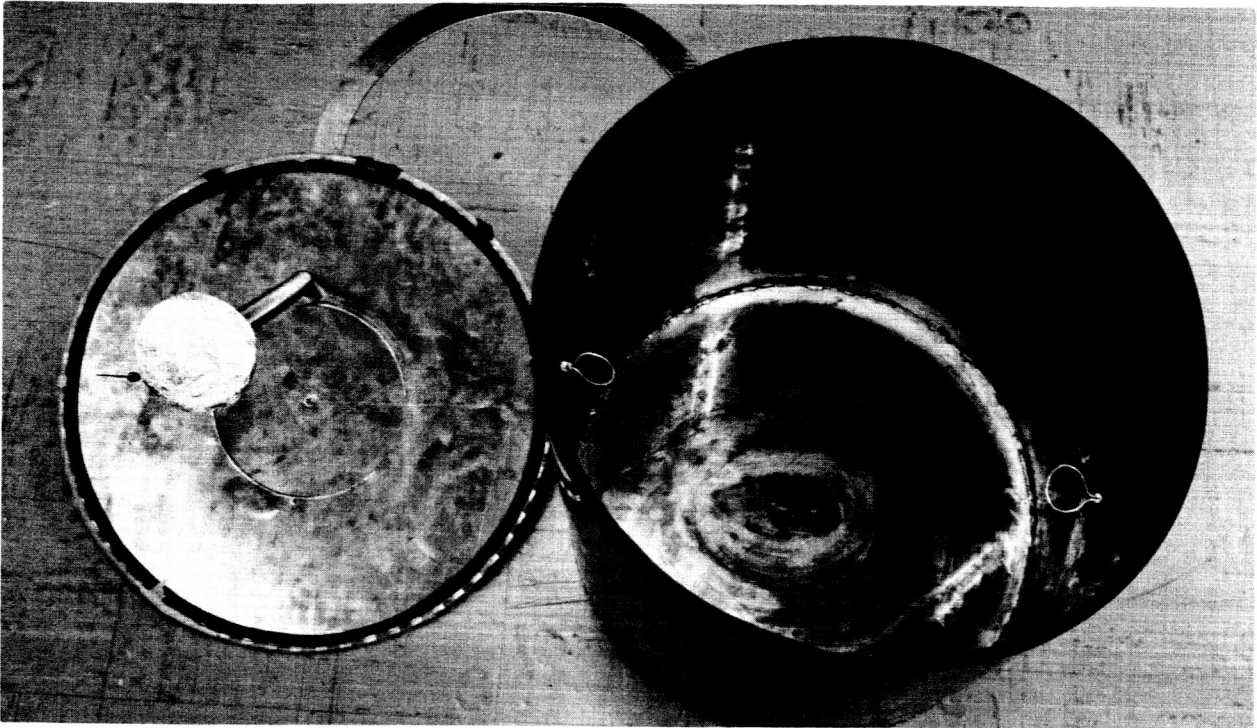
Fig. 3-14 Twenty-Two and One-Half Inch Laboratory Tank, Loop Probes

NOTES:
1. DIELECTRIC, POLYSTYRENE PELLETS
2. O—O NORMAL FILL
3. X—X SIMULATED ZERO "g" FILL
4. CURVES FOR TM_{011} MODE
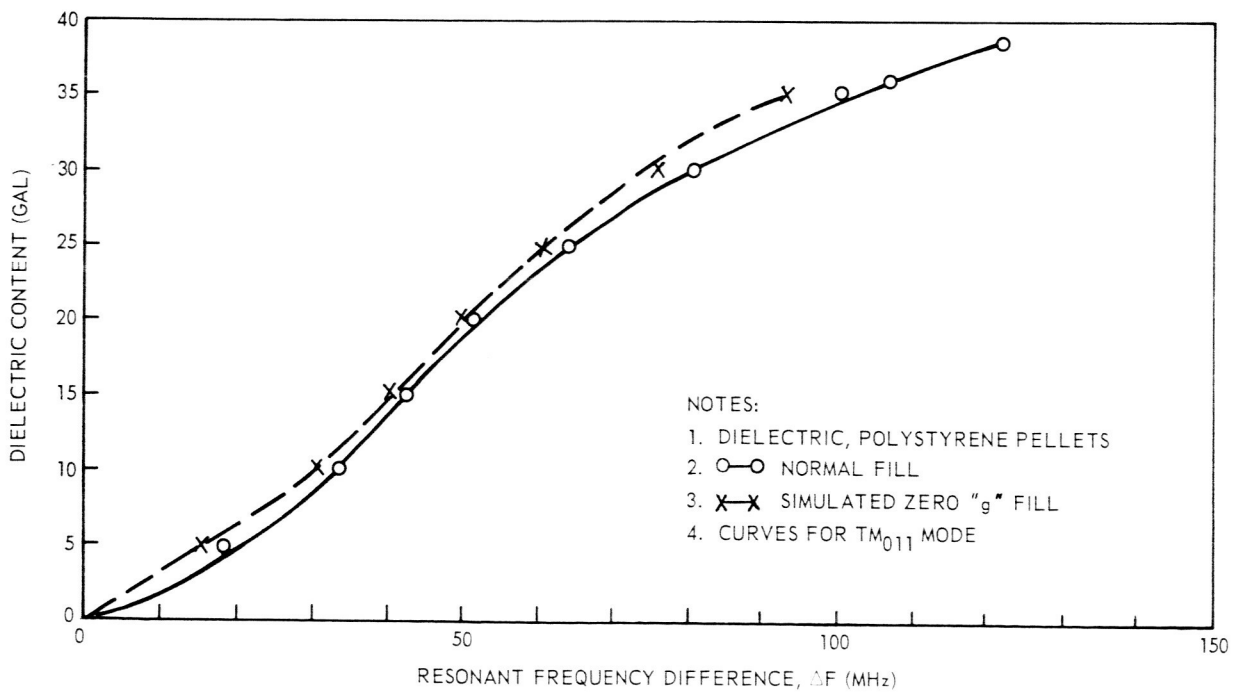
Fig. 3-15 Simulated Zero G Data Plot

3-17

Section 4

DEVELOPMENT PROGRAM

The development program, the second part of the investigation and development of an RF liquid-level sensing technique, included the following:

- RP-1 experiments
- Simulated zero g experiments
- LH_2 experiments
- LOX experiments
- RF system design for the Saturn S-IVB Battleship

Large tanks were used for the experiments with RP-1 and LH_2, and the 24-in. tank was used for LOX testing.

4.1 LIQUID ROCKET FUEL EXPERIMENTS

Tests utilizing RP-1 in a modified Agena tank were conducted at Moffett Field in Hangar No. 1. The spherical portion of the Agena tank was selected because the size and shape closely resembled the 60-in. independent development tank* used for the LH_2 experiments. This selection permitted the results to be more directly compared than would have been the case if any other of the available tanks had been used.

The modified Agena tank weighed approximately 545 lb and had a capacity of approximately 575 gal. The RP-1 weighed 6.64 lb per gal at 72°F and at standard atmospheric pressure. The environment during the testing was sufficiently uniform so that a weight-to-volume correction factor was not required. Figure 4-1 is a photograph of the installation.

---

*The independent development tank was fabricated by Lockheed for a company-sponsored program.

4-1
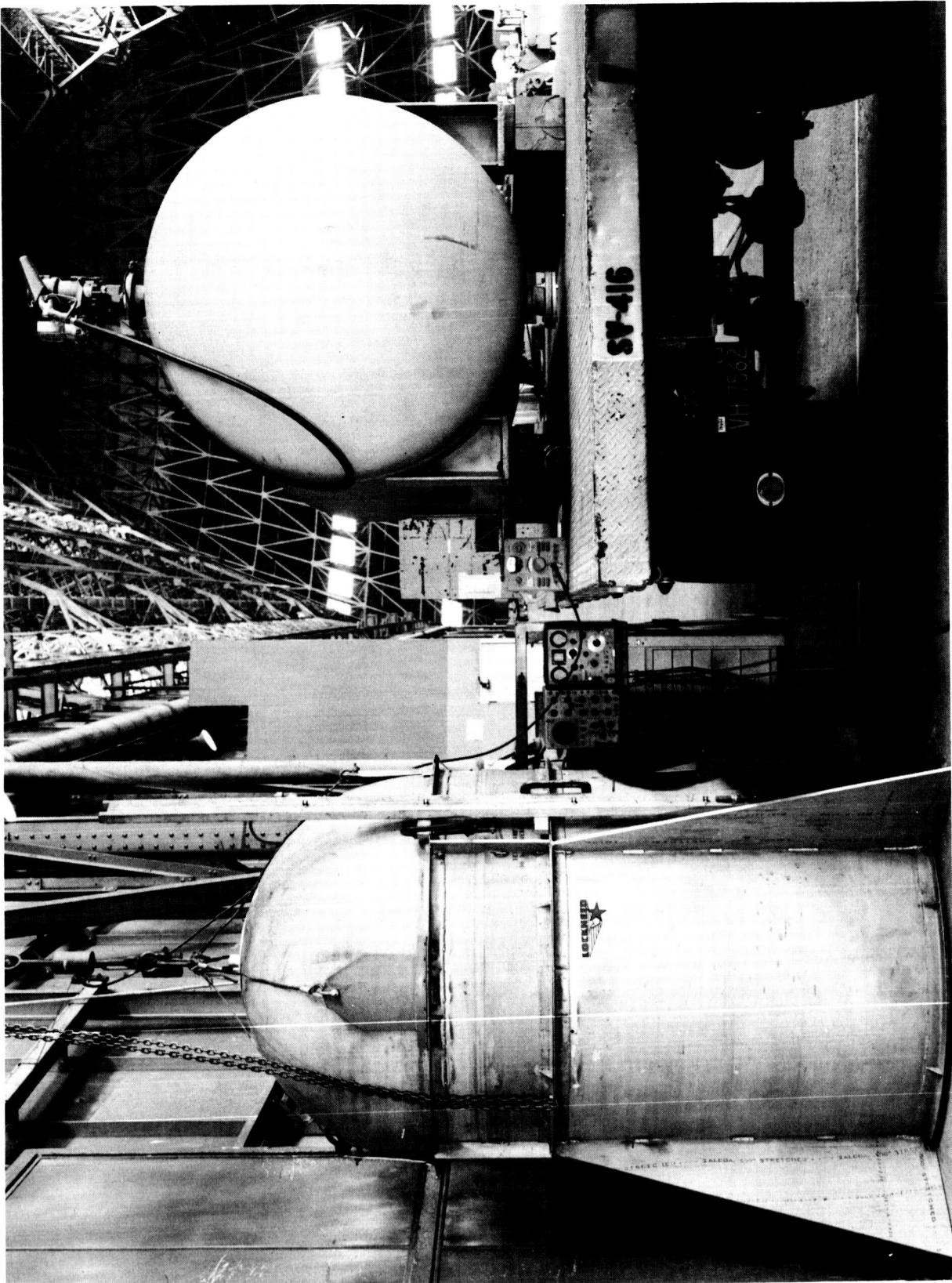
Fig. 4-1 Modified Agena Tank for RP-1 Experiments

The experiments included the following

    a.   Basic tank measurements to determine resonant frequency characteristics

    b.   Measurements of various probe designs

    c.   Measurements to determine the effects of various surface conditions including slosh

    d.   Measurements to determine the effect of modifying the internal configuration by extending fill lines into the tank

4.1.1 RF Systems

The two types of RF systems were used for exciting the tank. A block diagram of the manually tracked system is shown in Fig. 4-2. The tank was swept with a Telonic HD1A sweep generator, and the resulting sweep from the tank was displayed on an oscilloscope. The HP 608D signal generator provided a marker that was manually positioned upon the resonant peak. The frequency of the HP 608D was mixed with the reference frequency from a HP 608C to provide a difference frequency that was displayed on a HP 524B counter.

The second type was the self-oscillating system. The block diagram of this system is shown in Fig. 4-3. Two Conductron C-401 amplifiers were placed between the input and output probes of the tank and thereby produced an oscillating loop. The frequency of the oscillating loop was mixed with the frequency of a reference oscillator, and the difference frequency was displayed on a HP 524B counter. Variations of this basic system were used throughout the RP-1 experiments.

4.1.2 Supporting Instrumentation

A BLH* load cell in combination with a BLH Type N indicator was used to measure the weight of the RP-1. The load cell had a calibrated accuracy of +0.3 percent and a repeatibility of ± 0.25 percent. Instrumentation for measuring the volume of the RP-1 was a Tokheim flowmeter. Even though the flowmeter was not accurately calibrated against a standard, an analysis of the data showed that it provided more consistent readings than did the load cell.

---

*Baldwin Lima Hamilton

4-3
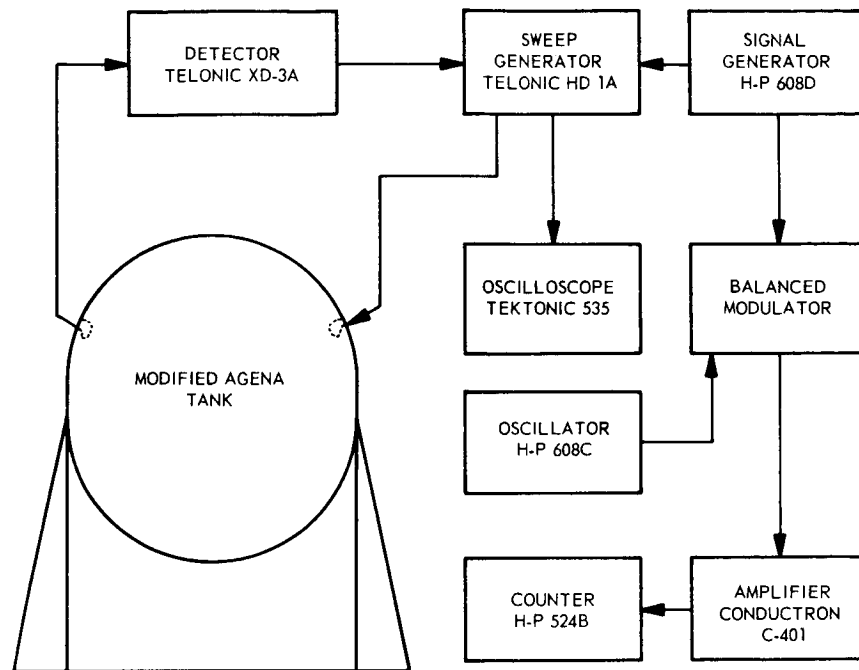
Fig. 4-2 Manually Tracked RF System, RP-1 Experiments

4.1.3 Preliminary Experiments

The placement and configuration of the RF probes required preliminary data regarding the resonant characteristics of the tank. A block diagram of the measuring system is shown in Fig. 4-4. A radio-frequency carrier modulated by a 1000 Hz signal was fed into one probe of the tank from a HP 608C signal generator. The signal was detected at the other probe, and the amount of attenuation was recorded from the HP 415B VSWR meter. With 2-1/2-in. diameter loops placed diametrically opposite each other at the base of the upper hemispherical end, it was found that many modes were propagated. Figure 4-5 is a plot of the modes. Many of the cylindrical modes were supressed, while the spherical modes were undisturbed when the loops were replaced with 3-in. long dipoles located on the top and bottom of the tank. (See Fig. 4-6 and compare with Fig. 4-5.) The addition of 2-in. and then 6-in. diameter discs to the ends of the dipoles increased the amplitude of several of the spherical modes. The resulting plot of the first three spherical modes as the tank was filled with RP-1 is shown in Fig. 4-7.

4-4
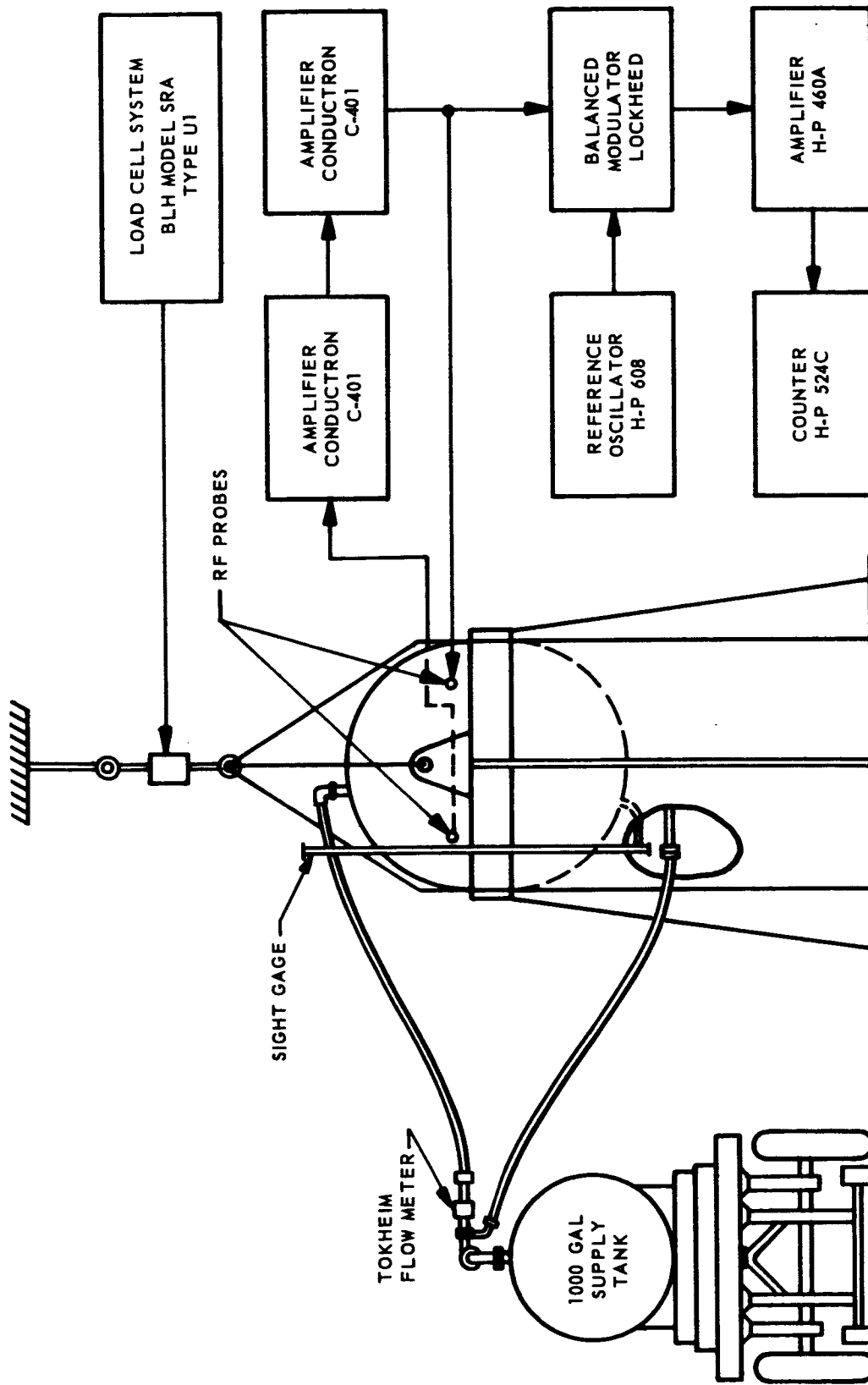
Fig. 4-3 Self-Oscillating RF System for RP-1 Experiments
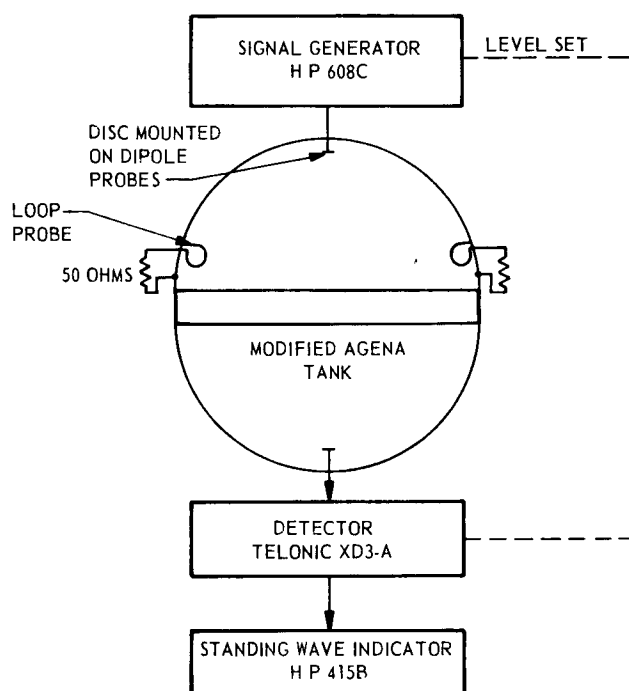
Fig. 4-4 Resonant Frequency Mode Determination, Block Diagram

LOCKHEED MISSILES & SPACE COMPANY
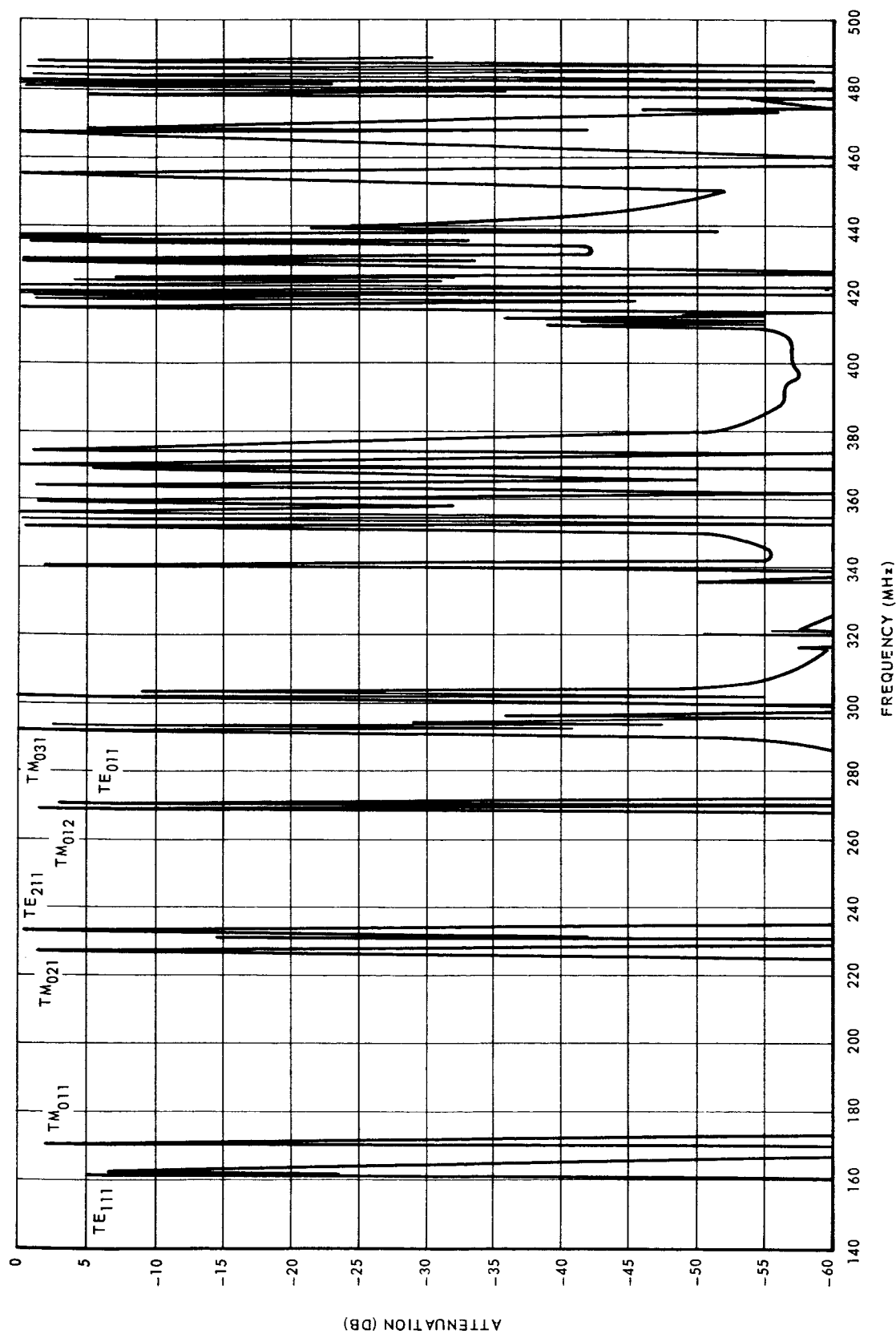
Fig. 4-5 Resonant Frequency Mode Plot, Empty Tank,
Two and One-Half Inch Loop Probes on Side

4-7
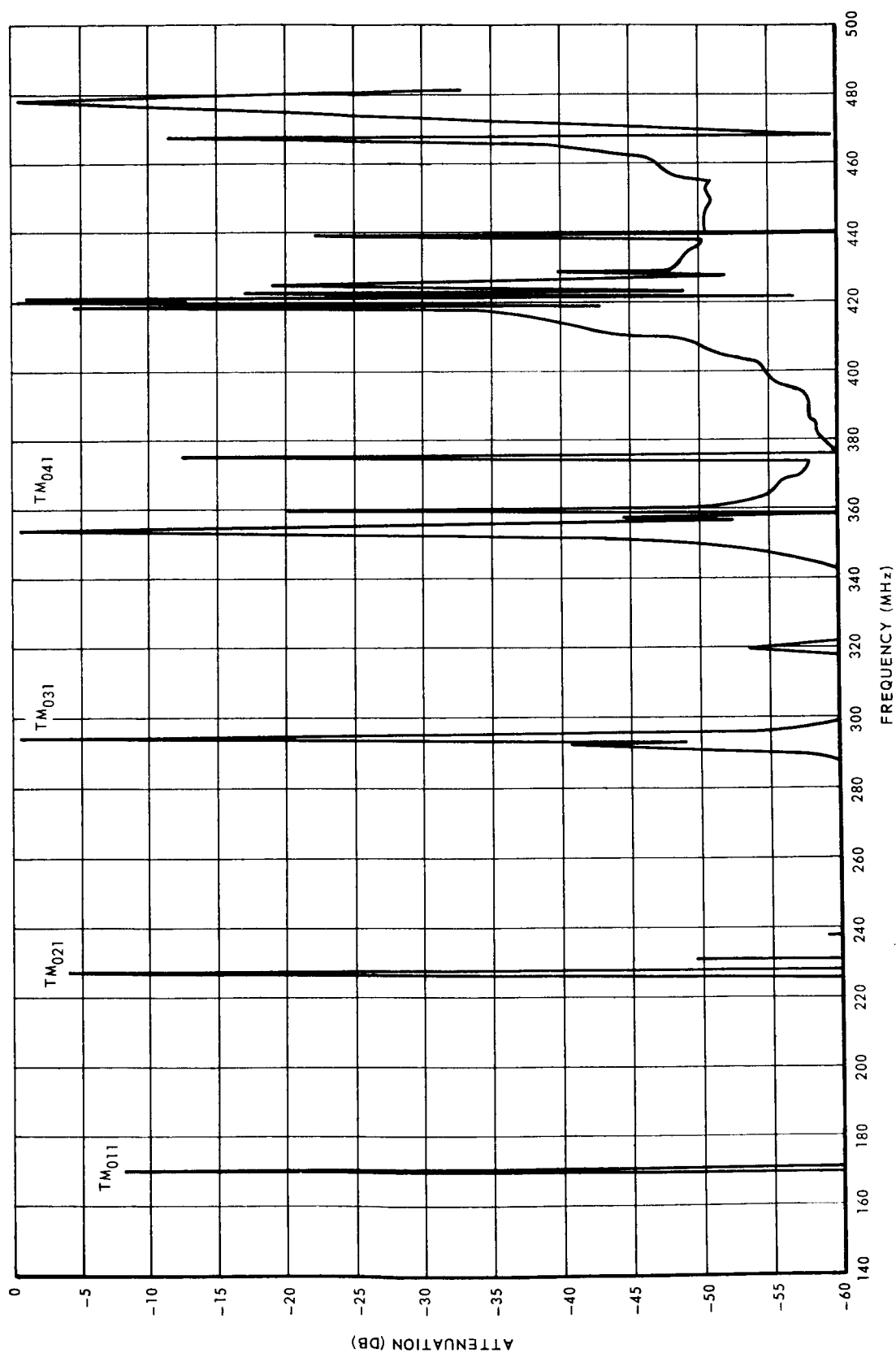
Fig. 4-6 Resonant Frequency Mode Plot, Empty Tank, Three–Inch
Long Dipoles, Top and Bottom
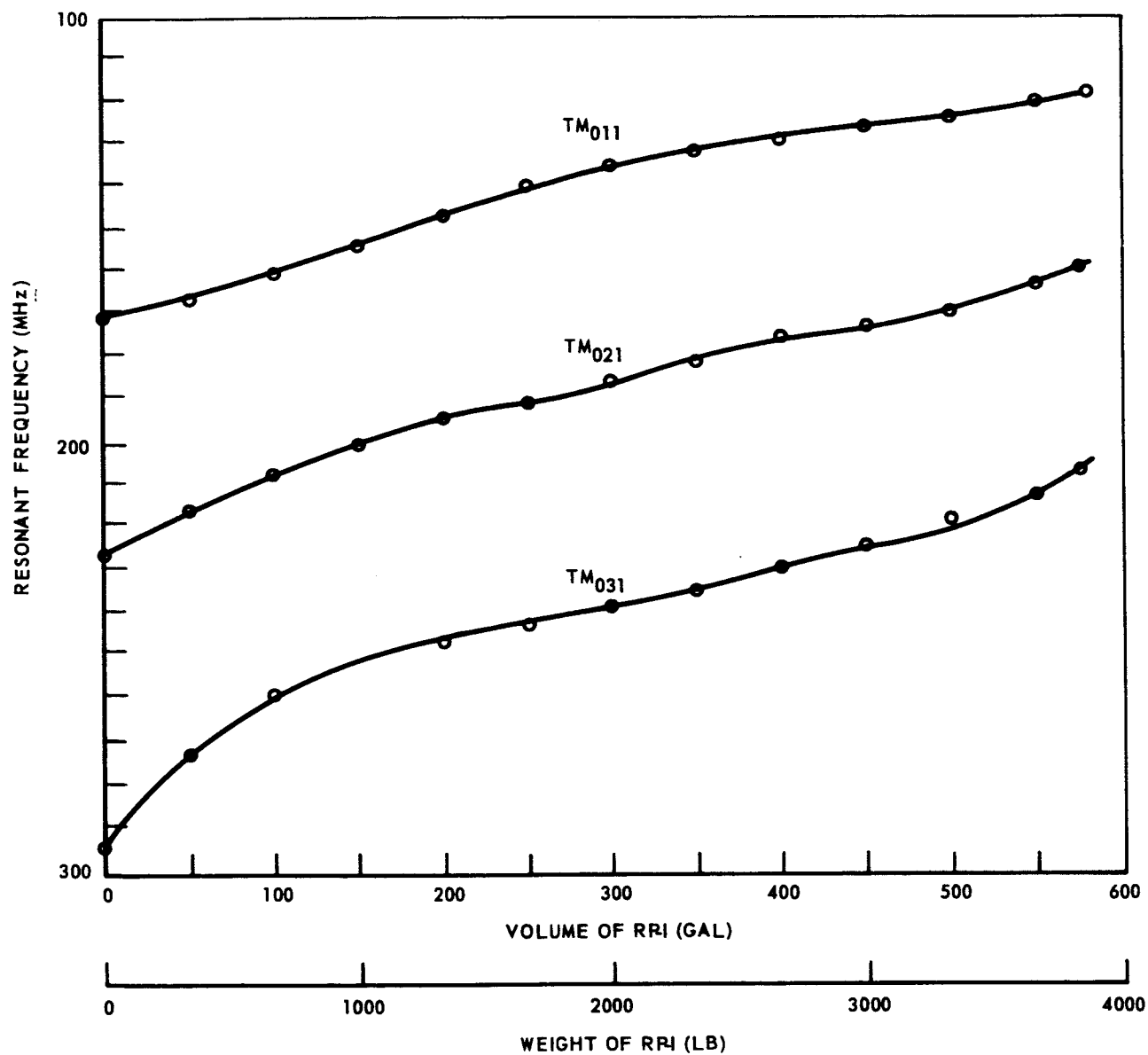
Fig. 4-7 Resonant Frequency Characteristics, RP-1 Fill Cycle

4.1.4 Series 1 Experiments

A series of six experiments was conducted with the RF system operating in the TM_{011} mode. A pair of dipoles with 6-in. diameter discs were located in the top and bottom of the tank as shown in Fig. 4-4. The self-oscillating RF system (Fig. 4-3), was used for test runs 1, 5, and 6; the manually tracked system was used for runs 3 and 4. Both techniques were applied for exciting the tank during test run 2. Test run 5 was used for calibration, and the resulting change is resonant frequency versus RP-1 content is plotted in Fig. 4-8. The curve is typical and representative of all of the TM_{011} mode plots for RP-1. To maintain self-oscillation over the entire fill, it was necessary to correct the phase of the circuit by making cable length adjustments. Also, to prevent mode jumping, it was necessary to add a low-pass filter to the oscillating circuit.

4.1.5 Series 2 Experiments

To determine the effect on the RF liquid-level sensing system of various internal fill and drain line configurations, a series of three experiments were conducted. A 2-in. diameter steel pipe was placed along the major axis, and measurements were taken for various lengths of the pipe extending into the tank. The change in resonant frequency was noted with the pipe both grounded and ungrounded at the top of the tank. Also the pipe was extended into the entire length of the tank and grounded at each end of the tank. The tank was excited through both the loop probes and the dipoles. The results of these experiments demonstrated that the simulated fill line suppressed the spherical modes and enhanced the TE_{111} and TE_{211} cylindrical modes. The length of the pipe extending into the tank caused little or no effect up to approximately 10 percent. The major change occurred at about 15 percent, and little additional change was noted beyond the 90 percent of tank length.

The manually tracked system was used for exciting the TE_{211} mode, and the resulting change in resonant frequency versus RP-1 content is shown in Fig. 4-9. The self-oscillating system operated in the TE_{111} mode; Fig. 4-10 is a plot of the results. As noted above, it was necessary to change the cable length and to add a low-pass filter to sustain the self-oscillation.
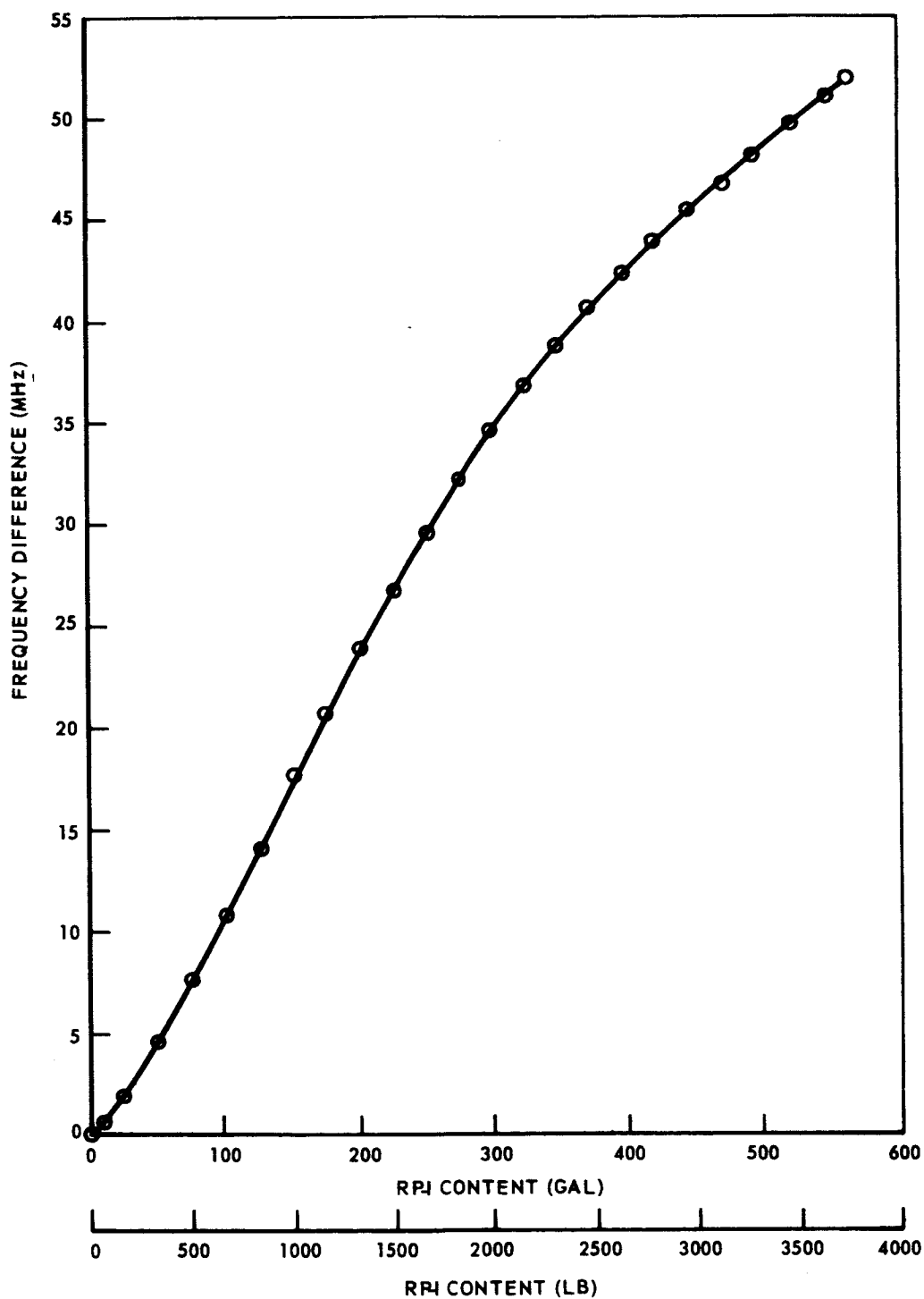
Fig. 4-8 Resonant Frequency Difference Vs. RP-1 Content, TM_{011} Mode, Self-Oscillating Run 5

4-11
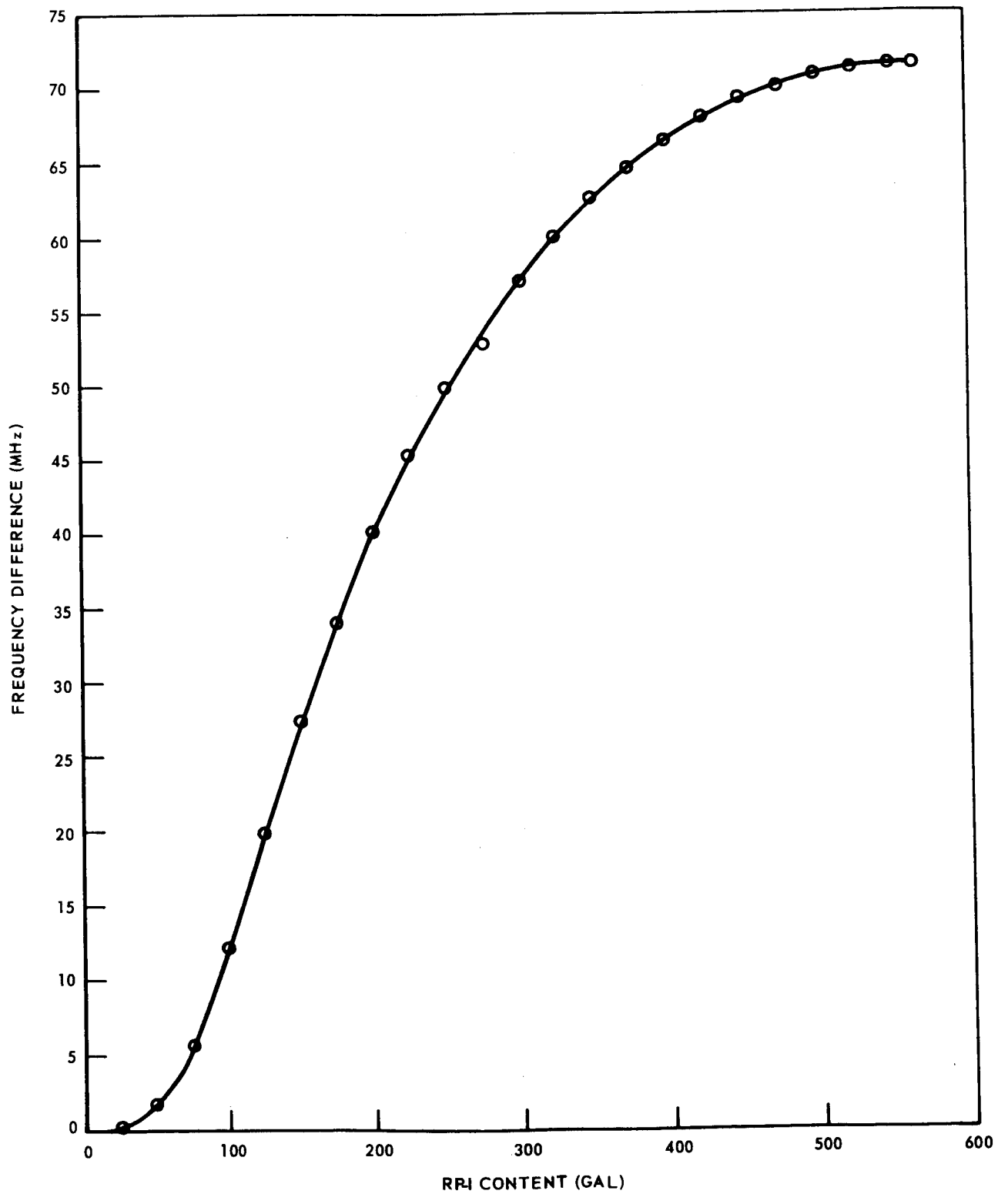
Fig. 4-9 Resonant Frequency Difference Vs. RP-1 Content, TE_{211} Mode, Manually Tracked Run 7

4-12
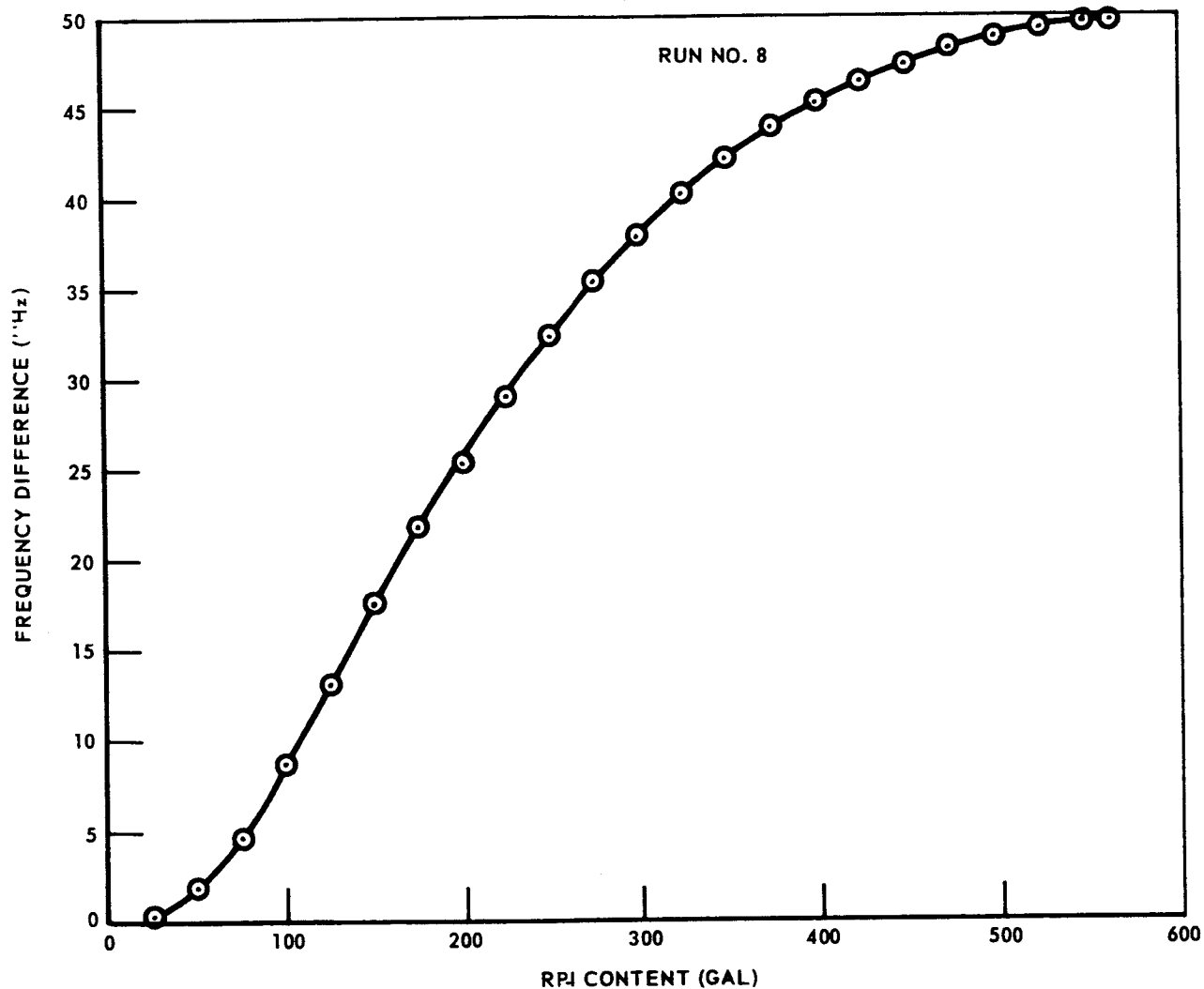
Fig. 4-10 Resonant Frequency Difference Vs. RP-1 Content, TE$_{211}$ Mode, Self-Oscillating Run 8

4-13

4.1.6 System Accuracy Determination

One of the experimental runs, test number 5, was selected for a calibration run. The RP-1 was measured and weighed very carefully and, as closely controlled increments of the liquid were added, the resonant frequency was detected. The resonant frequency at a particular level on all subsequent test runs was read off the calibration curve, and the apparent volume of RP-1 was noted. The actual volume was subtracted from the apparent volume, and the resultant difference was divided by the total volume of the tank to obtain the full scale error.

Figure 4-11 is a plot of the RF system accuracy. The values presented were referenced to the volume as determined by the load cell measurements as a standard. Figure 4-12 shows the accuracy plots as referenced to the volume determined by the flowmeter. An error band indicating the maximum deviation has been added to each plot.

A significant portion of the total error band of ± 0.5 percent may be attributed to the calibration accuracy (+ 0.3 percent) and repeatibility (± 0.25 percent) of the load cell.

The error band obtained from the flowmeter data was the same as that obtained from the load cell data except for the first half of run 2 and the complete test run 6. The greatest error determined for run 6 was 0.35 percent. The self-oscillating system was used for these runs. The results indicated an improvement offered by the self-oscillating system over the manually tracked system.

4.1.7 Surface Effects

A series of experiments was conducted for the purpose of determing the influence of changing surface conditions on the stability of the RF liquid-level sensing system. The first group of tests consisted of filling the tank to a particular level, recording the resonant frequency, tilting the tank, determining the angle, and recording the change in resonant frequency; and continuing this sequence for different angles of tilt and different volumes. Both the manually tracked and the self-oscillating systems were
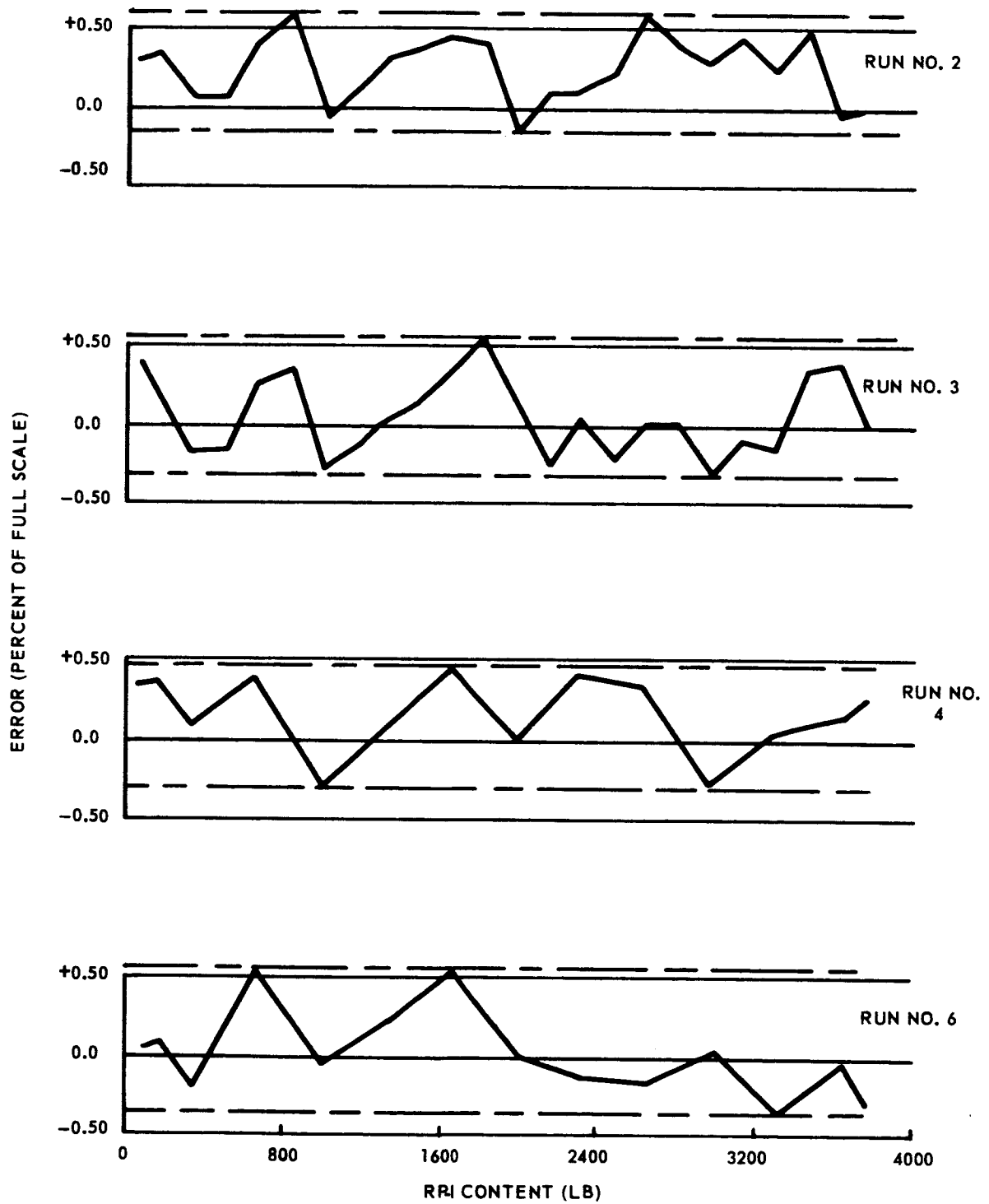
Fig. 4-11 RF Liquid Level Sensing System Accuracy, Load Cell

4-15
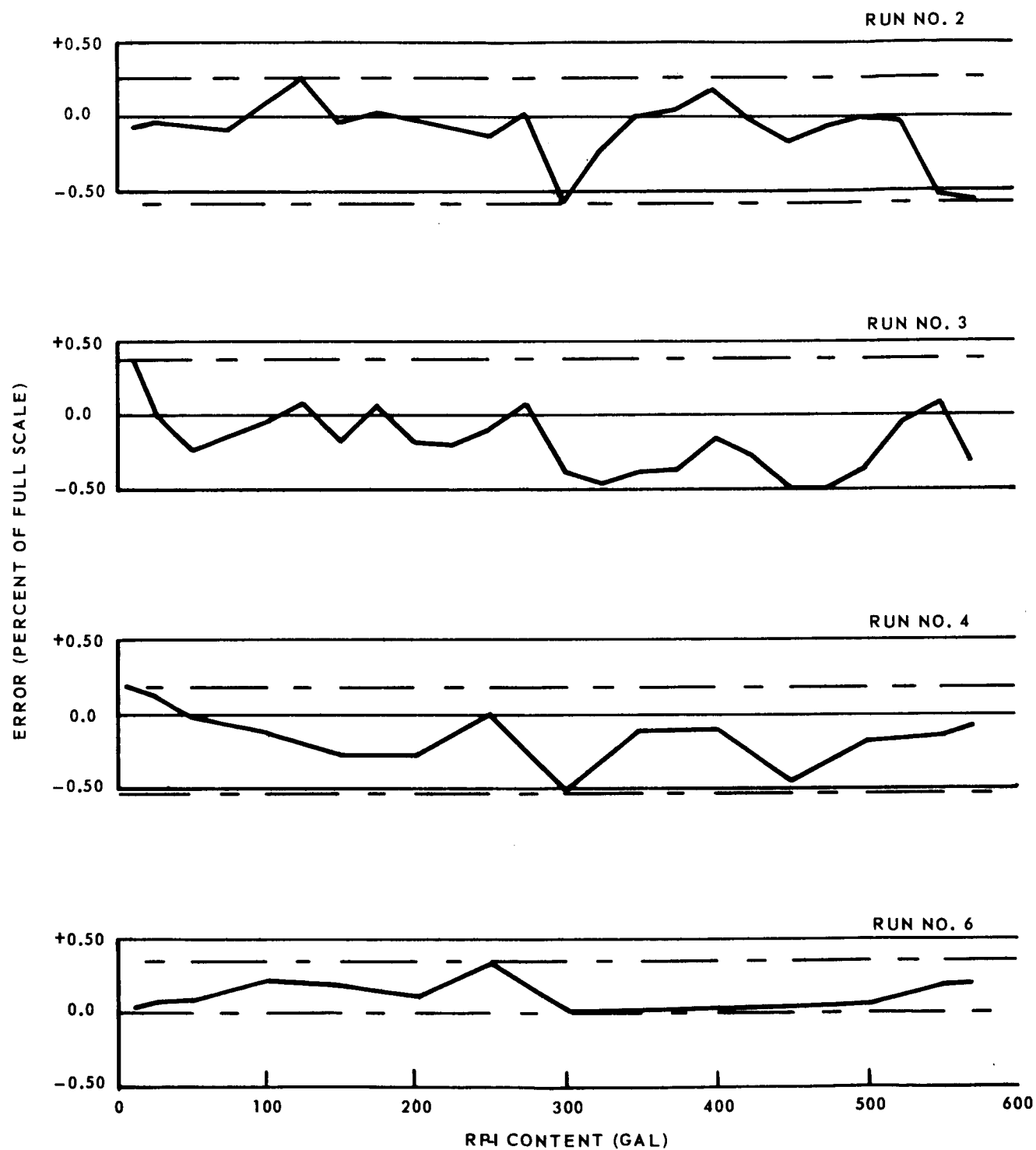
Fig. 4-12 RF Liquid Level Sensing System Accuracy, Flowmeter

4-16

used. Table 4-1 and Table 4-2 list the results. For the second series, the side-wall mounted probes were used (versus the top and bottom locations), and the tank was tilted near the parallel plane of the probes and then near the perpendicular plane of the probes. The results are shown in Table 4-3.

A third experiment was conducted to determine the effect of slosh on the stability of the RF sensing system. A stability check of the TM_{011} mode was made by filling the tank with 200 gal of RP-1 and recording changes in the resonant frequency as the tank was set into motion to create sloshing of the RP-1. The motion of the liquid caused the resonant frequency to become 0.38 MHz lower and 0.24 MHz higher than the 145.50 MHz recorded at rest. These changes correspond to a total deviation of -1.6 percent to +1.0 percent. An averaging of the change would result in an error of -0.3 percent.

4.1.8 Impedance and Phase Measurements

The final series of the experiments was made to determine the impedance and phase characteristics of the TM_{011} mode. These characteristics were determined during an RP-1 fill by using a HP 803A VHF bridge that was fed by a HP 608C signal generator. The HP 417A VHF detector was used for determining the minimum signal. The impedance characteristics are plotted in Fig. 4-13, and the phase angle versus volume of RP-1, in Fig. 4-14. The changes of load impedance from capacitive to inductive and back to capacitive demonstrated the need for adjusting the cable length to sustain self-oscillation over the entire fill range. The input impedance and phase characteristics of the Conductron amplifiers that were used in the oscillating circuit were quite constant. Mode jumping was attributed to phase shifts in the other components of the circuit, i.e., the cables, probes, and tank.

4.2 SIMULATED ZERO G EXPERIMENTS

The 22-1/2-in. diameter copper tank described in Par. 3.5 was used for the simulated zero g experiments. Polystyrene pellets with a dielectric constant of 1.7 were used to simulate a liquid for most of the experiments. A mixture of the polystyrene pellets

Table 4-1

SURFACE EFFECTS ON MANUALLY TRACKED RF SYSTEM,
TM_{011} MODE, DIPOLE PROBES

Tilt Angle (deg)	Resonant Frequency (MHz)	Change in Frequency (MHz)	Apparent Change in Content (lb)	Full Scale (3780 lb) Error (%)
100 GAL = 664 LB -17.5 PERCENT				
0	159.052	0.000	—	—
27.3	158.850	+ 0.202	9.63	0.25
38.6	158.689	+ 0.363	17.30	0.45
200 GAL = 1328 LB -35 PERCENT				
0	145.500	0.000	—	—
19.0	145.039	+ 0.461	25.80	0.69
23.0	145.026	+ 0.474	26.50	0.70
31.0	144.538	+ 0.962	53.70	1.42

Table 4–2

SURFACE EFFECTS ON SELF-OSCILLATING RF SYSTEM,
TM$_{011}$ MODE, DIPOLE PROBES

Tilt Angle (deg)	Resonant Frequency (MHz)	Change in Frequency (MHz)	Apparent Change in Content (lb)	Full Scale (3780 lb) Error (%)
50 GAL = 332 LB –8.9 PERCENT				
0	165.500	0.000	—	—
5	165.512	– 0.012	0.723	0.02
10	165.561	– 0.061	3.67	0.10
14.5	165.648	– 0.148	8.92	0.24
19	165.765	– 0.265	15.9	0.42
23	165.935	– 0.435	26.2	0.69
27.3	166.110	– 0.610	36.8	0.97
31	166.293	– 0.793	47.7	1.26
38.6	166.456	– 0.956	57.5	1.52
100 GAL = 664 LB –17.5 PERCENT				
0	159.052	0.000	—	—
5	159.049	+ 0.003	0.230	0.01
10	159.039	+ 0.013	0.992	0.03
14.5	159.031	+ 0.021	1.60	0.04
19	159.015	+ 0.037	2.82	0.07
23	158.984	+0.068	5.18	0.14
27.3	158.950	+ 0.102	7.80	0.20
31	158.939	+ 0.113	8.63	0.23
38.6	159.001	+ 0.051	3.89	0.10

Table 4-3

SURFACE EFFECTS ON SELF-OSCILLATING RF SYSTEM,
TE$_{111}$ MODE, SIDE-MOUNTED DIPOLE PROBES

Tilt Angle (deg)	Resonent Frequency (MHz)	Change in Frequency (MHz)	Apparent Change in Content (lb)	Full Scale Error (%)
TILT PARALLEL TO PROBES (Content 50 gal — 332 lb — 8.9 percent)				
0	159.500	0.000	—	—
5	159.486	+0.014	0.126	0.01
10	159.429	+0.071	0.636	0.02
14.5	159.323	+0.177	1.59	0.04
19	159.175	+0.325	2.91	0.08
23	158.986	+0.514	4.60	0.12
27.3	158.743	+0.757	6.80	0.18
31	158.565	+0.985	8.85	0.24
38.6	158.250	+1.250	11.2	0.30
TILT PERPENDICULAR TO PROBES				
0	159.500	0.000	—	—
5	159.495	+0.005	0.045	0.01
10	159.483	+0.017	0.153	0.01
14.5	159.435	+0.065	0.583	0.02
19	159.297	+0.203	1.82	0.05
23	159.111	+0.389	3.49	0.09
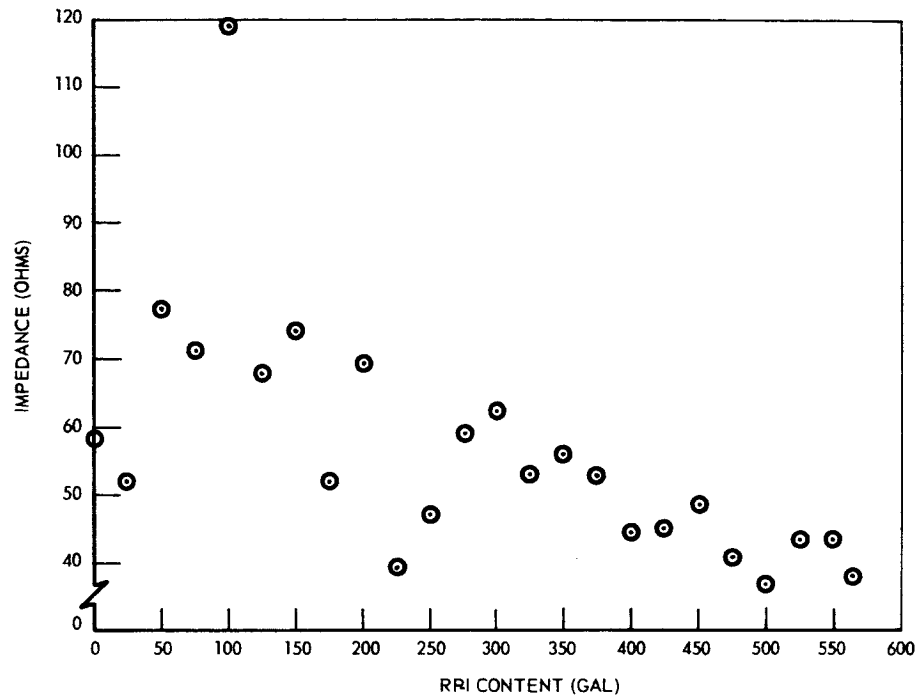
Fig. 4-13 Impedance Characteristics, TM_{011} Mode
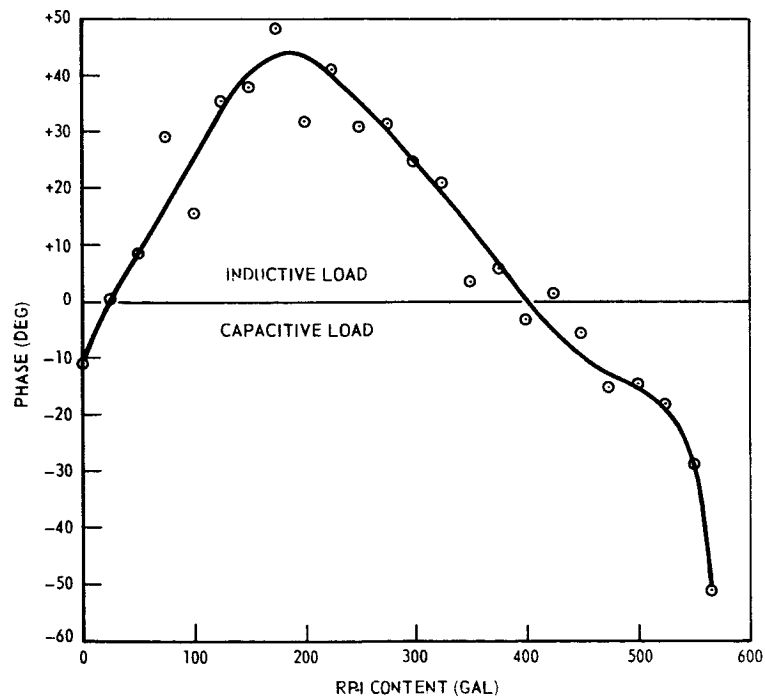
Fig. 4-14 Phase Characteristics, TM_{011} Mode

4-21

and polyurethane foam to obtain a dielectric constant of 1.15 was packaged in polyethylene bags and used for one series of experiments. A block diagram of the RF system is shown in Fig. 4-15.

4.2.1 Preliminary Experiment

For this series of experiments, the three lowest modes dominant in the copper tank (TM_{010}, TM_{011}, and TE_{111}) were used. Two 2-in. discs mounted on dipoles and located in the center of the top and bottom of the tank were used for exciting the TM modes. Two 1-in. loops located 180 deg apart and half-way between the center and side wall on the top of the tank were used to excite the TE_{111} mode. The resonant frequencies and frequency differences for all three modes were obtained as the tank was filled. The results are shown in Table 4-4. These measurements, which were made with the surface of the pellets leveled, served as the standard for comparison.
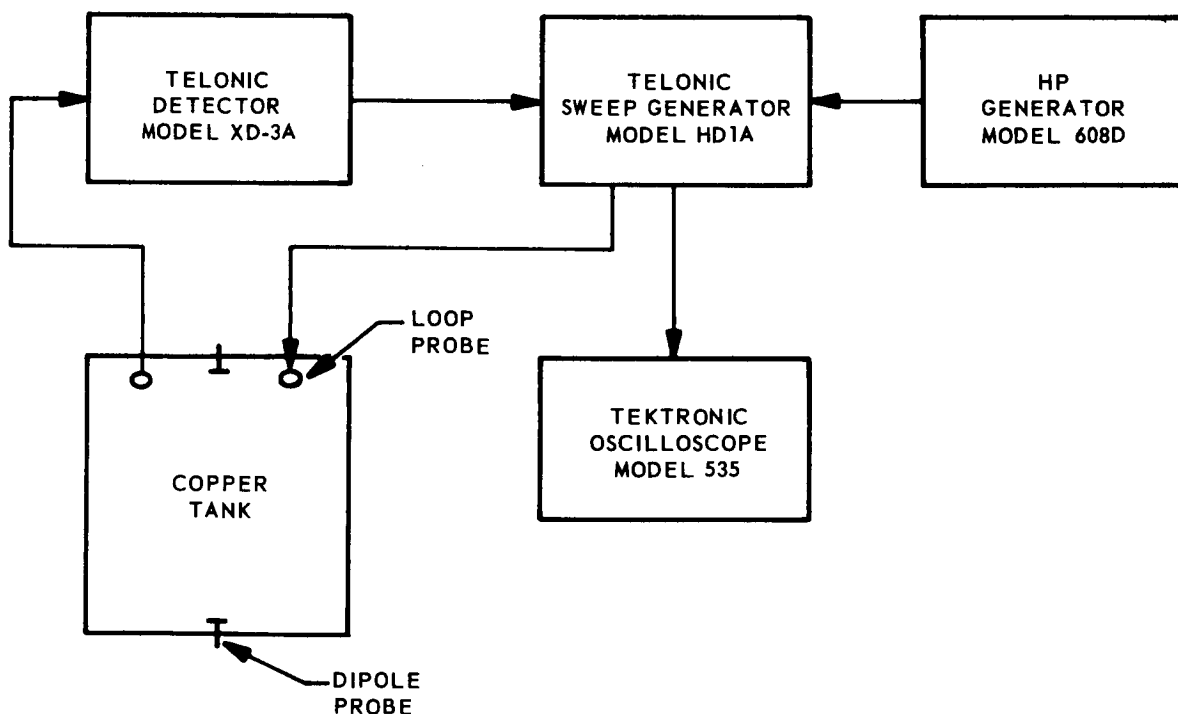
Fig. 4-15 Zero G Simulation, RF System

4-22

Table 4-4

BASIC RESONANT FREQUENCY VALUES FOR COPPER TANK

Volume of Polystyrene Pellets (gal)	TM_{010} Resonant Frequency (MHz)	TM_{010} Resonant Frequency Difference (MHz)	TE_{111} Resonant Frequency (MHz)	TE_{111} Resonant Frequency Difference (MHz)	TM_{011} Resonant Frequency (MHz)	TM_{011} Resonant Frequency Difference (MHz)
0	399	0	405	0	476.5	0
1	396	3	404	1	474	2.5
2	394	5	402	3	470	6.5
5	376	23	399	6	456	20.5
10	360	39	378	27	445.5	31.0
15	341	58	347	58	436	40.5
20	328	71	326	79	426	50.5
25	319	80	310	95	412	64.5
30	312	87	302	103	395	81.5
35	305	94	297	108	374	102.5
38	301	98	296	109	358	118.5

4.2.2 Fiberglass Tube Experiments

Three fiberglass tubes 22.5 in. long, with inside diameters of 12.5, 8, and 4 in. and walls 1/4 in. thick, were used to position the polystyrene pellets for the first series of simulated experiments.   Each tube was placed in various positions throughout the tank, and the pellets were placed either outside of the tube (leaving the tube empty to serve as a void) or filled inside (leaving the remainder of the tank empty).   As the pellets filled the outside of the tube, the indicated volume was less than the actual volume. As the pellets filled the inside of the tube, the indicated volume was greater than the actual volume.   The data from these experiments are presented in Table 4-5.

Table 4-5
SIMULATED ZERO G EFFECT WITH CYLINDRICAL GEOMETRY

Tube Diameter (in.)	Tube Pellets Outside/Inside	Distance From Tank's Axis to Tube's Axis (in.)	Actual Volume (gal)	Resonant Frequency Difference (MHz)	Apparent Volume (Calibrated) (gal)	Difference in Volume (gal)	Error in Volume (%)
TM_010 MODE							
12	Outside	0	25	32	8	-17	-42.5
12	Outside	5	28	62.5	16.5	-11.5	-28.4
8	Outside	0	33	60.5	16	-17	-42.5
8	Outside	5	34	78	24	-10	-25.0
8	Outside	7	35	88	30.5	- 4.5	-11.3
4	Outside	0	39	85.5	29	-10	-25.0
4	Outside	3	38	88	30.5	- 7.5	-18.8
4	Outside	6	38	92.5	33.5	- 4.5	-11.3
4	Outside	9	38	99	38.5	+ .5	+ 1.25
12	Inside	0	11	69	19.5	+ 8.5	+21.2
8	Inside	0	5	43.5	10.5	+ 5.5	+13.8
8	Inside	5	5.3	34.5	8.3	+ 3	+ 7.5
8	Inside	7	5.3	23.5	6	+ .7	+ 1.75
4	Inside	0	1.3	18	5	+ 3.7	+ 9.25
4	Inside	3	1.4	13	4	+ 2.6	+ 6.5
4	Inside	6	1.4	9.5	3	+ 1.6	+ 4.0
4	Inside	9	1.4	3.8	1.5	+ .1	+ .25
TM_011 MODE							
12	Outside	0	25	54	21	- 4	-10.0
12	Outside	5	28	75.5	28.5	+ .5	+ 1.25
8	Outside	0	33	83	30.5	- 2.5	- 6.25
8	Outside	5	34	97	33.8	- .2	- 0.5
8	Outside	7	35	102	34.8	- .2	- 0.5
4	Outside	0	39	104.5	35.5	- 3.5	- 8.75
4	Outside	3	38	101	34.4	- 3.6	- 9.0
4	Outside	6	38	106	35.8	- 2.2	- 5.5
4	Outside	9	38	110	36.7	- 1.3	- 3.25
12	Inside	0	11	59.5	23	+12	+30.0
8	Inside	0	5	34	11.5	+ 6.5	+16.3
8	Inside	5	5.3	31	10	+ 4.7	+11.8
8	Inside	7	5.3	24	6.7	+ 1.4	+ 3.5
4	Inside	0	1.3	15	3.5	+ 2.2	+ 5.5
4	Inside	3	1.4	13	3	+ 1.6	+ 4.0
4	Inside	6	1.4	8.3	1.8	+ .4	+ 1.0
4	Inside	9	1.4	4	1	- .4	- 1.0
TE_111 MODE							
8	Outside	0	35	84.5	21.5	-13.5	-33.8
8	Inside	0	5	27	10	+ 5	+12.5
4	Outside	0	38	100	28	-10	-25.0
4	Outside	3	38	101.5	28.7	- 9.3	-23.2
4	Outside	6	38	105	31.5	- 6.5	-16.3
4	Outside	9	38	108	36	- 2	- 5.0
4	Inside	0	1.5	6.5	5.3	+ 3.8	+ 9.5
4	Inside	3	1.3	6	5	+ 3.7	+ 9.25
4	Inside	6	1.3	3.5	3.8	+ 2.5	+ 6.25
4	Inside	9	1.3	1.2	2	+ .7	+ 1.75

4.2.3 Fiberglass Tube Effect

The fiberglass was selected as a convenience and unfortunately introduced a significant shift in the resonant frequency. Measurements were made to determine the amount of deviation caused by the fiberglass tubes, and the results are tabulated in Table 4-6. The smallest change was noted for the smallest tube when located close to the tank wall. The same results were observed with the pellets where the least deviation was produced as the pellets filled either the outside or inside of the 4-in. tube located against the tank wall. These effects may be predicated by inspecting the field patterns presented in Figs. A-1 through A-3.

A further test to determine the effect of the fiberglass tubes was performed with a mixture of pellets and foam. Bags containing the mixture were stacked along the walls of the tank so that a void of approximately 15-in. diameter was formed. The resulting full scale errors were: (1) TM_{010} mode, 28 percent; (2) TM_{011} mode, 25 percent; and (3) TE_{111} mode, 14 percent.

Table 4-6

EFFECT OF FIBERGLASS TUBE POSITION

Tube Diameter (in.)	Distance From Tank's Axis to Tube's Axis (in.)	TM_{010} Resonant Frequency (MHz)	TM_{011} Resonant Frequency (MHz)	TE_{111} Resonant Frequency (MHz)
None		399	476.5	405
12	0	389	469	
12	5	390	470	
8	0	385	467	400
8	5	390.5	471	
8	7	394.5	473	
4	0	390	470.5	401
4	3	391	473	401.5
4	6	395	474.5	403
4	9	399	476.5	404.5

4.2.4 Spherical Void Experiment

To simulate a zero g condition more truly, a spherical void representing the ullage was created by positioning an inflated balloon in the center of the tank. Pellets were then packed around the balloon, and the resulting resonant frequencies were recorded. The results of the experiment are listed in Table 4-7.

4.2.5 Tank Orientation Experiment

A series of experiments was performed with the tank resting on its side and partially filled with the bags placed uniformly on the tank wall. Two orientations were used; one with the loop probes in a vertical position and the other with the probes in a horizontal position. The results are shown in Table 4-8 for contents of 25 and 50 percent.

Table 4-7

ZERO G SIMULATION WITH SPHERICAL GEOMETRY

Mode	Actual Volume (gal)	Resonant Frequency Difference (MHz)	Apparent Volume (Calibrated) (gal)	Difference in Volume (gal)	Error in Volume (%)
10 IN. DIAMETER SPHERE					
TM_{010}	36	85.5	28.5	-7.5	-18.8
TE_{111}	36	101.0	28.5	-7.5	-18.8
TM_{011}	36	113.5	37.5	+1.5	+ 3.75
16 IN. DIAMETER SPHERE					
TM_{010}	30	61	16	-14	-35.0
TE_{111}	30	63	16.2	-13.8	-34.5
TM_{011}	30	85	31	+ 1	+ 2.5

Table 4-8

TANK ORIENTATION EXPERIMENT

Mode	Quantity of Dielectric (capacity, %)	Resonant Frequency (MHz)			Error (largest change, %)
		Tank Vertical	Tank Horizontal		
			Probes Vertical	Probes Horizontal	
TM_{010}	0	400	400	400	0
	25	394.5	395.5	395.5	0.25
	50	386	386.5	388	0.51
TM_{011}	0	476	476	476	0
	25	470	473	473	0.64
	50	464.5	464.5	464.6	0.02
TM_{111}	0	405.5	405.5	405.5	0
	25	398.5	399	399	0.12
	50	391	391	392	0.25

4.3 LIQUID HYDROGEN EXPERIMENTS

The LH_2 experiments consisted of four fill and drain cycles and were conducted on the cryogenic test pad at the LMSC Santa Cruz Test Base. An overall view of the test pad (Fig. 4-16) shows the 18-foot diameter vacuum chamber, the vacuum system, the liquid nitrogen storage tank, and the LH_2 dewar.

4.3.1 Description of Test Vessel

A 60-in. diameter spherical tank (Fig. 4-17), designed for Lockheed independent development experiments, was used for the test vessel. The dimensions of this tank were very similar to those of the modified Agena tank that was used for the RP-1 experiments. (See Par. 4.1.) Figure 4-17 shows the relative locations of the RF loop probes and the instrumentation rake. Except for the supports for the three mounting

Fig. 4-16 Cryogenic Test Pad

holes, the tank had no other internal equipment or irregularities. A photograph of
the 60-in. tank, taken as it was being positioned inside of the vacuum chamber, is
shown in Fig. 4-18. Multilayered insulation had been applied to the outside of the
tank prior to enclosing the top access port and the bottom line with molded fiberglass.

4.3.2 RF System

A block diagram of the RF system is shown in Fig. 4-19. The system was the self-
oscillating type and differed from other self-oscillating systems described in this
report by the addition of a remotely controlled, variable phase-shifter. This was
added as an attempt to overcome the problem of sustaining oscillation (Par. 4.1.8).
A wide-band mixer was designed and fabricated to eliminate the requirement to adjust
the reference oscillator whenever the difference frequency exceeded the bandwidth of
the mixer. Because of its losses, the mixer was replaced with a 10 MHz General
Radio design. The reference oscillator was adjusted as necessary during the experi-
ments to keep the RF signal within the bandwidth of the mixer.

4-28

DETAIL A-A
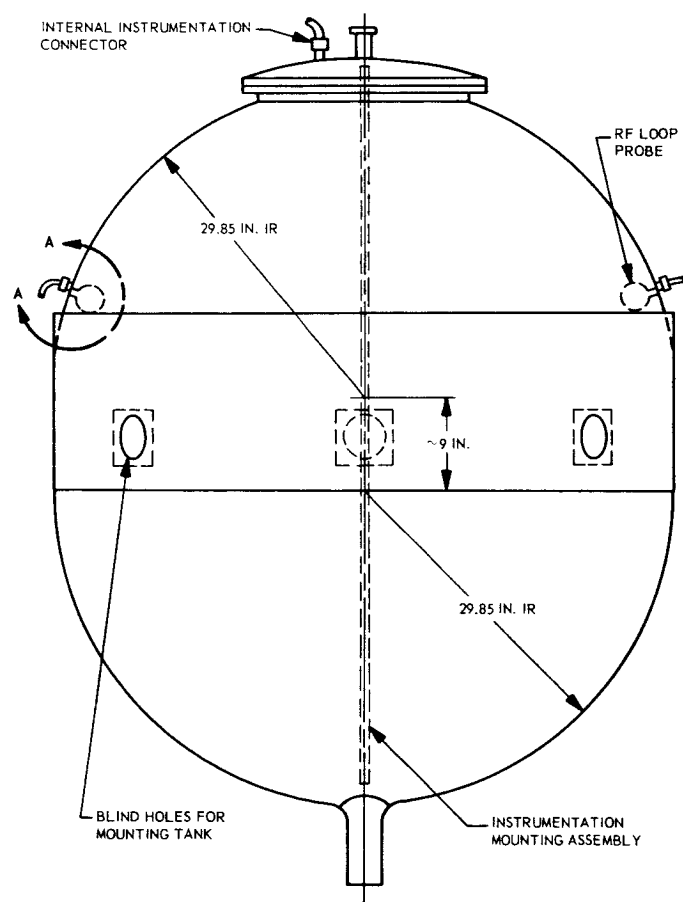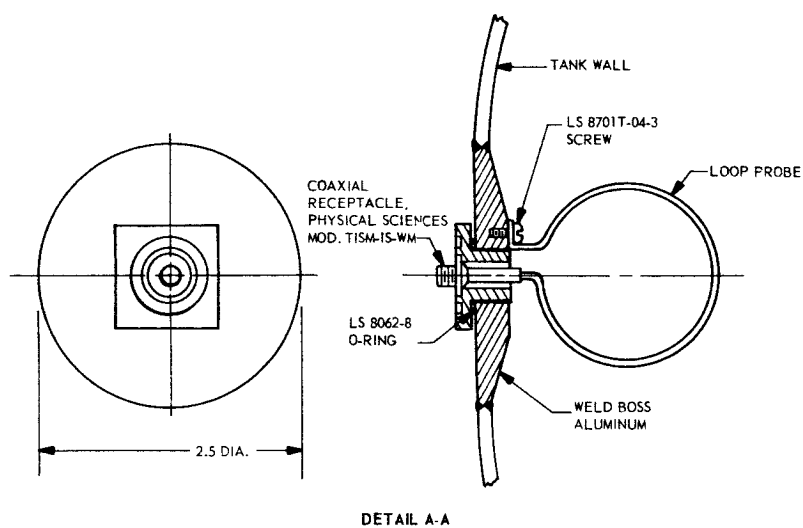
Fig. 4-17 Sixty-Inch Independent Development LH$_2$ Tank

4-29
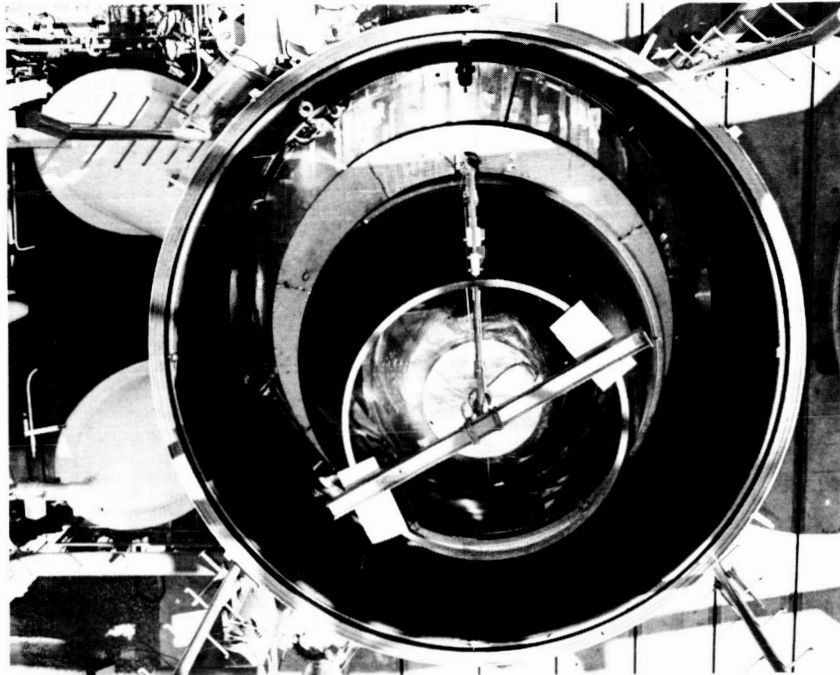
Fig. 4-18 Sixty-Inch Independent Development LH$_2$ Tank Being
Positioned in Vacuum Chamber
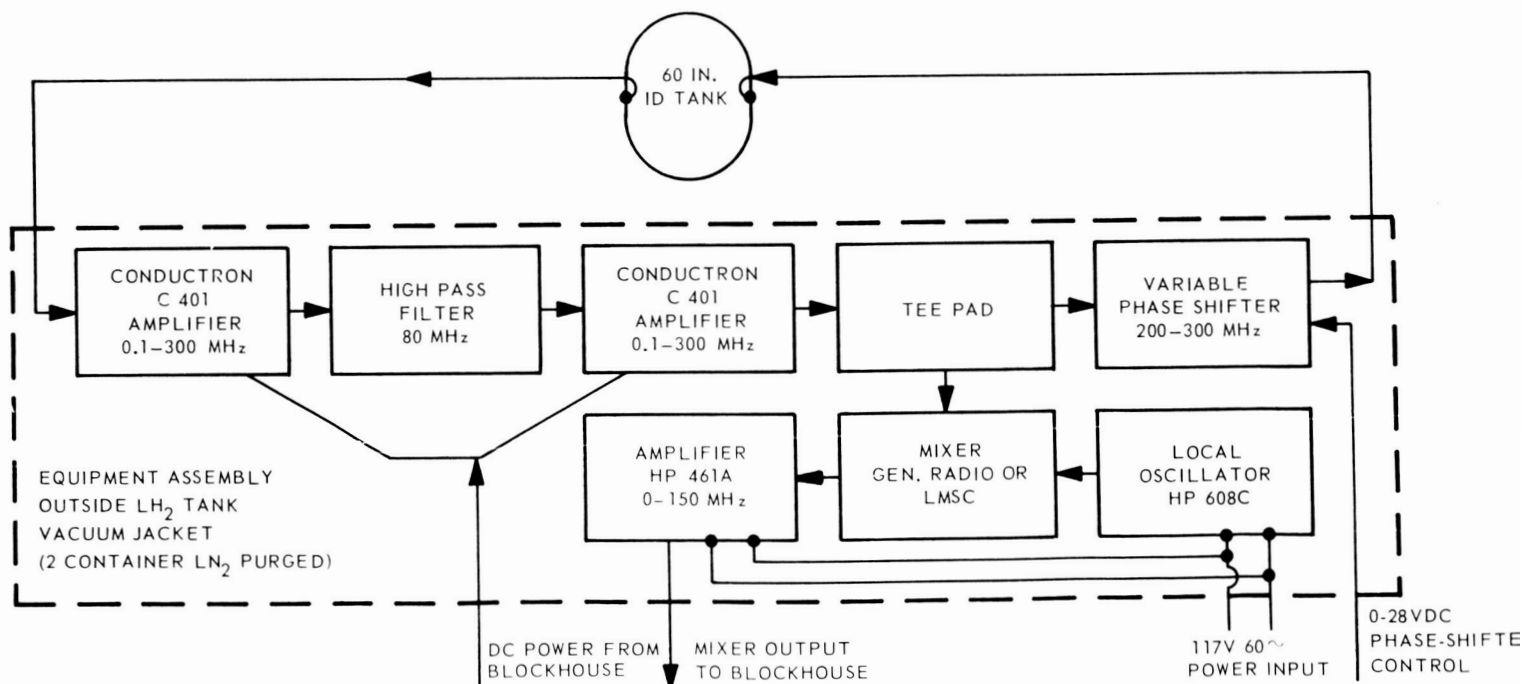
Fig. 4-19 Block Diagram of RF System for LH$_2$ Experiments

4.3.3 Data Acquisition System

A photograph of the blockhouse equipment used for recording the RF signal is presented in Fig. 4-20. This same type of equipment was used for all of the cryogenic testing. The lower panel contained a Veeder-Root mechanical counter that was driven by a 60-Hz synchronous motor. The output was accumulated in a HP 521A counter. The RF frequency was counted on a HP 524B counter, and the outputs of both counters were applied to a HP 560A printer for permanent recording. The measurements from the liquid-level comparing instrumentation were sampled and recorded on a Dymec Data System.

4.3.4 Test Number 1

Although all safety aspects of the entire cyrogenic test pad had been verified, a complete validation test of the LH_2 system had not been attempted prior to the first RF liquid-level sensing system test. Shortly after the 60-in. tank had been chilled and the LH_2 started to flow into the tank, a malfunction of the LH_2 system was detected. The RF system, which provided a good output signal at the start of the filling of the tank, indicated the change in tank dimension as the cold gas caused the tank to shrink. The RF system either jumped modes, or the system became unbalanced because of phase relationship shortly after the LH_2 started to flow into the tank. Because of the malfunction of the LH_2 system, the tank was emptied rapidly, and no measurements of the RF system were possible. It should be pointed out that the TM_{031} mode originally selected for operation was very weak prior to the start of the run, and the system was adjusted to operate in the TM_{021} mode.

4.3.5 Test Number 2

As was the case for test 1, the TM_{031} operating mode with an empty tank frequency of 294 MHz was too weak to use and the 228 MHz frequency was again used. These modes and frequencies were determined by making empty tank mode searches prior to the time that the 60-in. tank was installed in the vacuum chamber.
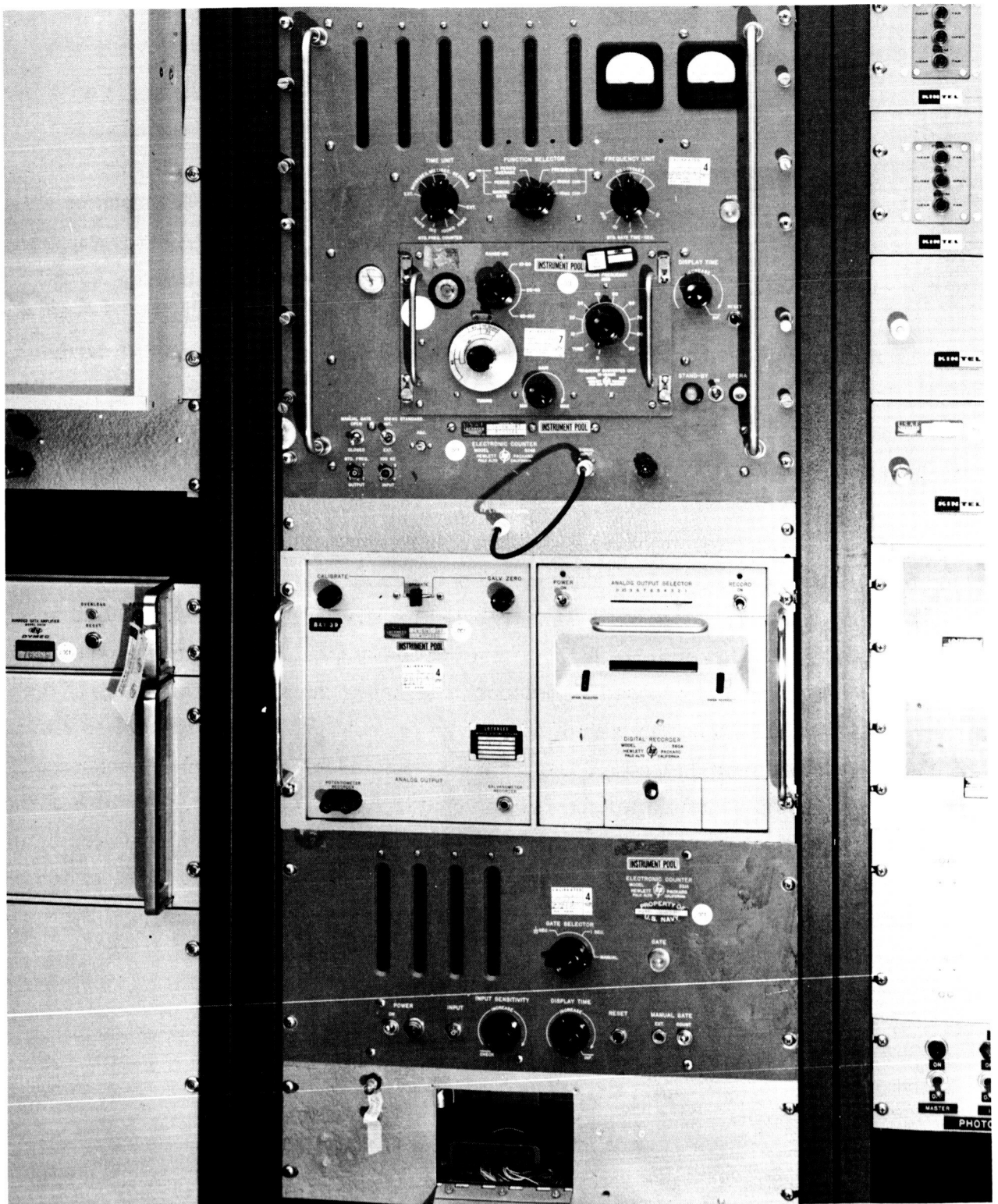
Fig. 4-20 RF Data Acquisition System

The RF system was placed in operation at the start of the chill cycle. Due to the normal chilldown procedure and adjustments to the liquid nitrogen, LH_2, and the vacuum systems, the start of the liquid hydrogen fill did not start until approximately 5 hours after the start of the countdown. The RF signal had been strong throughout this time, and the change in frequency correctly followed the chilling of the tank as well as the increase in tank size as the vacuum system pumped down the chamber.

Just as the LH_2 started to flow into the tank, the RF signal was lost. No indication of a signal could be observed on the oscilloscope. The tank was filled, and an inspection of the area was made to determine that it was safe for personnel to check the RF system on the pad.

The enclosure containing the electronics (Fig. 4-21) was hot to the touch. It was opened, and an inspection of the equipment revealed that the HP 608 signal generator had overheated. After the generator was allowed to cool and a fuse was replaced, the generator was placed in a separate enclosure. One of the other components, the mixer, had been damaged. This was repaired and the system was placed in operation again. The RF signal was stable and provided good amplitude. As the tank was emptied, the frequency of the RF system followed correctly over a very short change of volume and then dropped out. This confirmed an observation made from a review of the results of the first test: A proper phase balance could not be achieved with the existing equipment.

4.3.6 Test Numbers 3 and 4

Prior to the start of test 3, a careful inspection was made of the RF equipment to insure that no other damage had been incurred by the overheating of the reference oscillator. The mixer was tested and found to be faulty and was replaced with a General Radio design that had a limited bandwidth of 10 MHz. A phase shifter had been fabricated and was added to the RF circuit. The design was such that a potentiometer located in the blockhouse could control the correction angle. The design value was for a shift of 240 deg; however, the sensitivity provided a shift of only about 90 deg over a bandwidth of 240 to 300 MHz. The entire coaxial cable system was also inspected,
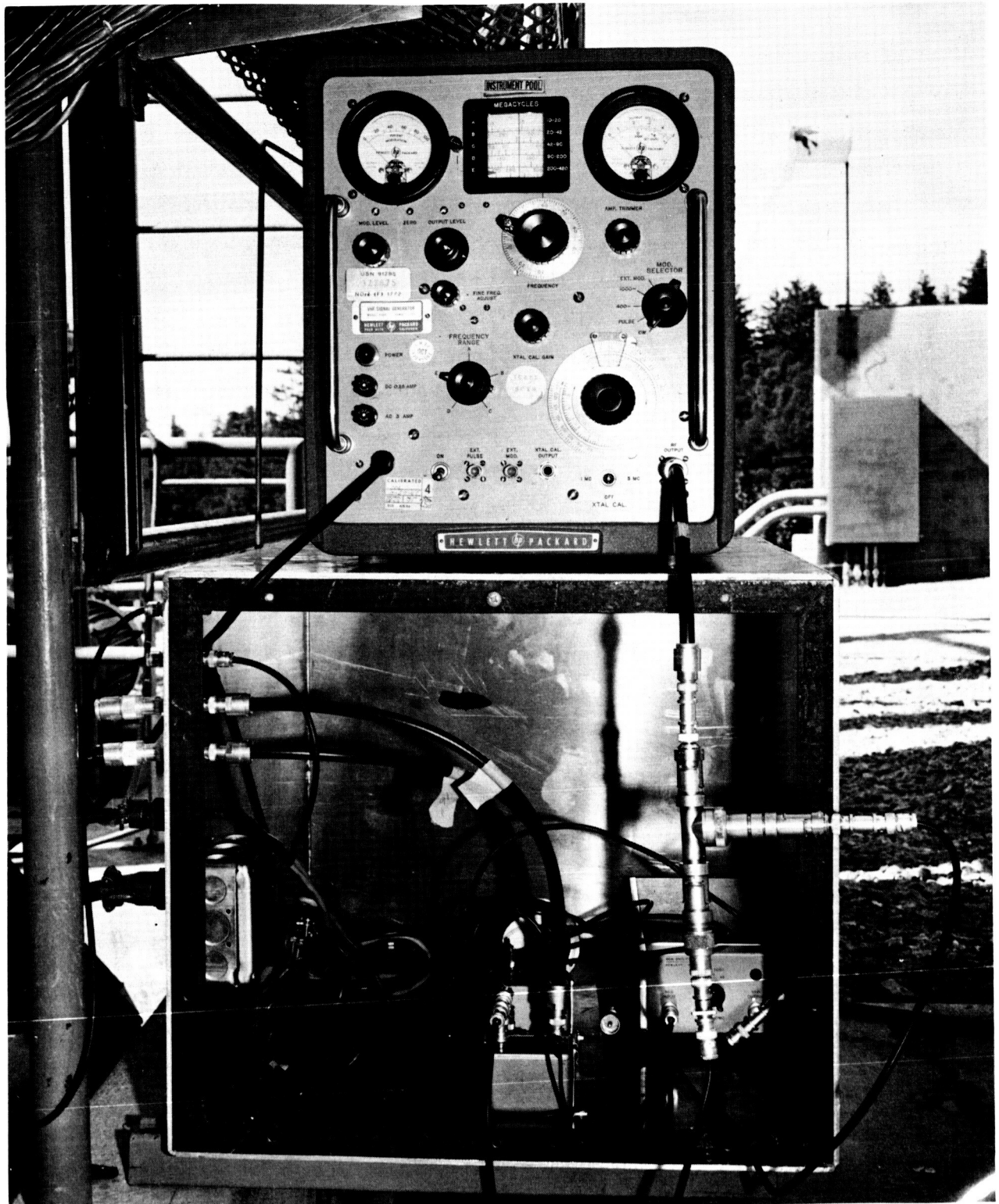
Fig. 4-21 Enclosure for RF System Electronics

4-34

and a few of the connectors were resoldered. A mode search of the tank was completed, and the TM_{031} mode at 294 MHz was strong. The system was adjusted for operation in this mode as originally planned.

The RF system provided a strong signal as the LH_2 fill for test 3 started. As the signal decreased in amplitude, the phase shifter was adjusted. The correction of phase, however, was not sufficient over parts of the frequency range. The fill was rather rapid, and adjustments of cable length to aid the phase correction was not possible. During the drain, cable adjustments were made that materially aided the performance of the system.

Figure 4-22, which is a plot of the resulting resonant frequencies, also shows the results of test 4. The data obtained from the comparing instrumentation were not sufficiently reliable to use for comparison. Thus, the plots are made on an elapsed time basis.

4.3.7 Evaluation of LH_2 Experiments

This series of experiments was scheduled at the earliest possible date based on the availability of the cryogenic test pad. Because of cost and schedule, it was not possible to install dipoles in the top and bottom of the 60-in. tank as was done for the RP-1 experiments. With the change to the dipole configuration for the RF probes, it was demonstrated that the self-oscillating system would perform over the entire range. The results of the LH_2 experiments contributed to the understanding of the limitations of the technique and pointed out areas that required further study and experimentation.
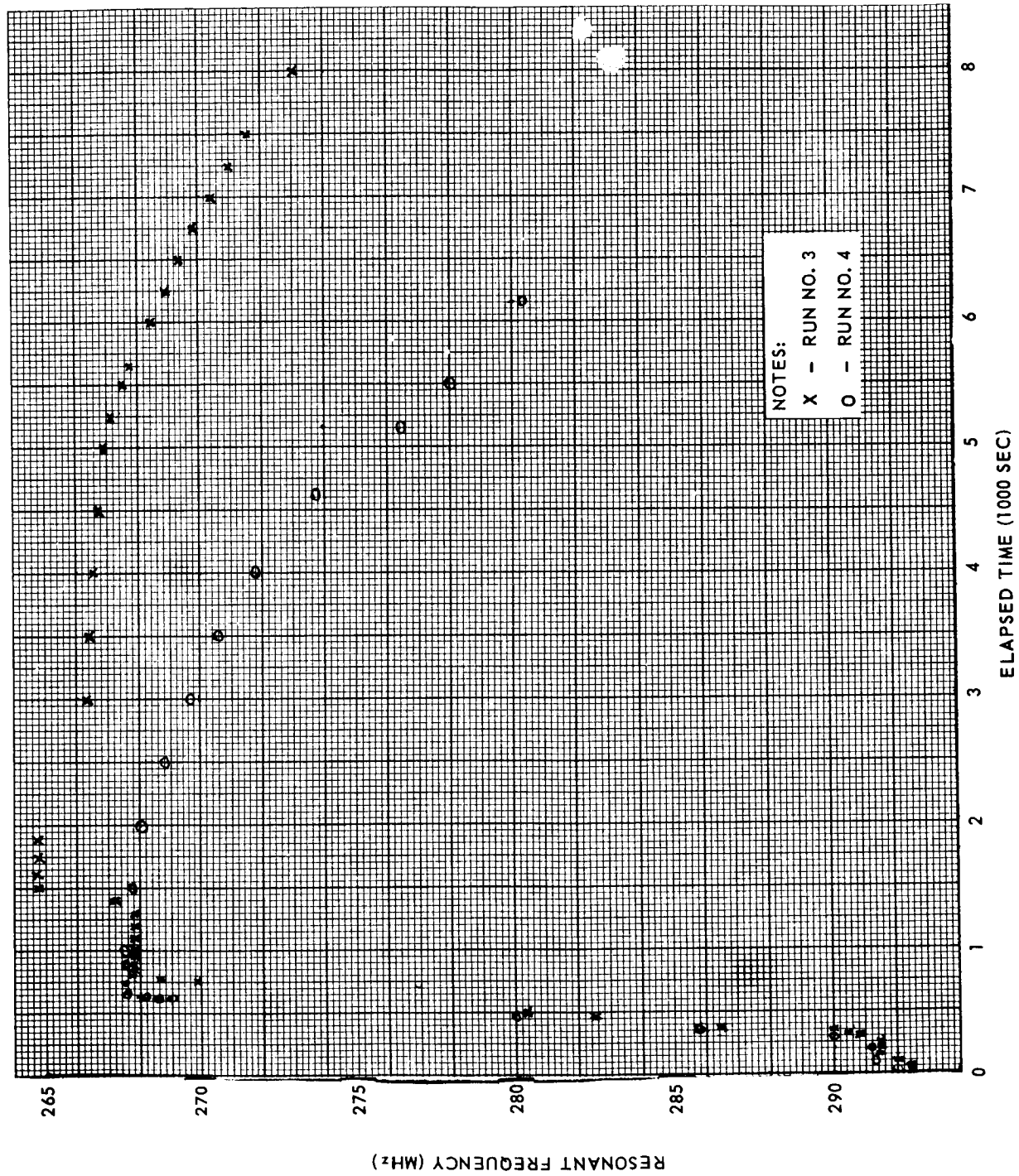
Fig. 4-22 Resonant Frequency Plot for LH$_2$ Runs 3 and 4

LOCKHEED MISSILES & SPACE COMPANY

4.4 LIQUID OXYGEN EXPERIMENTS

The LOX experiments consisted of a series of 20 tests that were conducted at the components testing laboratory of the LMSC Santa Cruz Test Base. The 24-in. diameter tank, previously used for the laboratory investigation, was used for the LOX series. (Illustrations of the tank and sectional views are presented in Figs. 3-8 and 4-23.) The experiments were designed to determine the effects of the paramagnetic property of LOX, of baffles, of fill lines, and of slosh on the performance of the RF liquid-level sensing system.

4.4.1 Supporting Instrumentation

The instrumentation rake is shown in position in Fig. 3-8. Twelve carbon resistors were equally spaced on the rake for discrete level indications. In addition to these, a Bendix optical point sensor was mounted at the 12-in. level of the tank. The test results from this instrumentation were disappointing. The carbon resistors, which had provided good liquid-level indications for the earlier LH_2 experiments, did not provide sufficient response for the LOX; they were replaced by thermocouples between the second and third tests. The response of the thermocouples was such that the determination of liquid level could not be made. A signal, indicating that the optical point sensor was covered, was recorded; however, the sensor behaved as though LOX were splashing over it throughout the remainder of the test. Even though the sensitivity was adjusted at the start of each test, no improvement in performance was achieved.

A differential pressure transducer (Fig. 4-23), installed between test runs 4 and 5, was selected because this type of transducer automatically compensated for the internal tank pressure changes that were caused by external heating and venting. This transducer essentially weighed the LOX and served as the reference for the remainder of the experiments. Approximately 0.9 psi was obtained for a full tank of LOX, and this pressure indication corresponded to a chart reading of 7.5. Good correlation was obtained during an individual test, and chart readings between 1.0 and 6.0 were quite consistent. Below a chart reading of 1.0, little resonant frequency
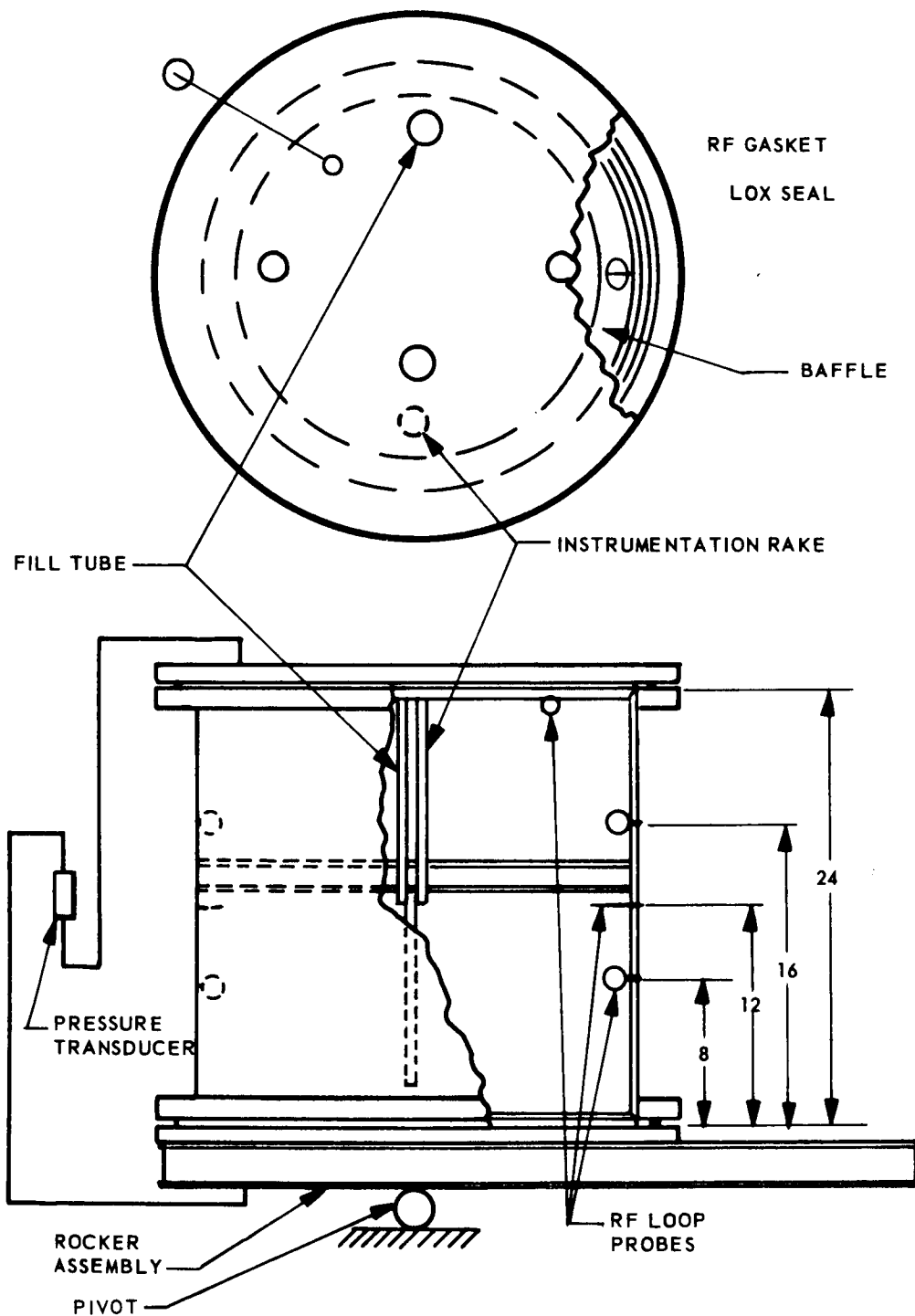
Fig. 4-23 Twenty-Four Inch Cryogenic Tank, RF Cable and Probe Configuration

4-38

change of the RF sensing system was noted, which indicated that readings between 0.0 and 1.0 essentially represented an empty tank condition. The discrepancies at the low end of the scale were attributed to the liquid or gas condition in the lead lines between the tank and the transducer. To a large degree, the condition was a result of the length of time for a test and the resulting frost buildup coupled with the venting condition during the time of recording. The blockhouse instrumentation was identical to that shown in Fig. 4-20 for the LH_2 experiments, except for the addition of a Brown recorder for the differential pressure measurement.

4.4.2 RF Liquid-Level System

Two types of RF investigations were made. First, a general survey was made of the modes within the tank to determine the preferred operating frequency and to search for potential problem areas; the survey was followed by the selection of an operating mode. Then, a self-oscillating system was set up by adjusting the reference oscillator and selecting cable lengths. A block diagram of the basic system is shown in Fig. 4-24.

Prior to the actual experimentation, a calculation was made so that the operating frequencies of the components could be estimated. A list of the calculated frequencies corresponding to the most probable operating modes is presented in Table 4-9.

In an RF system such as the one shown in Fig. 4-24, oscillation can and usually does occur simultaneously on a number of frequencies. The number of frequencies are limited by the bandwidth of the amplifier. Even with steps taken to suppress unwanted modes, the tank will have a number of responses at any fill level. Oscillation will occur at each frequency at which phase relationships are correct and losses are low. At any given fill level, the mode having the least loss will increase in ampltitude until it limits the amplifier, thus regulating at a level all of the other oscillatory responses. If two modes are close in frequency, they may cause a spurious response from the mixer. The only major problem, however, with multiple oscillation is that an unwanted mode may, at some fill levels, become so strong that the amplifier gain is forced below that necessary to maintain oscillation at a selected frequency. Once a suitable mode
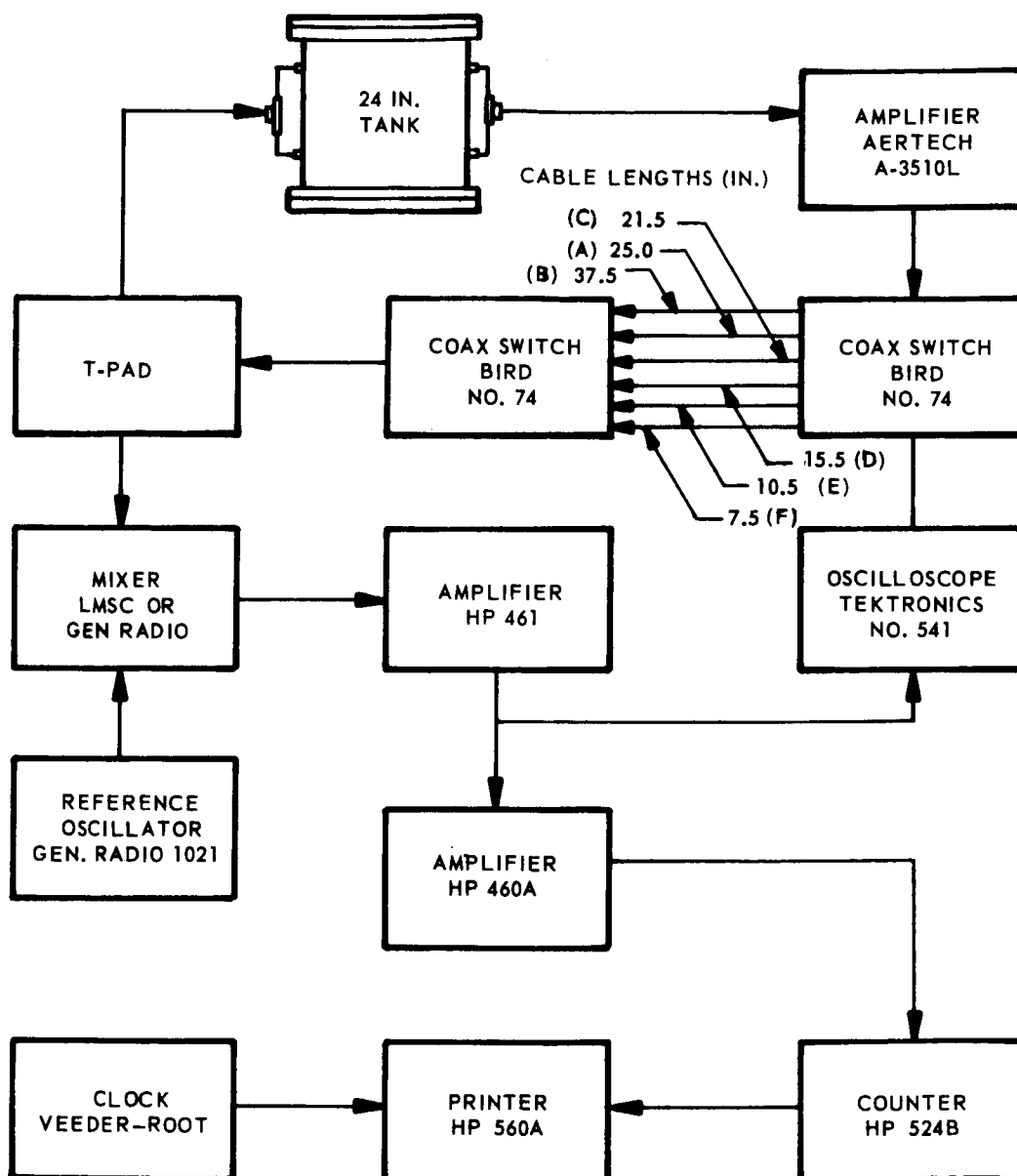
Fig. 4-24 RF System for LOX Experiments

4-40

Table 4-9

CALCULATED RF RESONANT FREQUENCIES FOR
LOX IN 24-IN. CRYOGENIC TANK

Mode	TM		TE	
	Empty	Full	Empty	Full
010	378	308	–	–
011	449	366	649	529
012	613	500	770	628
013	815	665	940	767
014	1004	819	1140	930
110	601	490	–	–
111	649	529	376	306
112	770	628	562	458
113	940	767	779	635
114	1140	930	1010	823
210	805	656	–	–
211	840	685	537	438
212	961	784	680	555
213	1083	884	865	705
214	1260	1028	1080	880
310			–	–
311			700	571
312			816	665
313			978	797
314			1170	954

Note: Calculations are based on equations of Appendix A, using
1.505 for the dielectric constant of LOX and the tank
dimensions of 24-in. diameter by 24-in. high.

has been selected, the unwanted modes may be eliminated by use of a bandpass filter. An unwanted mode or response near the frequency of the selected operating mode can usually be suppressed by modifications of the probe configuration or orientation.

Treatments such as those noted above were employed throughout the experiments. The reference oscillator was usually set approximately 9 MHz higher than the resonant frequency of the selected mode when that tank was filled with LOX. During a drain cycle, the LOX was dumped in increments of approximately 15 percent, and the reference oscillator was reset after the difference frequency had passed through zero and shifted to approximately 9 MHz higher. The reason for this was to maintain the frequency within the 10 MHz bandwidth of the General Radio mixer.

An illustration of a TE_{311} field configuration with optimum placement of probes is shown in Fig. 4-25. A fill line or capacitive probe positioned in a weak field position would not significantly degrade the performance of the RF system.

4.4.3 Test Conditions

Table 4-10 presents the schedule of the experiments and indicates the probe locations, the internal tank configuration, and the type of test. The first four tests were useful to the extent that both the LOX system and the RF system were evaluated, and corrections were made for control, recording, and performance. It was determined that the loop probes mounted in the top of the tank would not provide the desired excitation. The application of aluminum foil between the upper and lower ends and the cylindrical section of the tank for providing a continuous electrical path was marginal; thus, the foil was replaced with copper tubing. The placement of the foil may be seen in Fig. 3-8.

Instrumentation for level comparison was discussed in a previous paragraph. Two different length of fill lines were used for determining their effects on the RF system. A section of the baffle shown in Fig. 3-5 was installed for two tests.
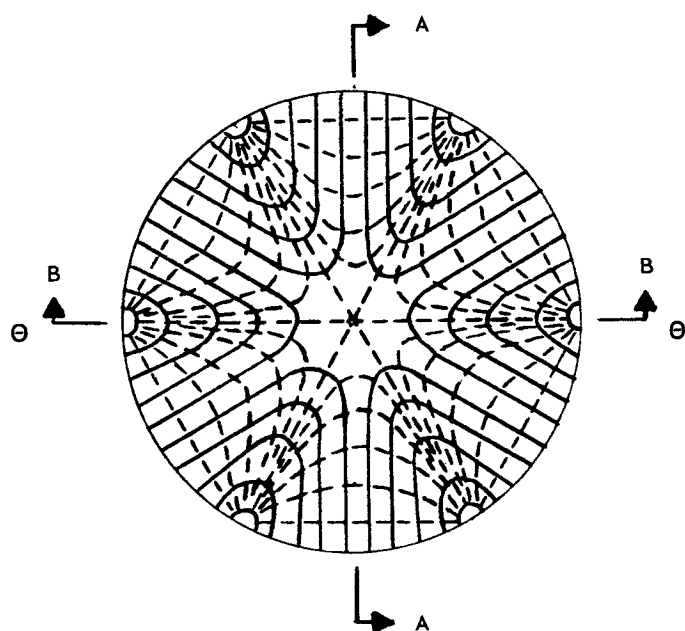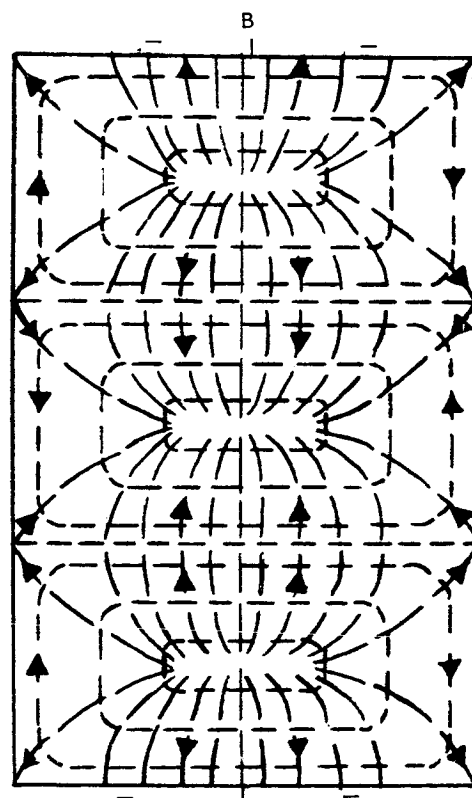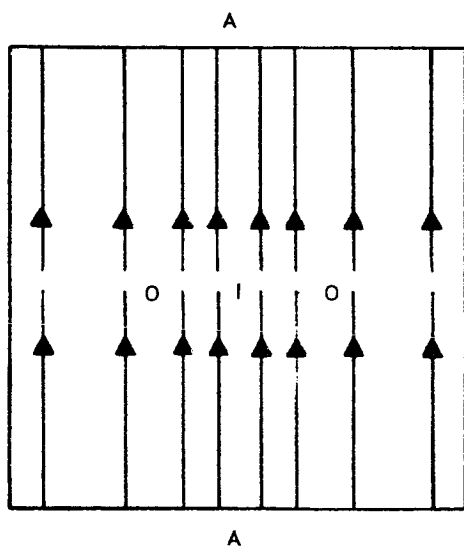
ALONG SURFACE
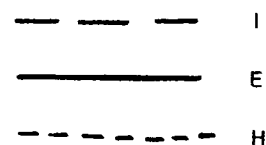
Fig. 4-25 TM$_{311}$ Mode Field Configuration, Right Cylinder

4-43

Table 4-10

LOX EXPERIMENTS

Test No.	Date	Probes No.	Probes Position	Internal Fill Tube (% of Tank Length)	Instr Rake	Baffle	Type of Test
1	10/27	2	Top	—	Yes	No	Equipment verification
2	10/27	2	Top	—	Yes	No	Instrument test
3	11/8	2	Top	—	Yes	No	Instrument test
4	11/8	2	Top	—	Yes	No	Instrument test
5	11/24	4	Sides	50	Yes	No	Mode exploration
6	11/24	4	Sides	50	Yes	No	RF system checkout
7	11/24	4	Sides	50	Yes	No	Self-oscillating system
8	12/3	4	Sides	100	Yes	No	Mode exploration
9	12/3	4	Sides	100	Yes	No	Self-oscillating system
10	12/7	4	Sides	—	Yes	No	Mode exploration
11	12/7	4	Sides	—	Yes	No	Cable length determination
12	12/7	4	Sides	—	Yes	No	Self-oscillating system
13	12/8	4	Sides	—	No	No	Mode exploration
14	12/8	4	Sides	—	No	No	Cable length determination
15	12/8	4	Sides	—	No	No	Self-oscillating system
16	12/10	4	Sides	—	No	Yes	Mode exploration
17	12/10	4	Sides	—	No	Yes	Cable length determination
18	12/14	4	Sides	—	No	No	Self-oscillating system
19	12/14	4	Sides	—	No	No	Slosh test
20	12/14	4	Sides	—	No	No	Paramagnetic effect

To be certain that a major influence of the paramagnetic property of LOX on the performance of the RF system be clearly shown, it was decided to make one test with liquid nitrogen. The dielectric constants of the two are very close to each other, and if parallel operation could be demonstrated, it could be positively stated that the magnetic property of LOX is not a significant consideration.

4.4.4 Mode Response Determination

Figures 4-26 through 4-30 show the mode plots for the various internal configurations of the 24-in. cryogenic tank. The mode plots were made from the measurements of the resonant frequencies obtained by exciting the tank with the output of a 150 to 950 MHz signal generator and detecting the resonant points. Although the complete range of the generator was used, only the range from 360 to 940 MHz indicated any usable data. The signal generator was connected to one probe (or a pair of probes), and the RF incident signal amplitude was detected on the opposite probe (or pair of probes).

The response with a fill line 50 percent of tank length and an instrument rake is shown in Fig. 4-26. (See Fig. 4-23 for an illustration of the tank and RF system circuit.) The RF coupling into the tank was arranged to accentuate the TM_{110} mode and to suppress as many other modes as possible. An additional pair of loops was located 180 deg apart at the midpoint of the tank, and the loops were oriented horizontally. This additional pair of loops was shorted to the tank wall to successfully suppress the even-order TE modes, e.g., TE_{nm2}, etc.

In Fig. 4-27, the conditions were the same as described above except that the fill line extended the full length of the tank and was grounded at both the top and bottom. In both cases, the responses of resonant frequency versus liquid volume were generally the same, with fairly strong TM_{110}, TE_{311}, and TE_{213} modes and a weak TE_{312} mode. A few other scattered responses were also detected.
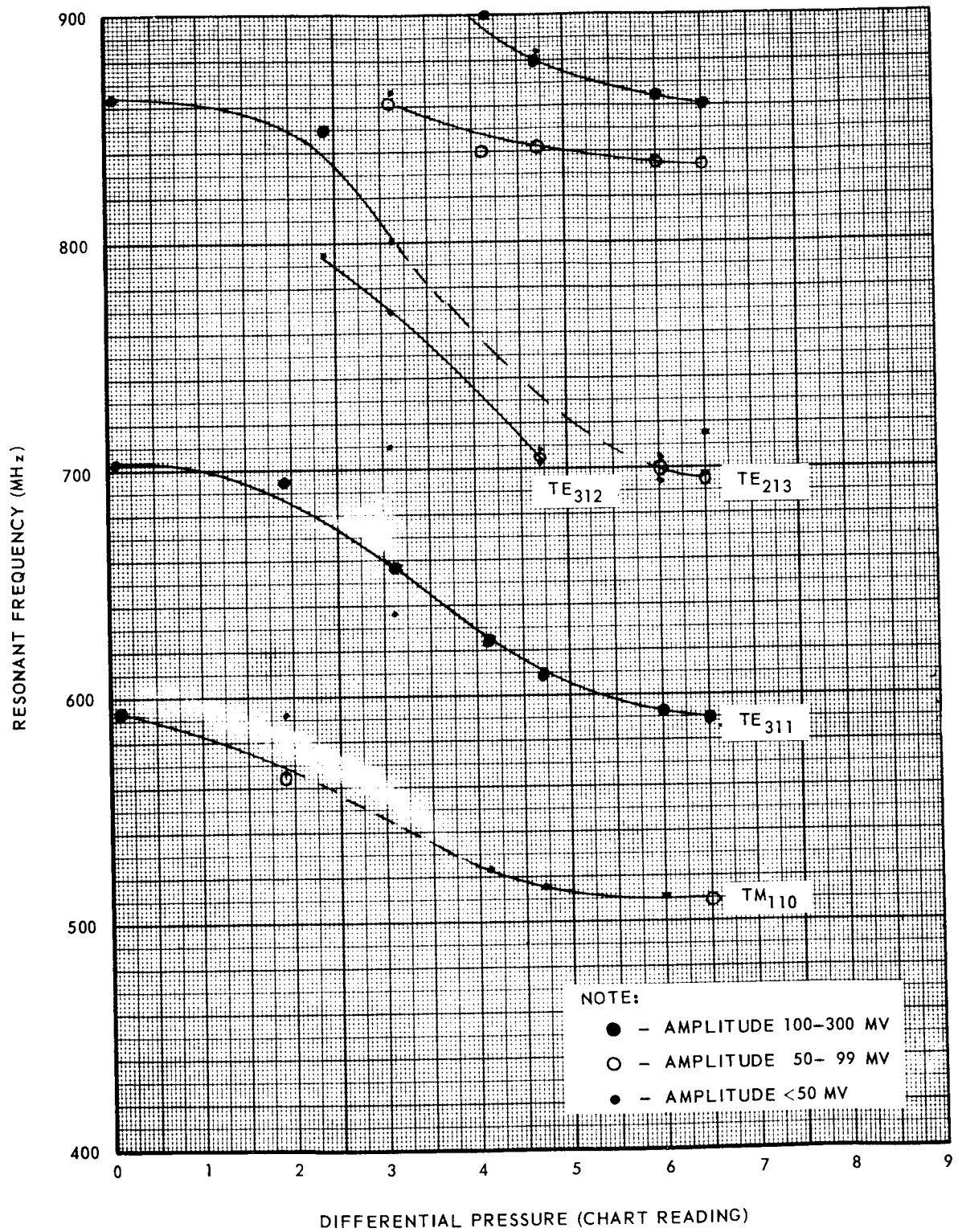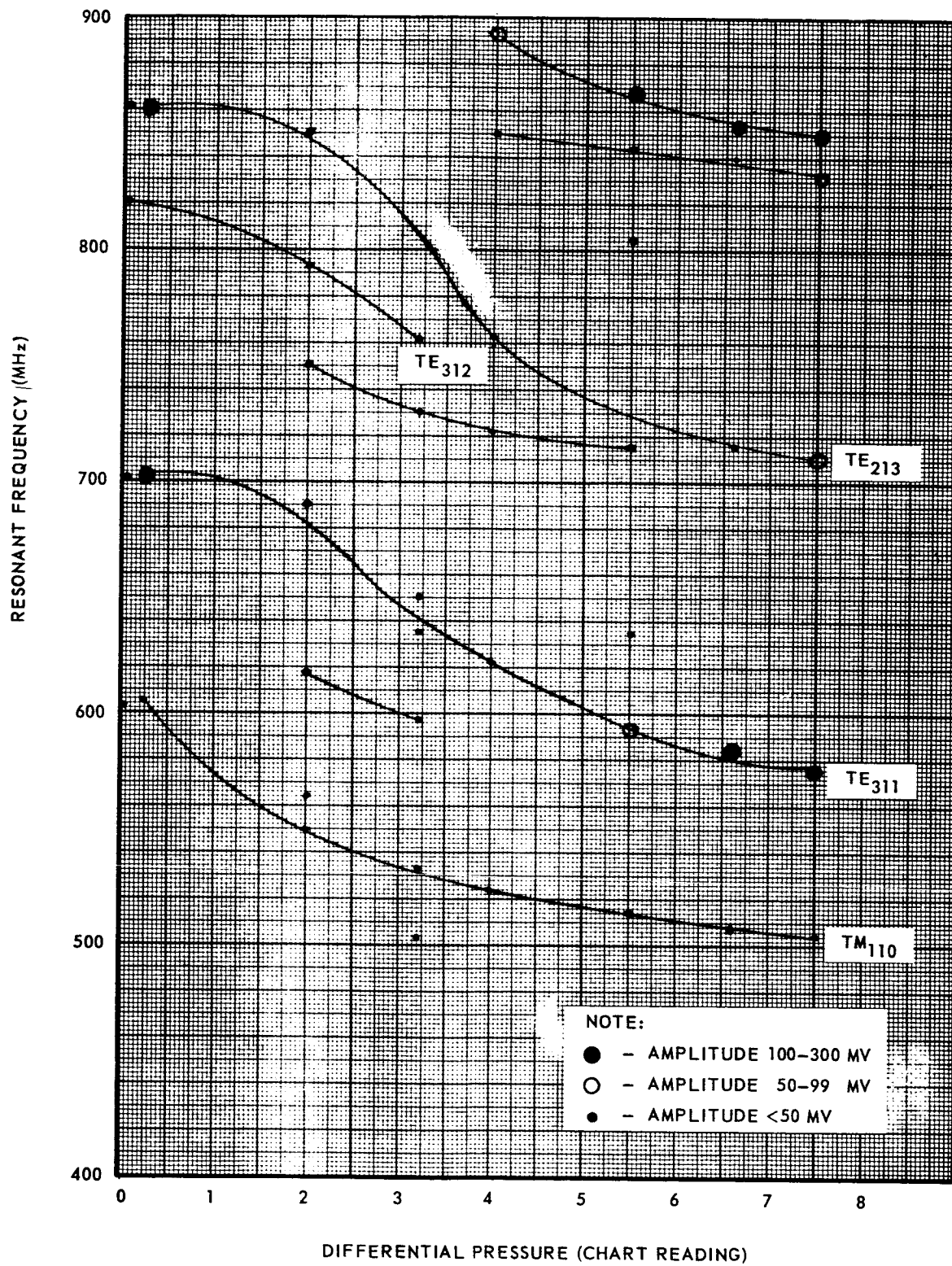
Fig. 4-26 Mode Plot, LOX Run 5

LOCKHEED MISSILES & SPACE COMPANY
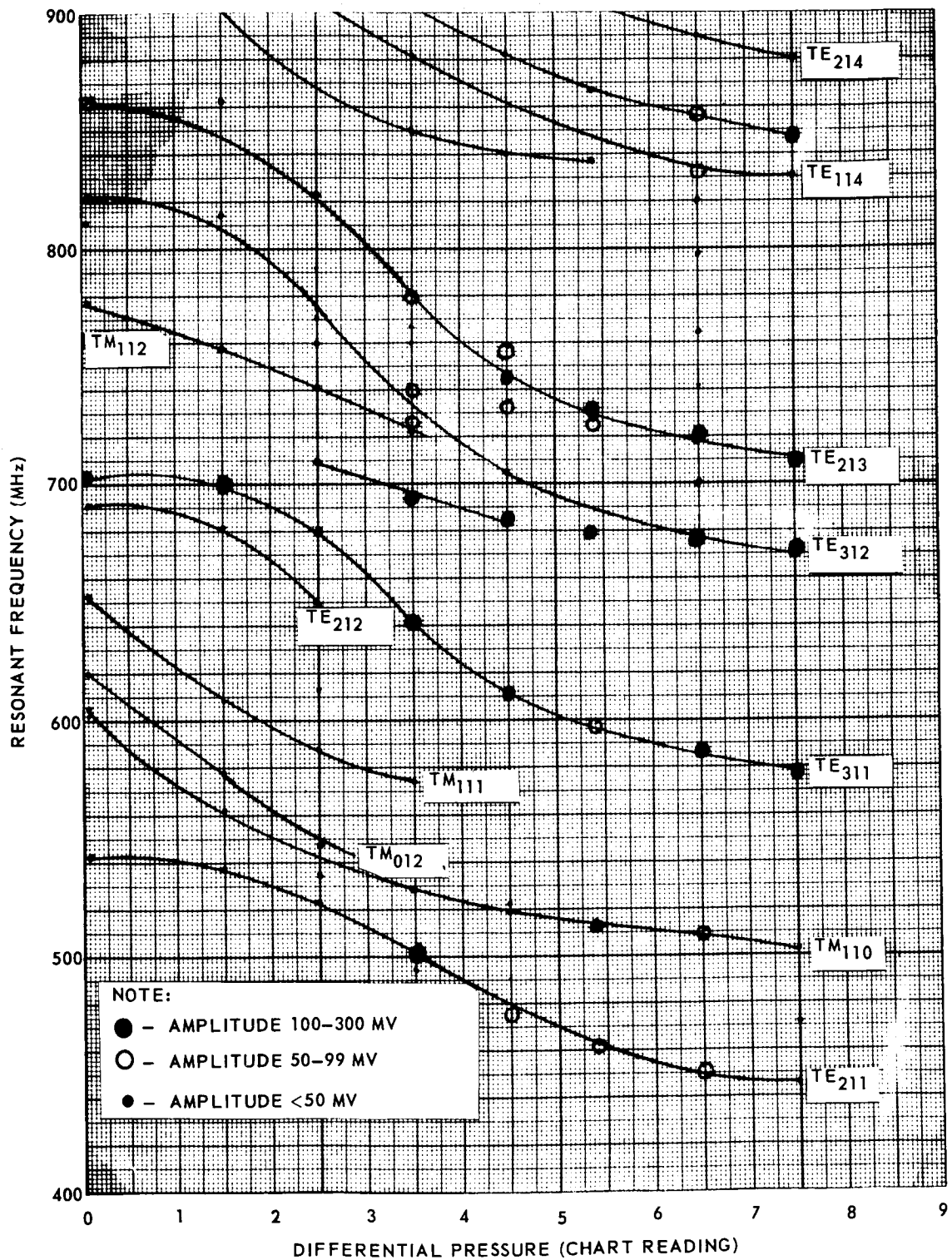
Fig. 4-27 Mode Plot, LOX Run 8

4-47

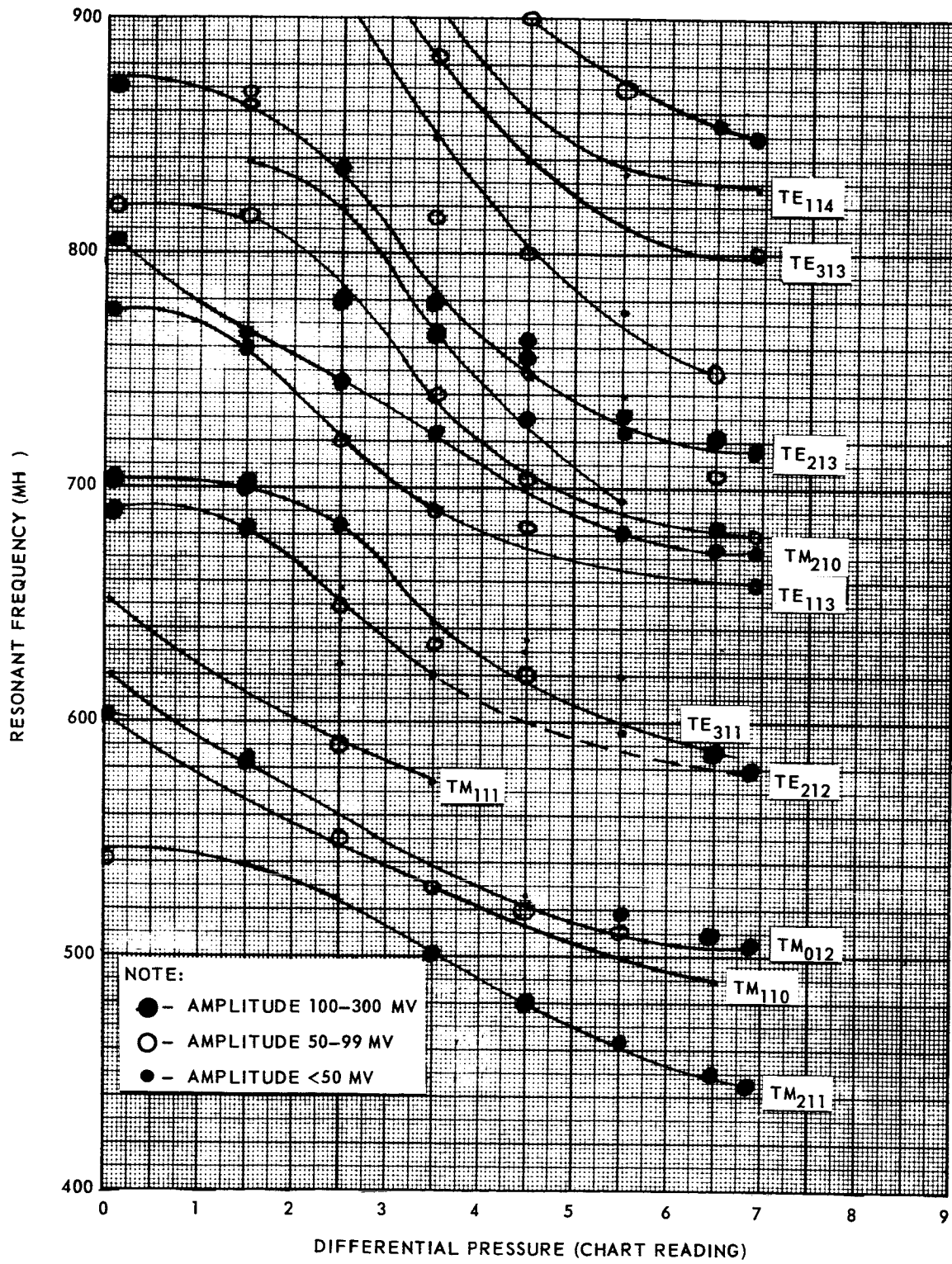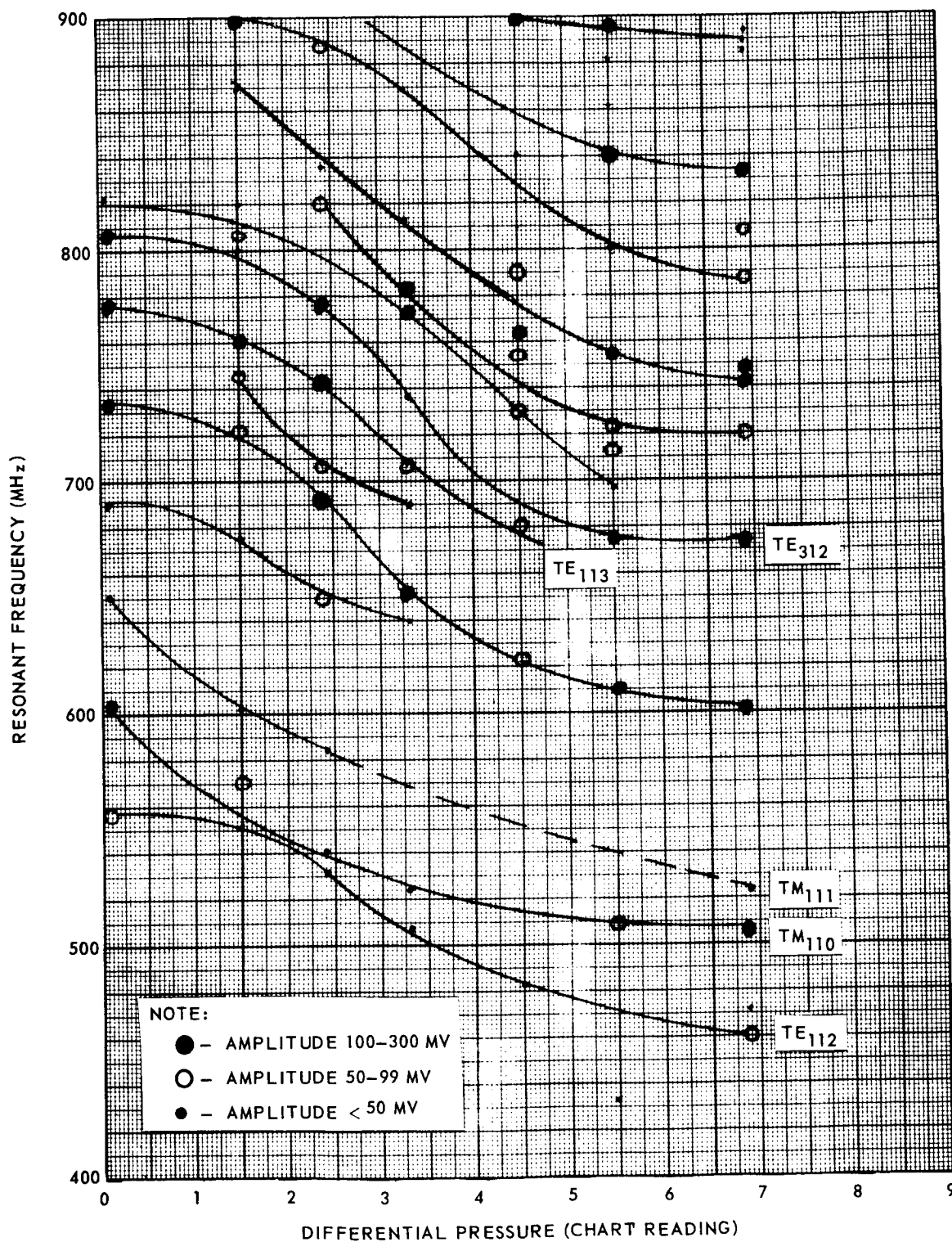Fig. 4-28 Mode Plot, LOX Run 10

Fig. 4-29 Mode Plot, LOX Run 13

4-49

Fig. 4-30 Mode Plot, LOX Run 16

LOCKHEED MISSILES & SPACE COMPANY

The results of tests 10 and 13 are shown in Figs. 4-28 and 4-29. The fill line was completely removed for these tests. The removal resulted in the appearance of modes that had been suppressed. The aluminum foil RF gasket had been replaced with a copper tube to overcome a high-resistance junction between the tank covers and the cylindrical section. The result of these two changes was the appearance of the TE_{211}, TE_{212}, TE_{113}, TE_{114}, TE_{214}, TM_{012}, TM_{111}, TM_{112}, and TM_{210} modes along with others not identified. In particular the TM_{012} mode was close to the TM_{110} mode and could easily be confused with it. Thus the desired objective of accentuation of the TM_{110} mode was not achieved.

It may be noted that the mode response shown in Fig. 4-29 is similar to those shown in Fig. 4-28 except that the amplitudes were substantially increased. This resulted from the removal of the instrument rake, which had absorbed energy from some of the modes. All of the later self-oscillating LOX experiments (15, 18, and 19) were made with the tank conforming to the mode plot shown in Fig. 4-29. The TE_{211} mode was used for the basis of the self-oscillating system.

4.4.5 Test Runs 5, 6, 7, 8, and 9

In the series of runs made on 24 November 1965, a mode plot was made first. The results were disappointing in that the TM_{110} mode responses were weak. Two UHF amplifiers had been connected in cascade; however, the system provided sufficient gain to sustain oscillation at only a few discrete frequencies. It is believed that the high, 300-ohm impedance and the lack of proper shielding resulted in self-oscillation around the amplifiers themselves.

In run 6, an attempt was made to follow the TE_{311} mode that appeared to be strong in the mode plot of run 5. The self-oscillating system was set up, and the tank was filled with LOX. Between full and about 60 percent volume, the frequency varied from 600 to 654 MHz, then settled at 648 MHz where it remained for the duration of the draining of the tank. The cause of the poor system performance was attributed to independent oscillation in the amplifier.

4-51

In run 7, an attempt was made to follow the TE_{213} mode. Again amplifier self-oscillation at 743 MHz took control and was unaffected by tank characteristics. When the tank was emptied, a strong signal was noted at the TM_{110} response at 600 MHz, but this mode died quickly as a function of fill and could not be detected with LOX in the tank.

An Aertech Model A-3510L amplifier, which had a gain of 20 db, replaced the UHF amplifiers for runs 8 and 9. The output level was flat within ±1 db between 500 and 1000 MHz and operated in a stable fashion at various cable distances from the output terminal, even with a short. The output power level was +1 dbm at 500 MHz and decreased to -0.9 dbm at 1000 MHz. An attempt was made to accentuate the TM_{110} mode, which had been weak in previous runs. The fill line was extended to the full tank length.

It may be noted in the mode plot of run 8 (Fig. 4-27) that there is a difference in amplitude between "cold-empty," that is, a cold tank before the LOX fill was started, and the later condition of "empty" at the end of run 8. It was believed that the trouble occurred from an open circuit in the Subminax cable harness. This same problem occurred throughout all LOX runs despite frequent cable replacements. The plot also shows that the TE_{213} and TE_{311} modes were strong and the TM_{110} mode was weak.

The results of LOX run 9, which was a self-oscillating test, are shown in Fig. 4-31. There was little correlation with the mode plot from run 8 (Fig. 4-27). The TE_{213} mode provided the best response, and the TE_{311} mode, the next best. Neither mode operated with the tank full. In the range between 500 and 630 MHz, a number of responses appeared that did not correlate with the mode plot. Although the Subminax cables were responsible for the lack of correlation between runs 8 and 9, the primary problem with the RF response of run 9 was attributed to the internal configuration of the tank.
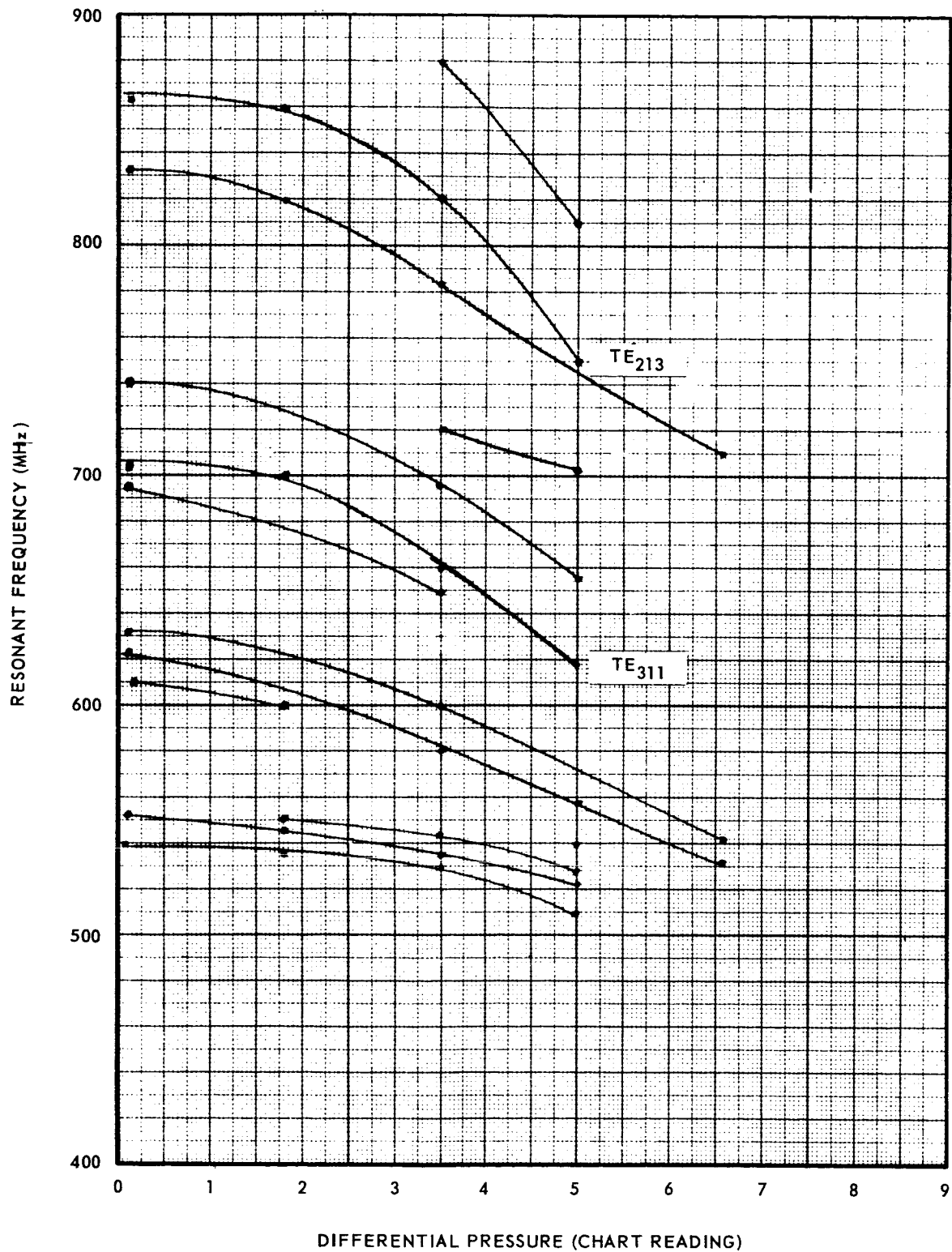
Fig. 4-31 Resonant Frequency Difference Vs. Differential Pressure,
LOX Run 9

4-53

4.4.6 Test Runs 10, 11, and 12

An effort was made to improve the response of the TM_{110} mode. After run 9, the tank was disassembled, and a 1/4 in. diameter, soft copper tube was added to replace the aluminum foil in an attempt to improve the RF gasket. (See Fig. 3-8.) By comparing the mode plot of Fig. 4-28 with that shown in Fig. 4-27, it may be seen that a host of new modes appeared. Some of these were due to better circulation of currents at the end junctions, while others were due to the removal of the full-length fill line. The amplitude of the TM_{110} mode was slightly improved by these modifications.

The TE_{211} mode appeared to be promising; however, when the self-oscillating system was energized, the TE_{311} mode was the only one that would sustain oscillation. In run 11, a self-oscillating system was set up in accordance with the block diagram of Fig. 4-24. A fill was made, and the oscillating frequency of the system was checked near the expected values for the TE_{211} and TE_{311} modes. The coax cables were switched manually, and all switch positions resulting in oscillation were recorded at each level of fill. (See Table 4-11.)

Table 4-11

CABLE LENGTH SELECTION*

Differential Pressure	7.2	6.5	5.5	4.5	3.5	2.4	1.4	0.0
Frequency Cable	581 ABCE	587 ABCF	598 E**	611 B**	640 A	681 A	701 CE	701 CE
Frequency Cable					643 C	685 CE		
Frequency Cable	715 CE	720 EF	724 C	743 B				
Frequency Cable			725 E	737 F				
Frequency Cable			726 F					

*Cable lengths are presented in Fig. 4-24.
**Denotes weak response.

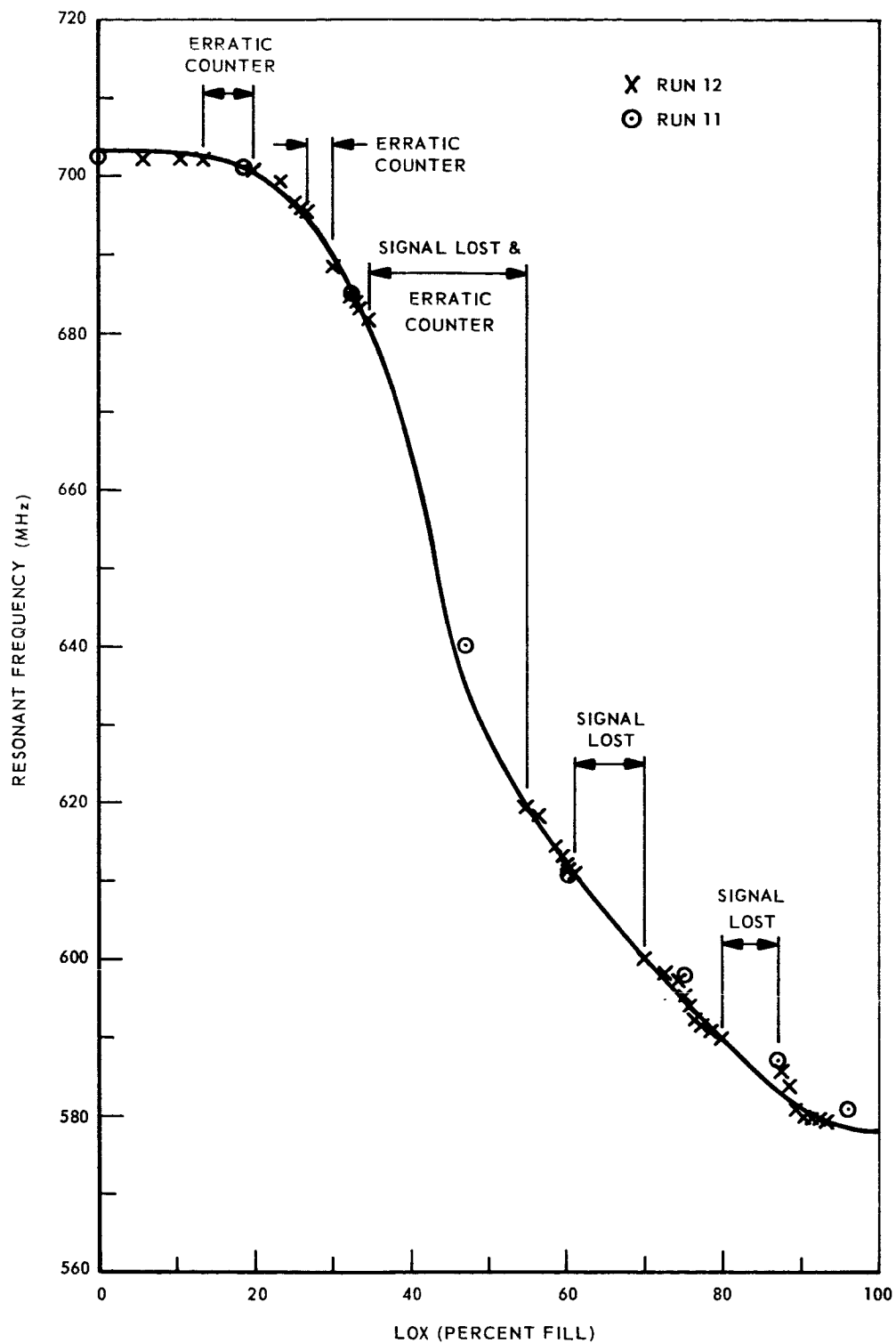Fig. 4-32 Resonant Frequency Difference Vs. Volume, LOX Run 12

For run 12, the cables were switched in accordance with the above table to obtain optimum oscillator phase relationship. Except for three points, the self-oscillating system performed continuously. Figure 4-32, which is plot of test results, shows points where self-oscillation was continuous but not recorded due to a printer malfunction caused by the time counter overloading the printer.

4.4.7 Test Runs 13, 14, and 15

These runs differed from runs 10, 11, and 12 only in that the instrument rake had been removed. The effect of this removal resulted in increased amplitudes for most all modes. In the frequency range between 700 and 800 MHz, several new strong responses appeared. Only three TM modes were identifiable, and of these only the TM_{210} mode was strong. As had been the case throughout this test series, the TE_{311} and TE_{211} modes were the most promising. Each, however, showed multiple responses within 2 or 3 MHz of one another over at least 30 percent of the tank volume, which indicated a tendency to jump modes. The TE_{211} mode and coax cable lengths corresponding to the volume of LOX were selected from the results of run 14.

Run 15 was conducted with the RF self-oscillating system. The results of the experiment are shown in Fig. 4-33. As noted in previous discussions, the bandwidth of the mixer was limited, so it was necessary to reset the reference frequency oscillator periodically during a test. Some of the error that may be observed in the plot of the data was due to the inability to monitor the exact reference frequency. At the differential pressure chart reading of 0.6 to 1.2 and at 6.8, it is believed that mode jumping occurred.

4.4.8 Test Runs 16 and 17

Runs 16 and 17 were made with a slosh baffle inserted in the tank. A section of the slosh baffle (Fig. 3-5) was used. Because of the side wall probe locations, it was not possible to insert the original baffle. A section consisting of two rings was cut from the baffle and located so that the baffle was resting on the center probes. Although good contact was made with the side wall at the warm tank condition, the reduced size did **not** offer as good electrical bond as desired.
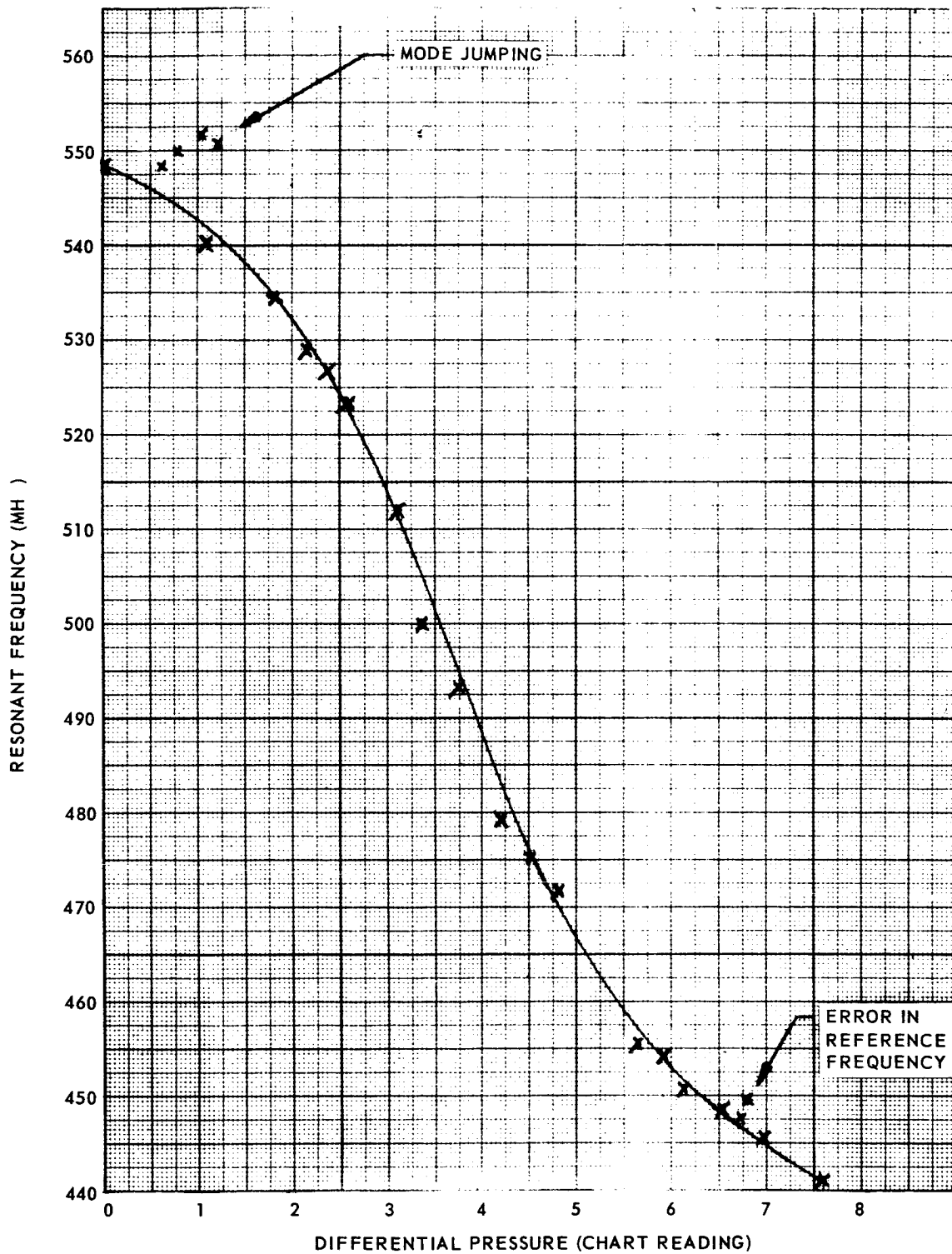
Fig. 4-33 Resonant Frequency Difference Vs. Differential Pressure,
LOX Run 15

The effect of the baffle was to divide the tank into three sections as shown in Fig. 4-34.

SIMPLIFIED RADIO FREQUENCY
MODEL OF TANK

ACTUAL PHYSICAL TANK
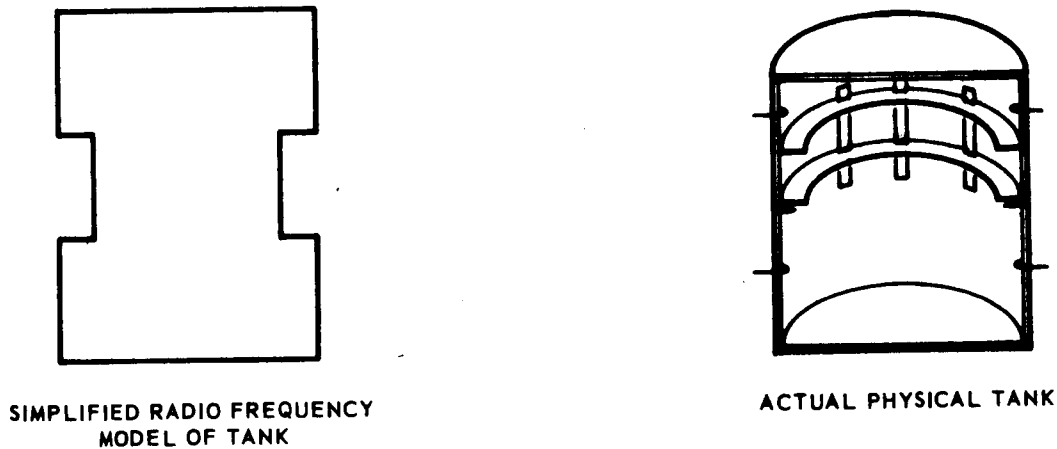
Fig. 4-34 Effect of Baffle

Note that some of the modes observed in run 16 (Fig. 4-30) appeared at the same frequencies, e.g. TM_{111} and TM_{110}. All responses decreased in amplitude. Several new responses also appeared that presumably, were generated in the three, short, non-closed cylindrical sections. A cable exploratory run (run 17) was made to determine whether or not self-oscillation could be maintained over a fill and drain cycle. A considerable amount of erratic behavior was observed. Part of the erratic behavior was believed to have been caused by intermittent contact of the baffle with the wall. A self-oscillating run was not attempted as it was felt that no useful information would have resulted. Relocation of the probes to the top and bottom of the tank and an improved ground between the baffle and the tank wall would have been beneficial.

4.4.9 Test Runs 18, 19, and 20

The baffle was removed and the tank restored to the same internal configuration as that used for runs 13, 14, and 15. The self-oscillating system was used for exciting the tank for all three runs. Run 18 was a duplication of run 15; an experiment to determine the effects of slosh was conducted during run 19. For both of these tests, the cable selection to maintain phase over the frequency range was based on the results of run 14. Test 20 was again a self-oscillating system run. Liquid nitrogen was used in run 20 in order that a direct comparison of the paramagnetic property could be obtained.

Fig. 4-35 LOX Run 18

Fig. 4-36 RF System Stability, LOX Run 18
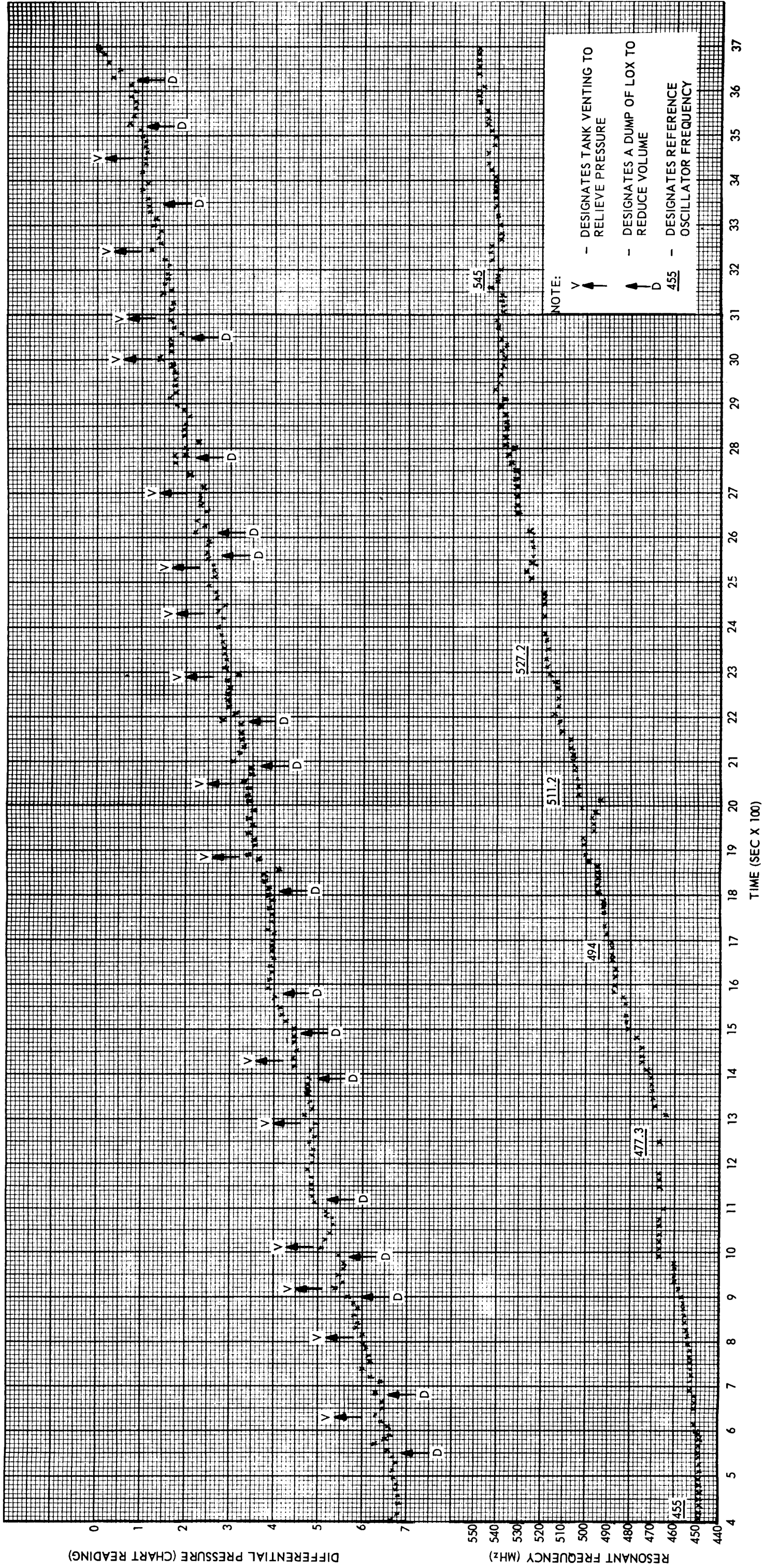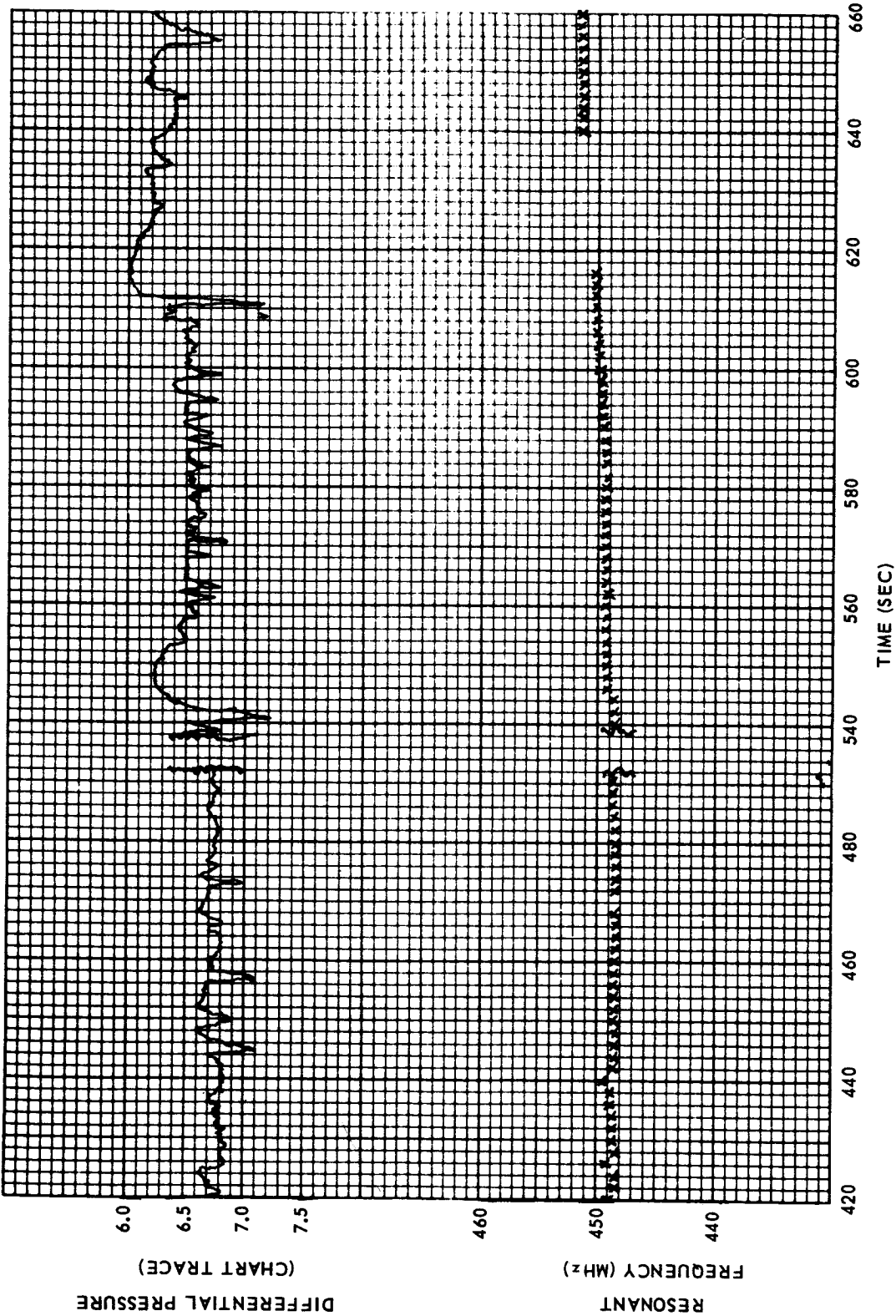
4-61

The data obtained from run 18 have been plotted in Fig. 4-35. To provide an overall appreciation of the performance of the RF liquid-level sensing system, the data have been presented in a time sequence and in a manner that illustrates the change in resonant frequency resulting from changes in the volume of the LOX. The lower plot is the resonant frequency; the reference oscillator frequency changes were made to maintain operation within the bandwidth of the General Radio mixer and to aid in the correction of phase angle in the oscillating circuit. The upper plot is a history of the output of the differential pressure transducer. Indicated on this plot are the venting of the tank to maintain pressure within the operating limit of the tank and also the times that the dump valve was opened to change the volume of the liquid oxygen.

To illustrate the stability of the RF liquid-level sensing system, an expansion of the data presented in Fig. 4-35 has been plotted in Fig. 4-36. This plot is typical for the response of the RF system. During the period shown, 420 to 660 sec, the tank pressure was relieved by venting to the atmosphere. This venting occurred at approximately 630 sec. The resonant frequency data were recorded and plotted at 2-sec intervals. The differential pressure readings were lost between 460 and 548 sec while the recording pen was being adjusted. Note the smooth shift in resonant frequency from 448.5 to 450 MH_z, which was caused by a normal boiloff of approximately 1-1/2 percent of the volume of the LOX. The venting caused a loss of an additional 1 percent, and the resulting change in resonant frequency may be noted. Also it should be pointed out that during the last dump, the differential pressure changed about 14 percent, while the RF system indicated a change of only 2-1/2 percent. The difference between these two readings correspond with the data obtained during the mode surveys and indicate that the tank was empty prior to the zero differential pressure recording.

One of the experiments conducted during the series of RP-1 experiments (Par. 3.4) was for the purpose of determining the effect of slosh on the stability of the RF liquid-level sensing system. The results of this experiment indicated that some change of resonant frequency did occur; however, the change was minor and the resulting error could be extracted or at least reduced by averaging the resonant frequency over a
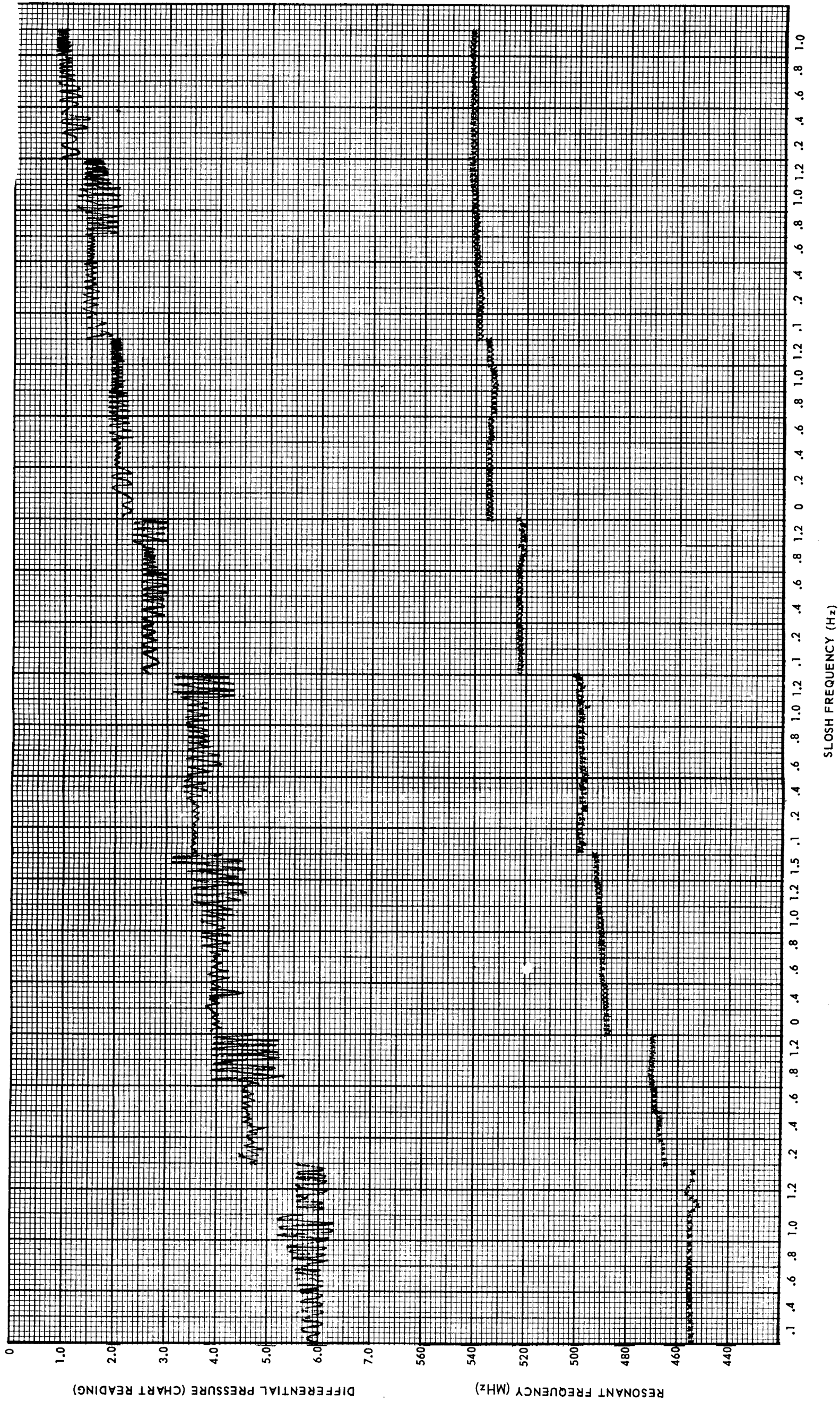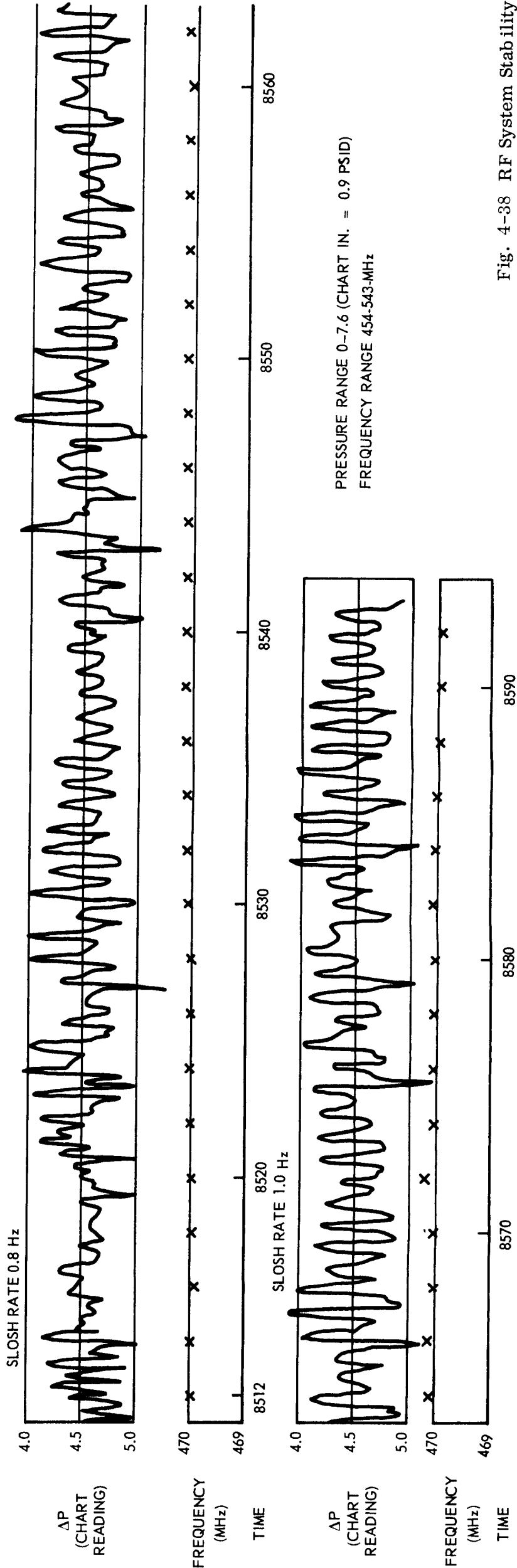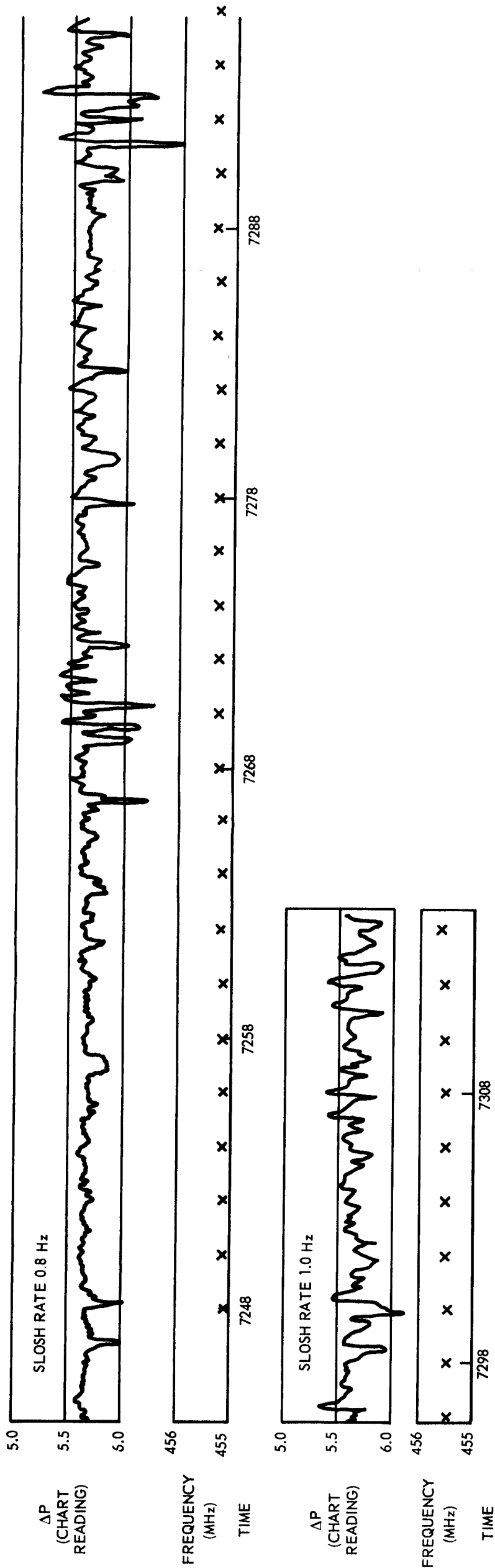
Fig. 4-37 LOX Run 19

Fig. 4-38 RF System Stability, LOX Run 19

PRESSURE RANGE 0-7.6 (CHART IN. = 0.9 PSID)
FREQUENCY RANGE 454-543-MHz

few readings. The physical arrangement for the RP-1 experiment limited the slosh test to a relatively small percentage of the capacity of the tank. The experimental setup for the LOX testing was such that the rate of slosh and the excursion were adjustable over a fairly wide range. Also, the installation provided for a complete coverage of the tank volume. LOX run 19 was conducted to obtain additional information regarding the performance of the RF system, and also to determine the behavior of the system under a dynamic condition with a cryogen. Figure 4-37 is a plot of the data resulting from the experiment, and Fig. 4-23 illustrates the pivot location for the rocking of the tank.

The tank oscillation was controlled at rates of 0.1, 0.2, 0.4, 0.6, 0.8, 1.0, and 1.2 Hz. Higher rates of 1.5 up to 2.5 Hz were used at the start of the checkout; however, these higher rates created an unsafe condition, and only once during the test was the oscillation allowed to reach 1.5 Hz. The level increments may be readily determined from the plot of the data. Except for one case near the start of the test, the resonant frequency changed in direct ratio to the boiloff rate at any particular level. The one exception occurred during a 1.2 Hz oscillation. At this time, the liquid was swirling rather than sloshing. This may be a truer behavior of the liquid. Under a condition of swirling, an averaging of readings would provide a more accurate measure. It was noted that during swirling, the resonant frequency did not exceed the true measure and, therefore, the highest frequency recorded would provide an even more accurate measurement.

An expanded scale for two slosh cycles is shown in Fig. 4-38. The differential pressure readings were traced from the strip chart. The total change in resonant frequency of 0.5 MHz or approximately 0.57 percent of volume corresponds to the amount of LOX lost by boil-off.

The results of the final experiment of the LOX series was made to obtain comparative data for determining the extent of the influence of the paramagnetic property of LOX on the performance of the RF system. Liquid nitrogen was selected for the comparing liquid because the dielectric constants of the two are close. Of course, the liquid

nitrogen is a much easier cryogen to handle than the LOX. The RF system was operated in the self-oscillating mode, and run 14 was used as a guide for the selection of cable lengths. The differential pressure reading for the liquid nitrogen of 5.5 corresponded to a reading of 7.5 for the LOX. The resonant frequency of 446 MHz was observed at the full tank condition for the liquid nitrogen, while it was 438 MHz for the LOX. Based on the difference in dielectric constant of 1.507 for LOX and 1.454 for liquid nitrogen, and the observed resonant frequency for the empty tank, the observed values agree with the calculated values. Almost identical performance was observed for the two liquids. If the paramagnetic property of LOX had any effect on the RF system, it was too minor to be detected. Figure 4-39 is a plot of the data for the liquid nitrogen experiment.
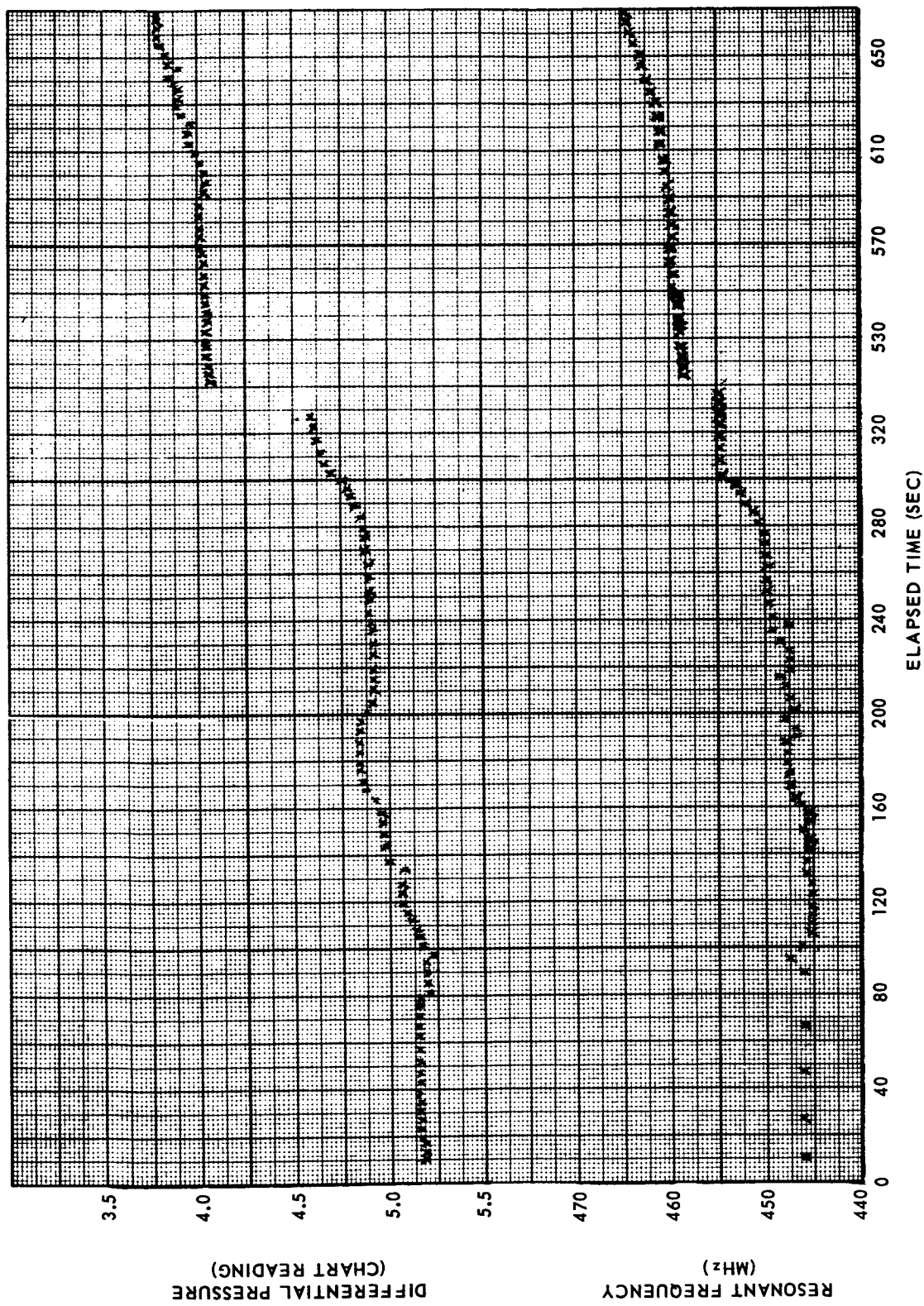
Fig. 4-39 Liquid Nitrogen Experiment, Run 20

4.5 RF SYSTEM DESIGN FOR SATURN S-IVB BATTLESHIP

The demonstration of the feasibility of the RF resonant cavity technique was sufficiently encouraging to add the design of a full-scale system. The Saturn S-IVB Battleship was selected for a test of the technique of determining the amount of propellant on board a space vehicle. To as great a degree as possible, standard commercial components were to be selected for the system, and no changes other than replacing two blind port flanges with RF probe assemblies were to be made to the S-IVB. The guidelines were to be followed, and the experience gained from the experiments were to be applied.

4.5.1 Design Considerations

The implementation of the RF liquid-level sensor would be greatly simplified if cavity excitation involved only one mode over the entire fill cycle. Where the placement or configuration of the coupling loops or probes were not restricted, most of the desirable operating modes could be excited so that other modes within the operating frequency range would be satisfactorily suppressed.

The selection of a particular mode to be excited is dictated by many considerations. It has been demonstrated experimentally that two types of modes (i.e., TE or TM) are each associated with a characteristic frequency versus a fill curve. Typically, the rate of change of frequency versus percent fill for a TM mode is the greatest near the empty condition and decreases as the tank fills. The rate of change of the resonant frequency of a TE mode is highest near the 50 percent level and is slower at both the near-empty and near-full condition.

Prior to selecting an operating mode, the effects of the tank geometry were considered. Internal instrumentation, supporting structures, pressurization vessels, general proportions of the tank, and end configurations were reviewed. The effect of the capacitive probe, including the supports and the hemispherical ends of the tank, upon a particular mode is difficult to evaluate. Had slosh baffles and fill or drain lines been included in the S-IVB, an even more complex design problem would have existed.

To demonstrate that effects of the internal tank irregularities could be reduced by proper mode selection and excitation, a model simulation program was undertaken. This simulation demonstrated that consideration for an RF level sensing system by the stage designers during the initial design phase would greatly enhance the performance of the RF liquid-level technique. The simulation program consisted of evaluating the excitation of selected modes in the cylindrical copper tank and subsequently extending the results by simulation in a $\frac{3}{13}$ scale model of the S-IVB.

At the outset of this simulation program, it was anticipated that the major difficulties to be encountered would result from the following:

       a. The capacity probe structure and associated mounting hardware

       b. The spherical shaped tank ends

       c. The pressurization vessels contained within the tank

The effect of the capacitive probe liquid-level sensor and associated mounting hardware upon the TE modes can best be considered by viewing the structure along the axis of the tank. At those stations along the tank where the capacity sensor is supported, the supporting structure constitutes a shorted loop as depicted in Fig. 4-40.

If this shorted loop were located so that its plane was orthogonal to the magnetic field, the fields would be greatly disturbed. The magnetic fields of the TE modes are such that this would be the case. If the supporting structure existed at only one station, say the midpoint, the effect would be more pronounced on the even numbered mode. This results from consideration of the variation of the magnitude along the length of the resonator. The magnitudes of the magnetic field in the Z direction for TE_{010}, TE_{011}, TE_{012}, and TE_{013} are depicted in Fig. 4-41.

The capacity probe is supported at four points, and as a result, the TE_{01q} modes are not satisfactory candidates for the Saturn design. It should be noted that if other irregularities within the tank are neglected, the effect upon the TE_{11q} and other higher order TE modes could be reduced by exciting the tank such that the location of the shorted loops on the circumference would be at a position where the Z components for the magnetic field are a minimum.
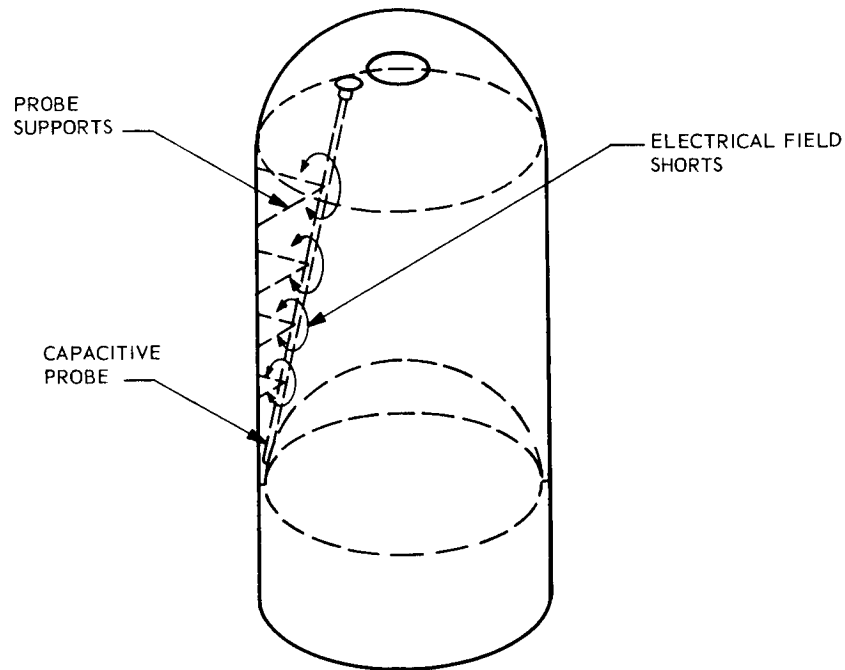
4-71

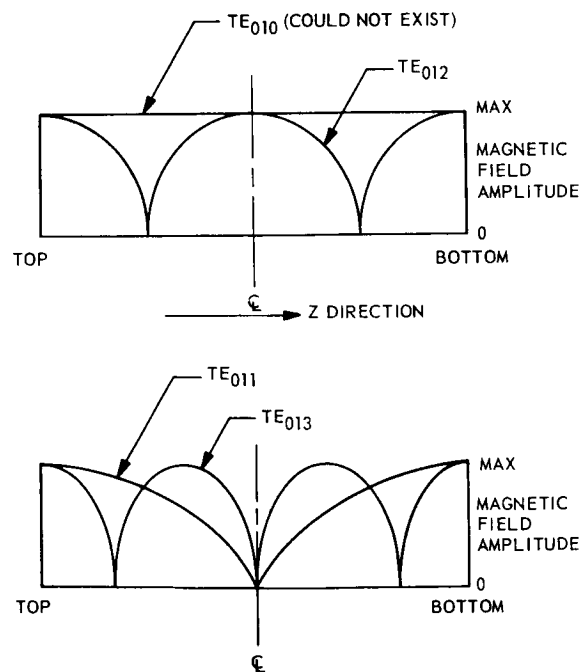Fig. 4-40 Effect of Capacitive Probe Supports, TE Field

Fig. 4-41 Field Patterns

4-72

The descriptive analysis of the fields for the TM mode is similar to that of the TE modes. The capacity sensor and associated supports again form shorted loops that affect those modes in which the magnetic field is orthogonal to the plane of the loops. (See Fig. 4-42.)

The affected modes would be the TM_{01q}; however, with proper excitation the effect upon TM_{01q} modes could be greatly reduced. The method of excitating the TM_{11q} modes is best understood by referring to a diagram (Fig. 4-43) of the H fields. The magnitude of the H field in the circumferential direction is zero in a plane 90 deg from the plane of maximum H_ϕ.

In the copper tank simulation program, it was decided to excite the TM_{110} mode selectively in a configuration that accommodated the capacity probe level sensor. To accomplish this excitation, it was necessary to suppress the TM_{111} and TM_{112} modes effectively. The method of suppressing the higher order TM mode involved the unique use of a multiple coupling loop.

This method of excitation is best understood by considering the variation of the H_ϕ with respect to the Z direction. Since the cylindrical resonator terminates in a short at both ends, the magnitude of the H_ϕ field, which varies sinusoidally with respect to the length, must be maximum at each end. The TM_{110} and the even higher order mode (e.g., TM_{112}, TM_{114}, etc.) are characterized by a maximum at each end and at the middle. The higher order odd-numbered modes (i.e., TM_{113}, TM_{115}, etc.) have a maximum at each end with a minimum at the center.

The prime inference from the above statements is the fact that the fields of the even-order modes are symmetrical in magnitude and polarity about the center, while the odd-order modes are symmetrical in magnitude about the center but opposite in polarity. As a result, it can be demonstrated that with two loops (each having identical orientation, located an equal distance from the center, and driven by in-phase currents) only even-order modes will be excited. Conversely, if this orientation were reversed, or if the loops were driven by out-of-phase currents, only the odd-order modes would be excited. In addition to the above, when the loops are located half-way between the
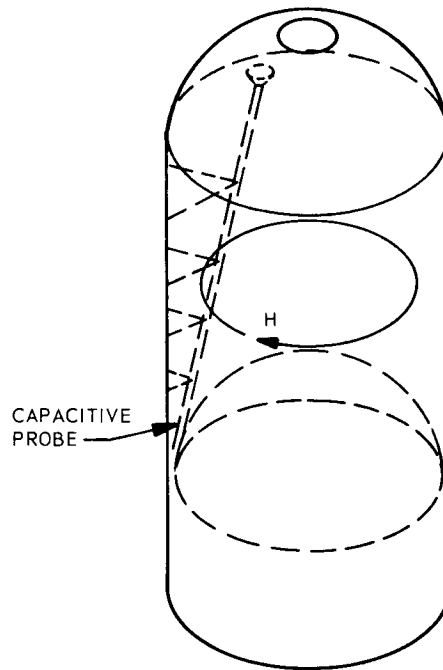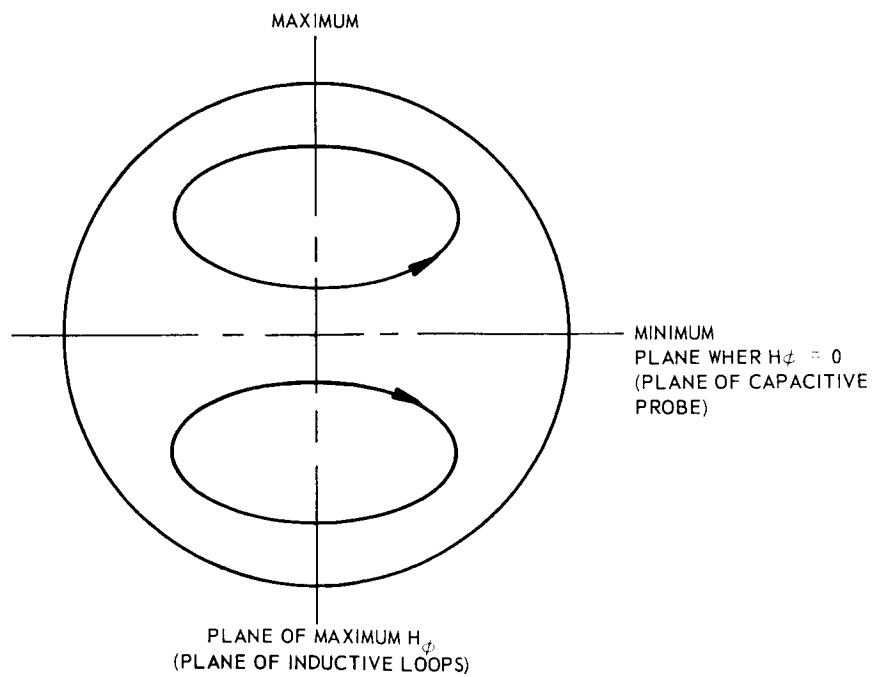
4-73

Fig. 4-42 Effect of Capacitive Probe, TM Field

Fig. 4-43 H Field Pattern

4-74

center and each end, the excitation of the TM_{112} mode will be negligible because the loops would then be positioned at the points of minimum field for this mode. This detailed coupling, therefore, is suitable for excitation of only the TM_{110} and TM_{114} modes, with the frequency of the TM_{114} mode being beyond the range of interest for RF liquid-level sensing.

The above concepts were demonstrated in the copper tank with a 1/4 in. copper tube positioned to simulate the capacity probe level sensor. Table 4-12 displays the frequency of various modes. The tank was excited by a Telonics sweep oscillator through a pair of inductive loops. The energy was extracted by a similar loop configuration and detected and displayed on an oscilloscope. (See Fig. 4-44.)

Since the results with the copper tank appeared to be satisfactory, a similar simulation to provide additional design information for the RF system was conducted in a $\frac{3}{13}$ scale model of the LH_2 portion of the Saturn S-IVB. The modified Agena tank used for the RP-1 experiments was reworked for the model as shown in Fig. 4-45. A copper tube was used to simulate the capacitive probe, and copper spheres were installed to simulate the pressurization bottles.

Table 4-12

RESONANT FREQUENCIES FOR 22-1/2 IN. DIAMETER COPPER TANK

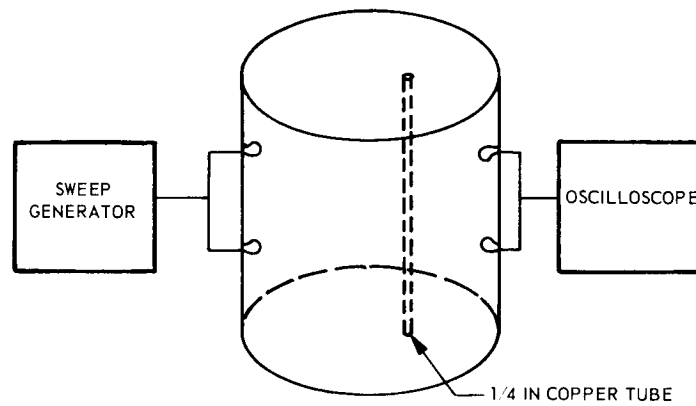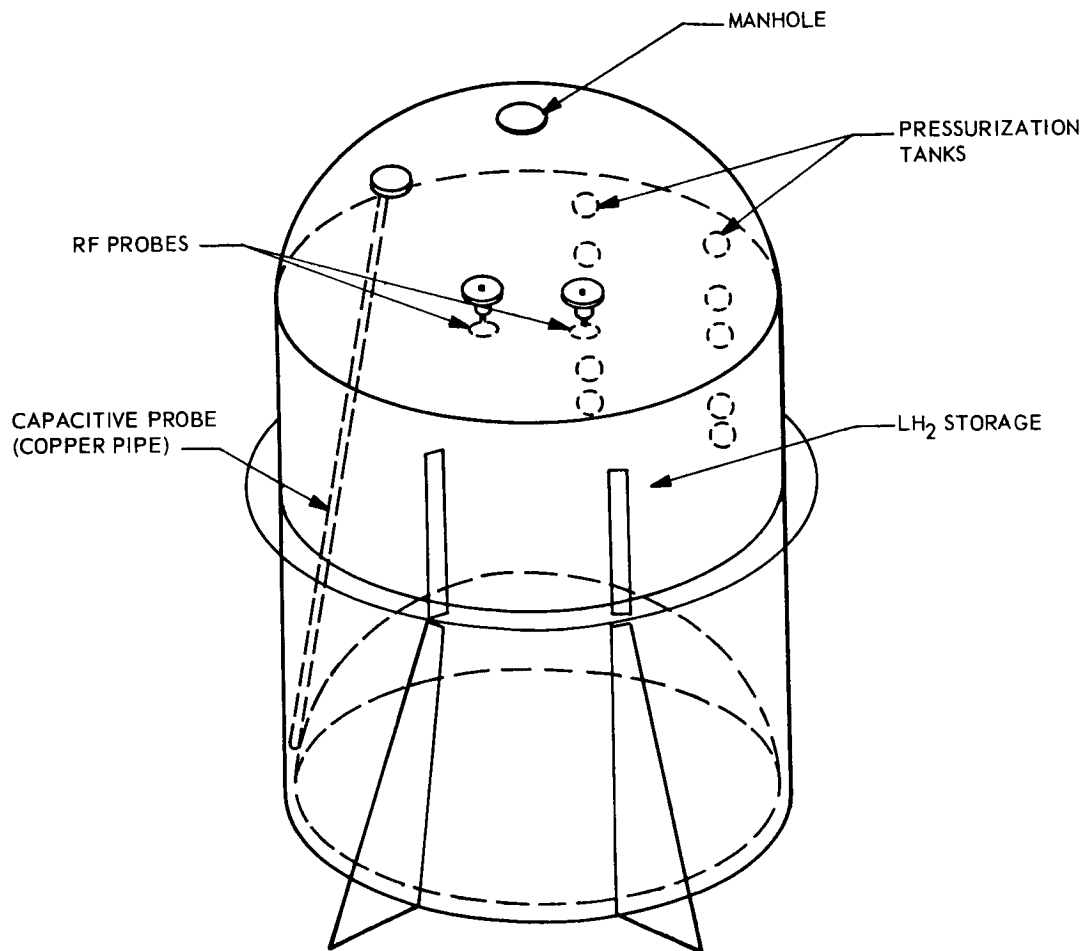| Mode Number	Frequency (MHz)	
	TE Mode	TM Mode
010		408
011	698	485
012	838	672
013	1030	900
014	1252	1150
110		642
111	408	698
112	618	838
113	862	1030
114	1115	1252
210		832
211	580	960
212	744	1010
213	945	1180
214	1190	1370

4-75

Fig. 4-44 RF Probe Configuration

Fig. 4-45 Scale Model of Saturn S-IVB

4-76

Initially, difficulties were encountered in exciting the desired mode, and several internal changes were made. The first problem, which will not occur in the Saturn S-IVB, was a high-resistance current path that was a result of the manner in which the tank was fabricated; the tank consisted of two flanged halves that were bolted together. An RF gasket was installed between the two sections, and the problem was solved. The second major problem resulted from the hemispherical ends and, in particular, the inverted hemisphere representing the top of the LOX tank. The difficulty was attributed to the increased length of the conduction current path, which results from this type of end configuration. Figure 4-46 illustrates the end effect.

In an attempt to reduce the effect of the end termination, and at the same time to maximize the sensed tank volume, two different screen configurations were introduced into the tank. The first configuration consisted of a 36-in. diameter screen disc installed 10 in. down from the top and an annular ring with an inside diameter of 18 in. effectively located at the lower end of the tank. In actuality, the bottom screen, which consisted of two sections as shown in Fig. 4-47, was sufficient to support the TM_{11q} modes.

The diameter of the top screen was later increased to 42 in., and the screen was mounted 19 in. down from the top of the tank. This configuration yielded a satisfactory mode.

A cursory examination of the irregularities in the Saturn tank; e.g., pressure vessels and capacity probe sensor, revealed that approximately one-half of the S-IVB LH_2 tank is free from obstructions. This led to the consideration of a tank configuration with a semicircular cross section.

The diagram (Fig. A-2) for the TM_{11q} modes illustrate that a plane may exist about which the fields are symmetrical, and to which all components of the electrical field are normal.

SATURN S-IV B

RIGHT CYLINDER
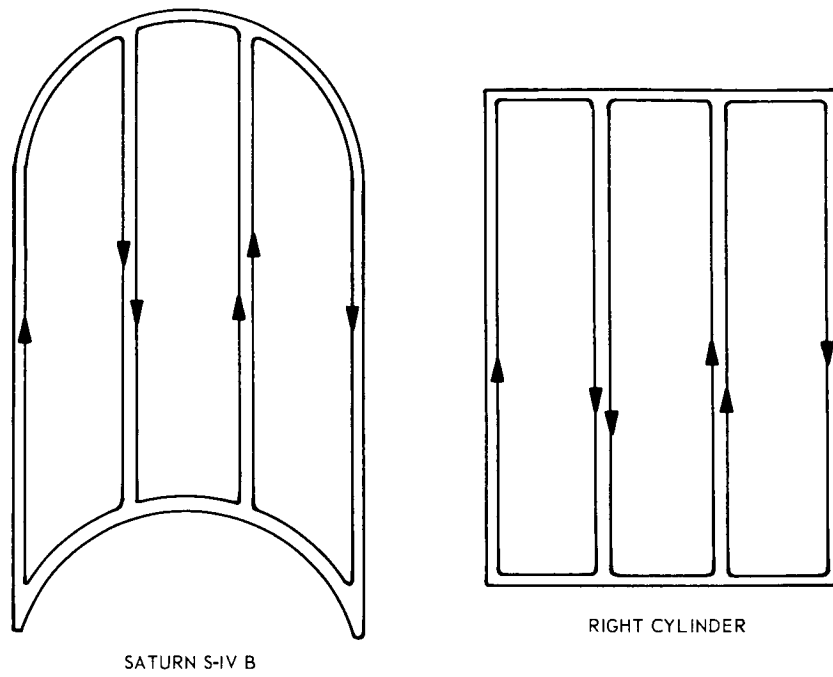
Fig. 4-46 Effect of Tank Geometry
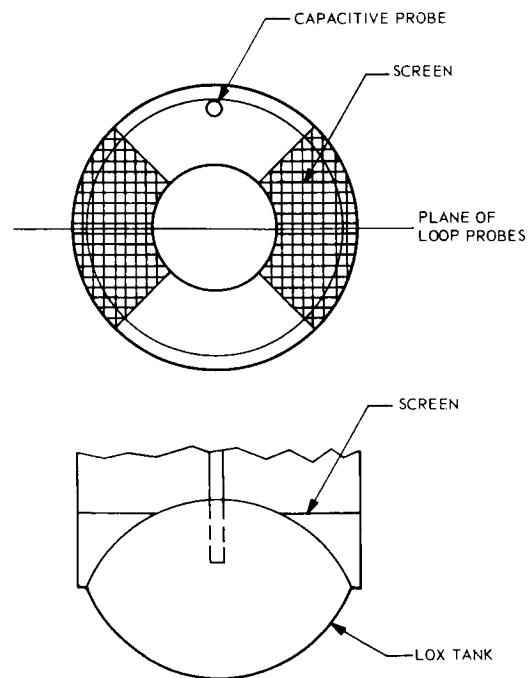
Fig. 4-47 RF Screen Configuration

4-78

To verify this observation, the copper tank was modified by the addition of a center plane made from a thin sheet of copper. Figure 4-48 illustrates the modification and the loop configuration used for exciting the tank. A composite material consisting of polyurethane foam and unexpanded polystyrene provided a dielectric approximating that of LH_2. The resonant frequency was followed through the fill cycle, and the resulting resonant frequency versus percent fill curve is displayed in Fig. 4-49. In all probability, the variation from the smoothed curve was a result of the lack of homogeneity of the two materials forming the dielectric.

The experiment was repeated as a self-oscillating RF sensing system. The results of the second experiment are shown in Fig. 4-50. A comparison of the experimental results for various dielectric constants are shown in Fig. 4-51.

Fig. 4-48 RF Probe Location

4-79

Fig. 4-49 Resonant Frequency Difference Vs.Volume, Half Tank

Fig. 4-50 Resonant Frequency Difference Vs. Volume, Self-Oscillating System

4-81
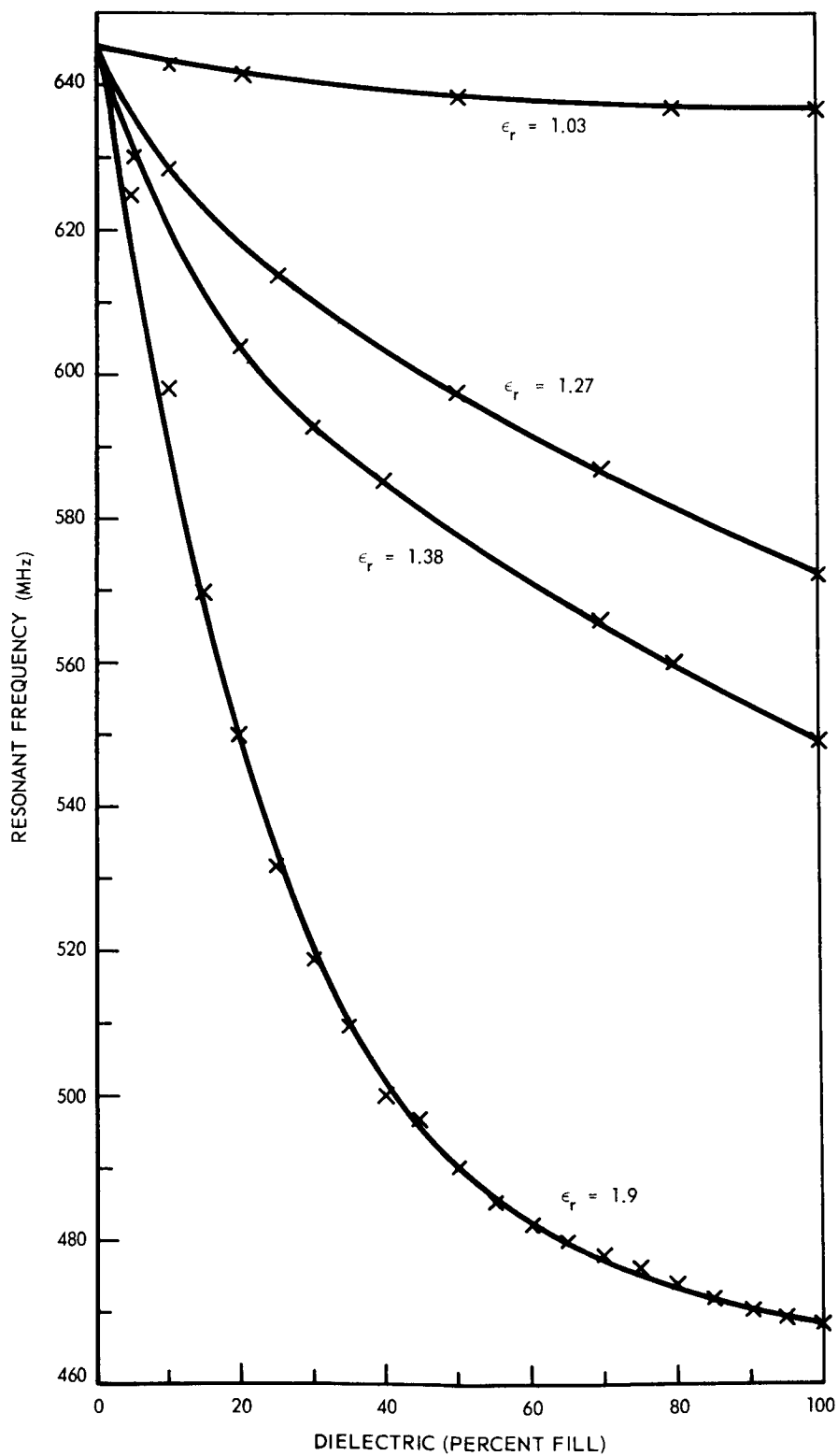
Fig. 4-51 Comparison of Experimental Results

4.5.2 Design Evaluations

This work demonstrated that an RF liquid level sensing system can be designed for operation with complicated internal tank configurations. To obtain 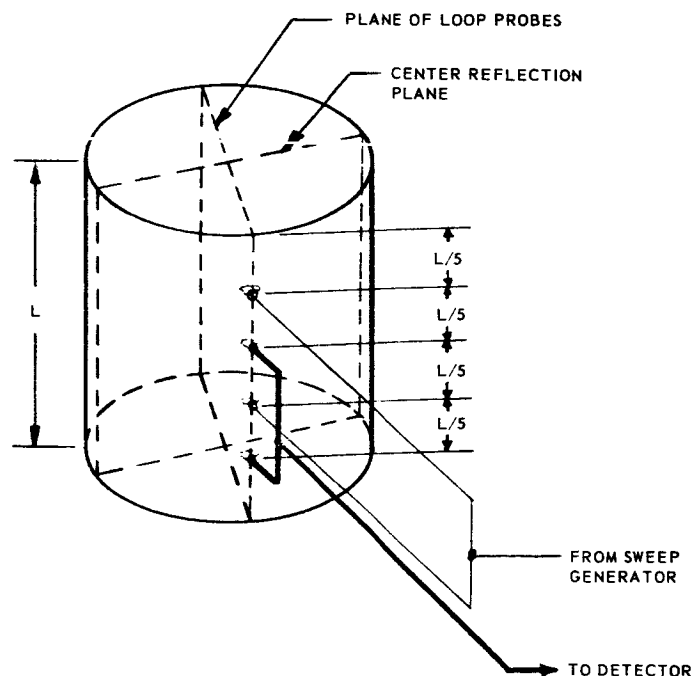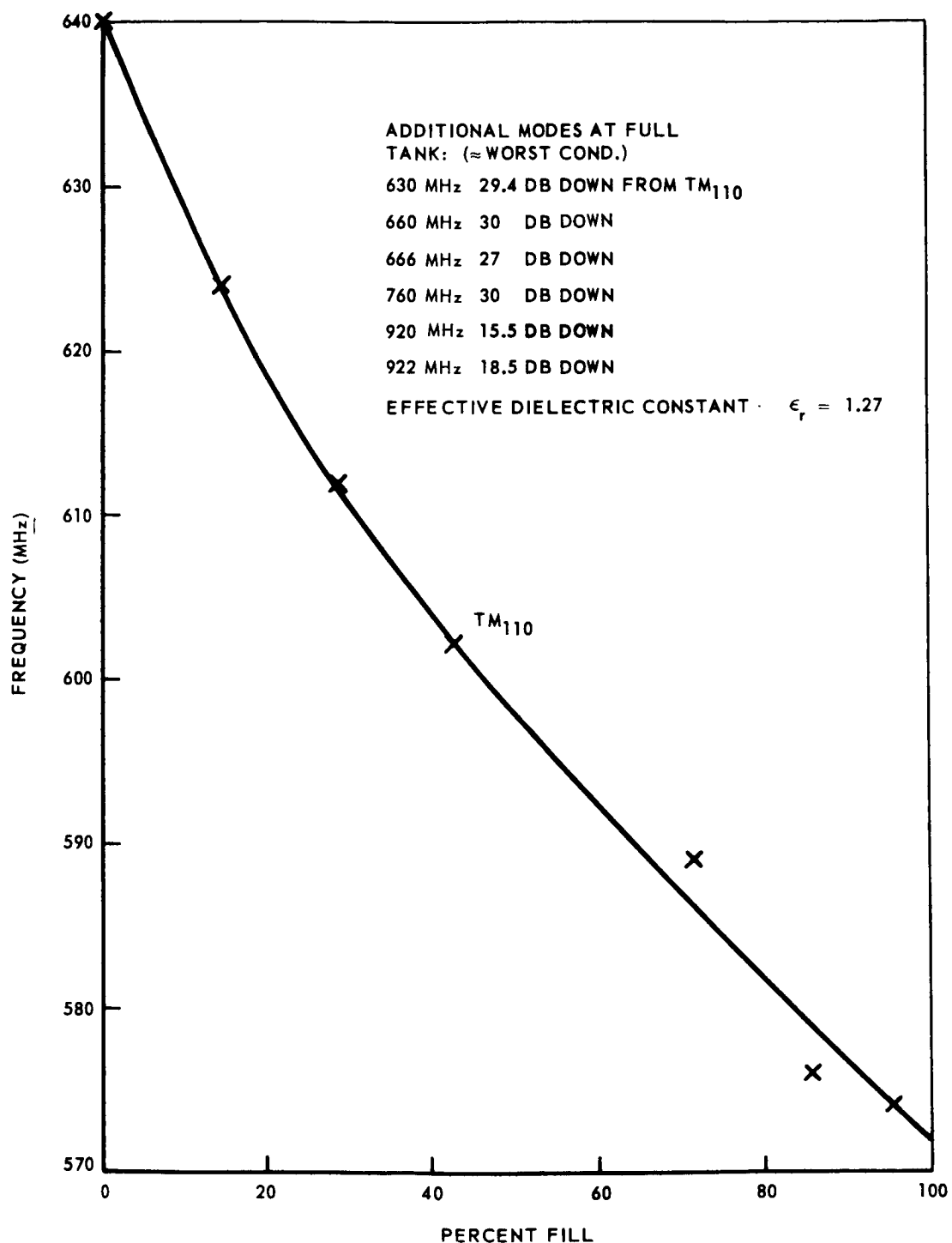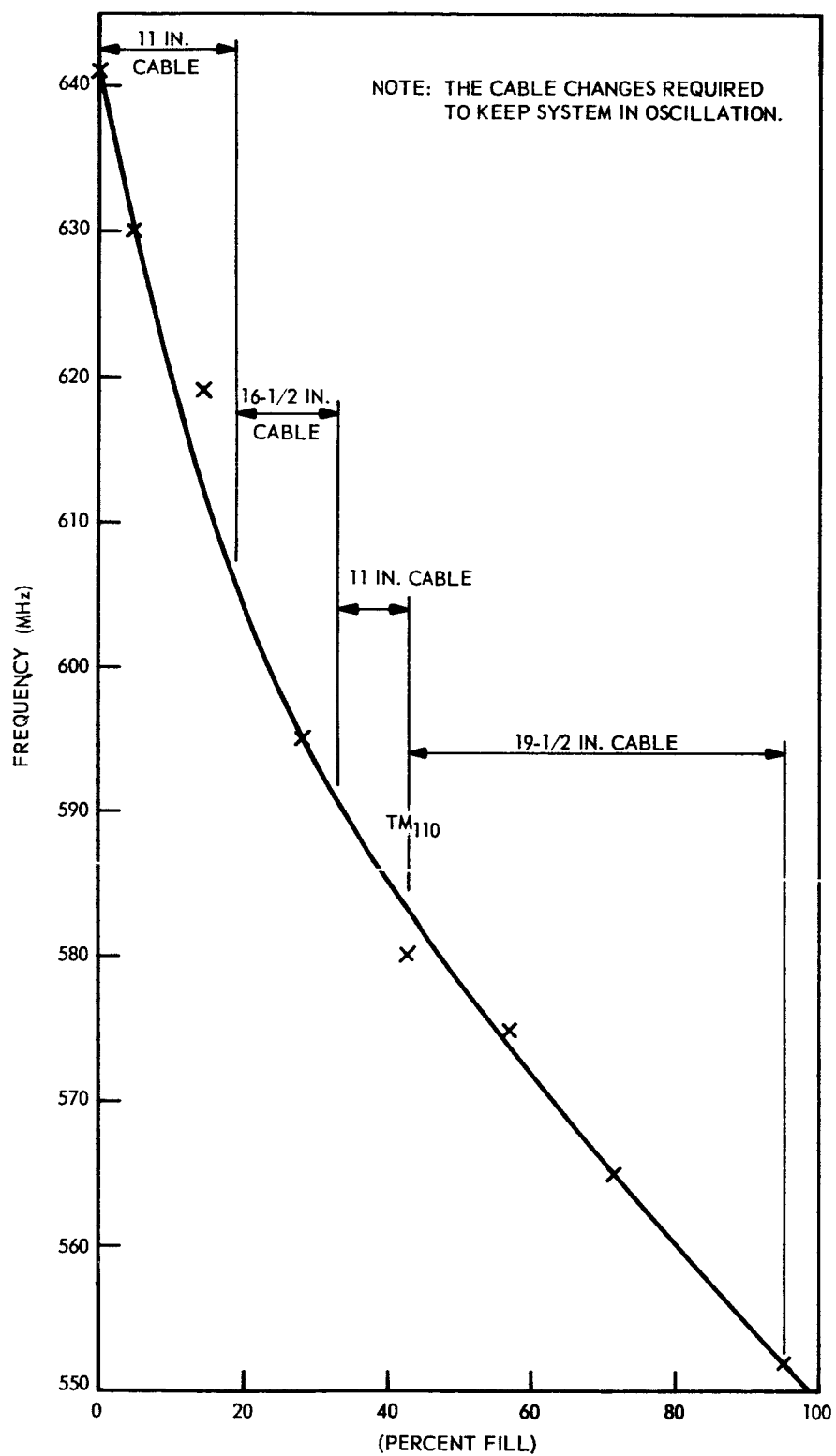optimum performance, it is necessary to select the probe location and operating mode carefully. Further, it was demonstrated that modifications such as the installation of screens would improve that RF system operation.

The above approach, while suitable for many applications, did not conform to the ground rules for the RF system design for the Saturn S-IVB Battleship. It was stipulated that only the available existing ports could be used to permit the system to be installed. Openings for installing the probes were made in the scale model to correspond to the positions of the available ports. Mode plots were made for combinations of ports that offered the most promise. This experimentation resulted in the selection of ports 15 and 18.

4.5.3 Component Selection

The resonant frequency was determined and recorded as the model was filled with the simulated LH_2 dielectric material. Sufficient material was on hand to fill the model to approximately 60 percent of capacity. Figure 4-52 is a plot of the results of the experiment.

By applying the 3/13 scale factor to the results, and by correcting for the value of the dielectric constant, it has been estimated that in the empty condition the resonant frequency of the S-IVB will be approximately 51 MHz. When the tank is full of LH_2, the resonant frequency should be approximately 46 MHz.

The RF liquid level sensing system that was designed for the Saturn S-IVB Battleship is illustrated in Figs. 4-53, 4-54, and 4-55.

Although the scale model system functioned fairly well, measurements made with the S-IVB tank might not extend beyond a relatively small portion of the fill. The available port locations are such that the most desirable modes cannot be excited. The mode selected for operation has not been fully identified. It is more sensitive to small changes in the interior configuration of the tank than are other modes, such as TM_{110}, TE_{311}, and TE_{211}, which were used in the later cryogenic experiments. For this reason, it cannot be forecast whether or not the LMSC scale model orientation can be successfully duplicated in the Saturn S-IVB Battelship.
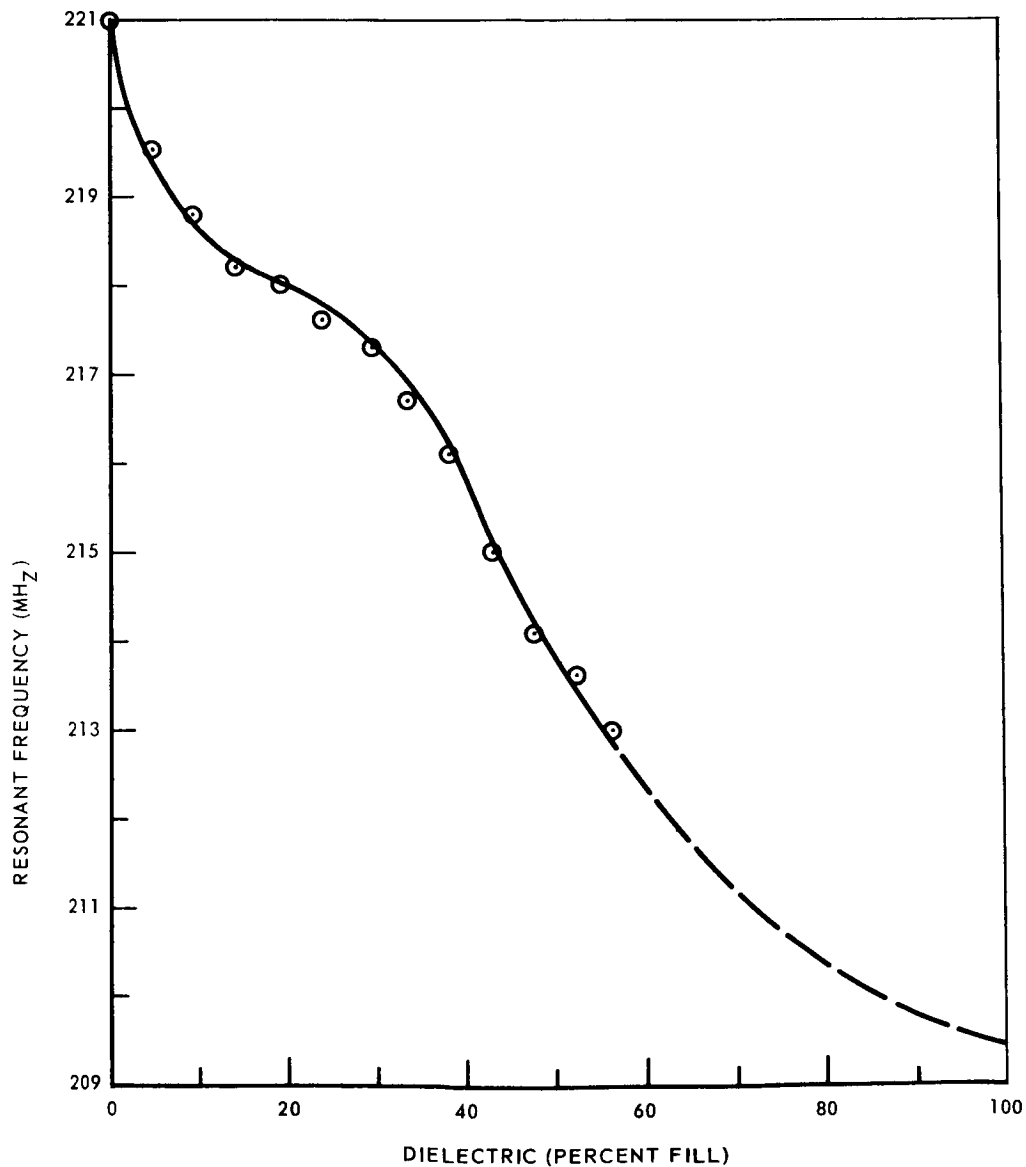
Fig. 4-52 Resonant Frequency Difference Vs. Volume, 3/13 Scale Model
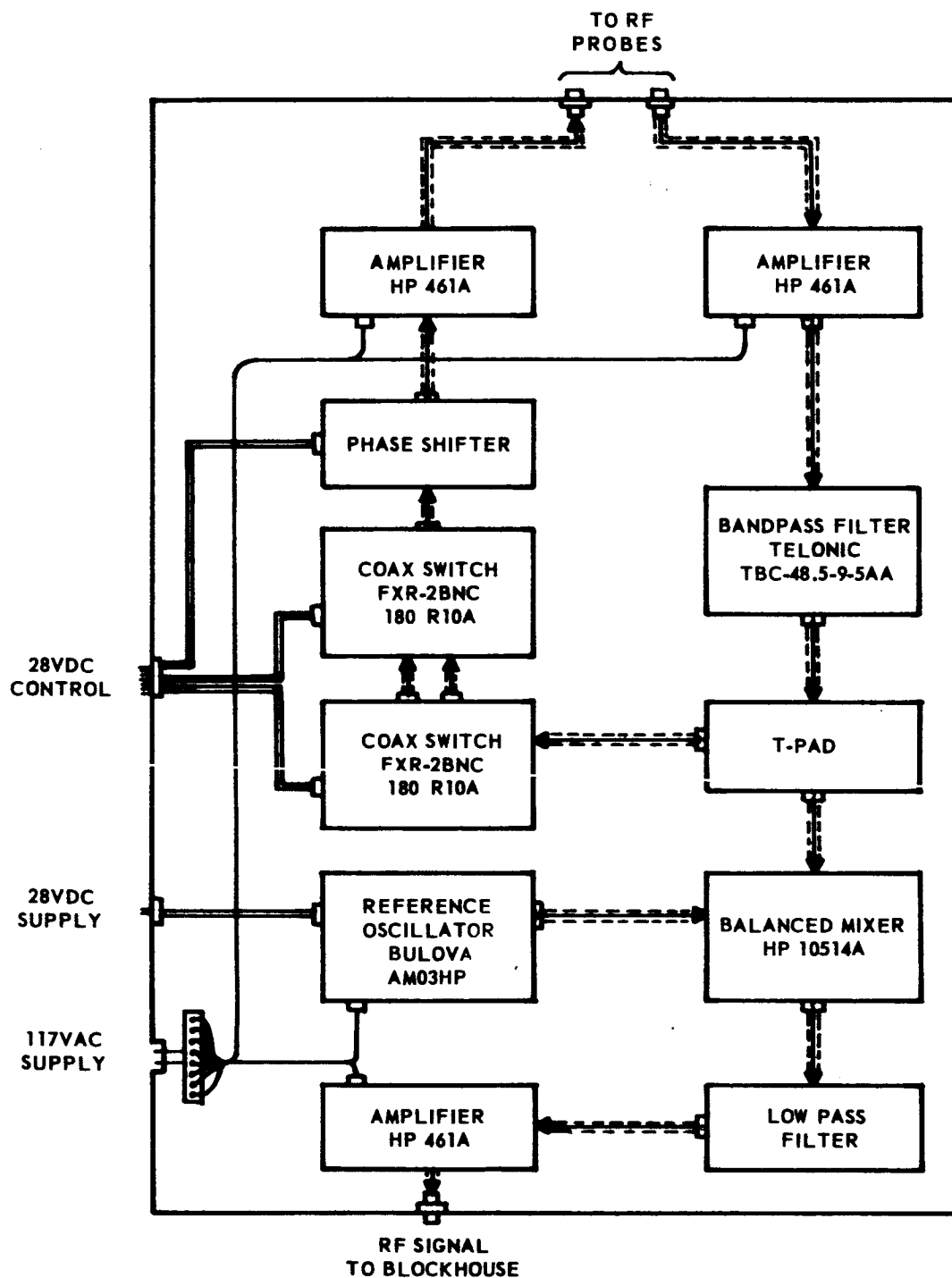
Fig. 4-53 RF System Block Diagram, Saturn S-IVB
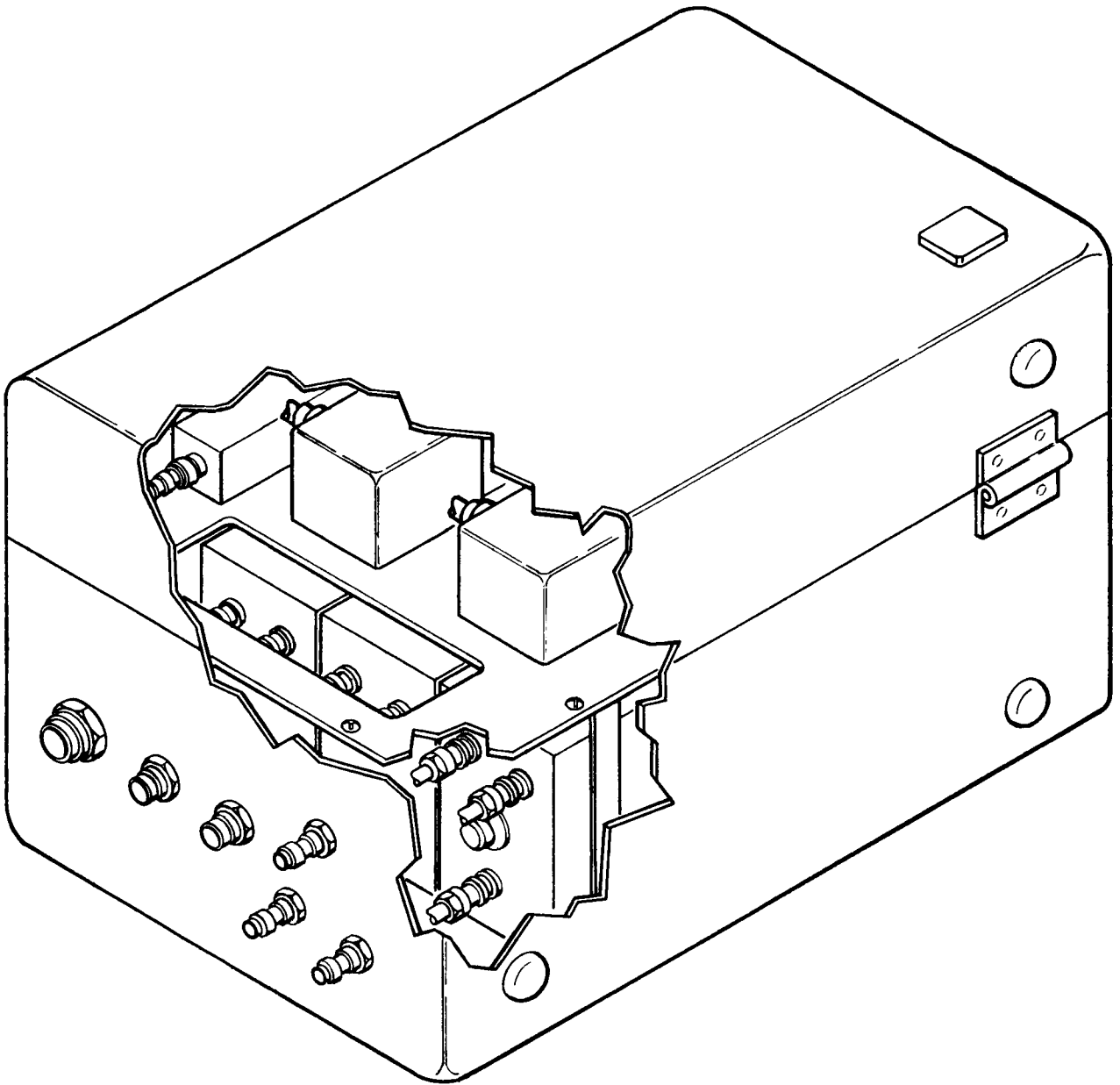
Fig. 4-54 Electronics Package, Saturn S-IVB

4-86

RF PROBE

THICK INSULATION

TANK WALL

GROUND PLANE
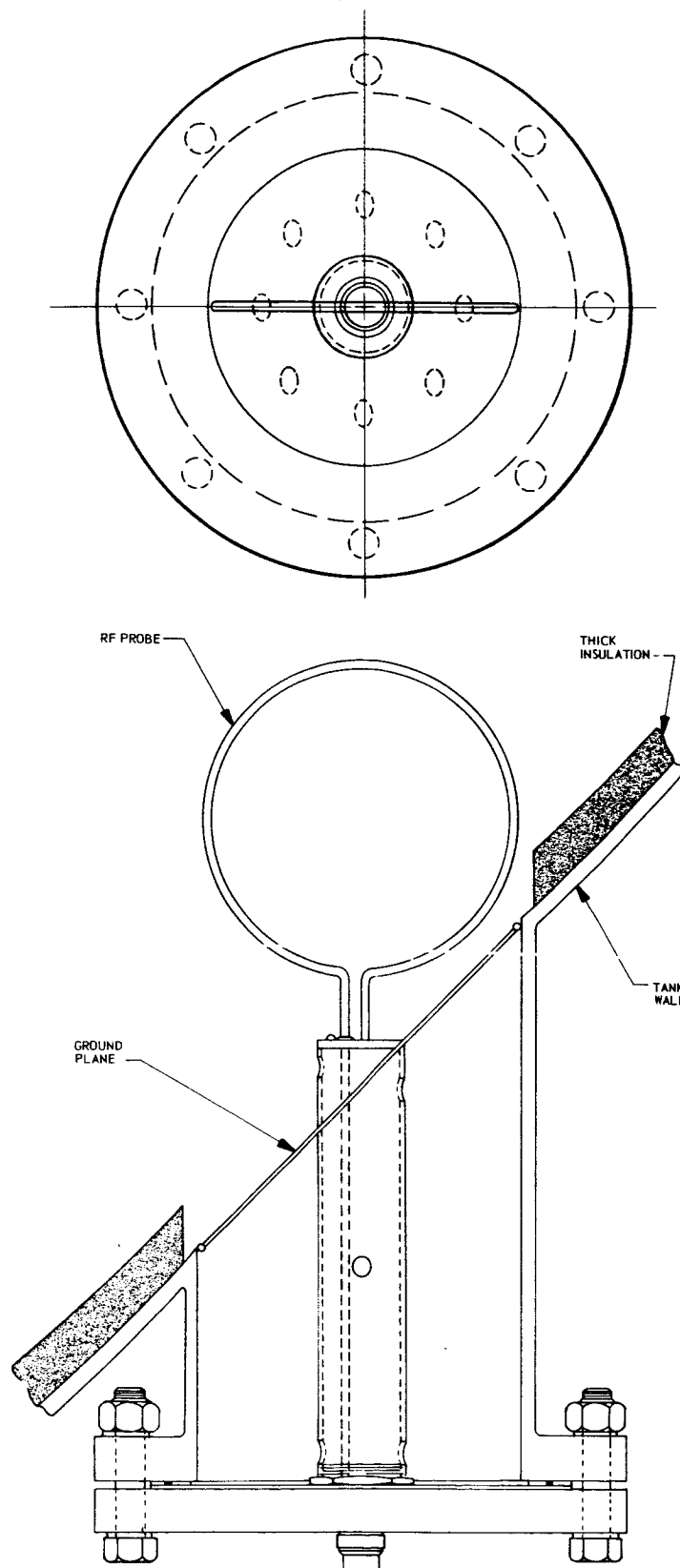
Fig. 4-55 RF Probe Assembly, Saturn S-IVB

4-87

Section 5

CONCLUSIONS AND RECOMMENDATIONS

5.1 CONCLUSIONS

Conclusions derived from the investigation and development of the RF liquid level sensing technique are as follows:

- The technique is feasible
- The technique is suitable for measuring LH_2, LOX, and RP-1, but is not limited to these liquids
- The technique offers a high degree of accuracy
- The technique may be applied to a wide variety of internal tank configurations
- The technique is suitable for dynamic as well as static operating conditions
- An installation of the system requires only minor modifications to a propellant tank
- The output of an RF liquid level sensing system is compatible with airborne and ground data systems
- The cost of an RF liquid level sensing system is nominal

The determination of the accuracy of the liquid-level sensing technique was limited by the accuracy of the available comparing instrumentation. Weighing and flow measurements provided the most accurate comparisons. Under static conditions, the measurement error of the RF system was demonstrated to be less than 1/2 percent. This value does not include the errors contributed to the comparing instrumentation. Although a wide range in accuracy was obtained for dynamic conditions, a considerable portion of the error may be extracted for a measurement by applying vehicle axis alignment data to a calibration curve for the RF liquid-level system. Under conditions of slosh, an averaging of measurements or a maximum RF reading results in a shift of less than 2 percent for a particular error measurement.

5-1

The application of the technique is not limited to a specific liquid or material. As demonstrated throughout the experiments, LH_2, LOX, and RP-1 may be measured. Also the system functioned well with liquid nitrogen and several combinations of dry materials. Inasmuch as the technique is based on the dielectric loading of a cavity, the dielectric property or constant of a material--whether it be solid, liquid, or gas-- is one of the more important considerations.

For practical applications, it is desirable to limit the change of resonant frequency. A reasonable working range would be for materials with a dielectric constant of 1.05 to 2.50. The importance of the dielectric constant is described in both Appendix A and Appendix B.

The installation of an RF liquid-level sensing system requires only minor modifications to existing tank designs. By careful selection of the operating mode, placement of probes, and selection of the electronic equipment, a satisfactory system may be added to an existing tank. A minimum of two probes has provided satisfactory operation. Better operation would be realized with the addition of two probes for exciting the tank and two probes for suppressing unwanted modes. The probe installation may be designed so that only access from the outside of the tank is required.

The output signal of the RF system is in the form of a sine wave of varying frequency. All that is necessary for data acquisition is a frequency counter or a frequency-to-voltage converter. Thus, the system is a practical one from a data handling point of view.

Although care must be exercised in the selection of the electronic components, only state-of-the-art designs are required. The selection of components and cables to maintain phase balance over a fairly broad frequency band is the only critical design problem for the electronics. A review of the equipment used throughout the experiments and the design for the S-IVB provides an appreciation of the low initial cost and maintenance that would be required for an RF system.

The system designed for the S-IVB Battleship shows that the placement of the RF probes is a limitation. Other limitations are as follows:

- The system cannot be an off-the-shelf type unless a standard sampling chamber is used. A standard sampling chamber could be a reflection screen design that would not interfere with the liquid flow, but it would add to the weight and cost. This approach would probably not be suitable for flight because of the orientation of the liquid.

- Although the system is suitable for most of the propellant tank designs in use today, it is not suitable for all configurations. Complex internal piping can suppress all operating modes. Also complicated configurations might prove unsuitable.

- The system cannot be readily calibrated on the bench. It must be installed in the tank for which it is designed and the empty tank frequency determined. From typical curves and mode plots, a calibration curve may be constructed. Refinement of the calibration curve would be obtained from the filling and draining history.

5.2 RECOMMENDATIONS

During the progress of the program, several recommendations were made—most resulting in changes to the scope of the program. Such recommendations included a more thorough series of zero g experiments, the design of a system for the Saturn S-IVB, and the combining of the LH_2 experiments with some independent development studies to permit more extensive experimentation with LOX and laboratory testing.

The additional recommendation to furnish the hardware for the S-IVB is being negotiated. All the recommendations were made with the cooperation of the George C. Marshall Space Flight Center (MSFC).

Because of the anticipated limited performance of the RF system for the S-IVB, it is recommended that after a few tests to evaluate the system components, the location of the probes be moved to more favorable positions. This should not cause more than minor adjustments to the other components.

LOCKHEED MISSILES & SPACE COMPANY

It is recommended that a prototype system be designed, fabricated, and installed as a passenger item on a Saturn flight vehicle. One of the objectives of this installation would be to obtain actual zero g performance data.

Section 6
REFERENCES

1. LMSC-A303541, January 1963 issue of <u>RIFT Monthly Technical Progress Report</u>, 20 February 1963 (C)

2. LMSC-A303670, February 1963 issue of <u>RIFT Monthly Technical Progress Report</u>, 20 March 1963 (C)

3. LMSC-NSP-64-03, December 1963 issue of <u>RIFT Monthly Technical Progress Report</u>, 20 January 1964 (U)

4. LMSC-A797508, <u>Analytical Studies of a Cavity Fuel Gage</u>, by A. D. Wasel, 2 January 1964 (U)

5. "Resonant Cavity Liquid Level Mass Sensor," Patent disclosure, LMSC Docket D-03-2295, 7 March 1963

6. "Resonant Cavity Liquid Level Mass Sensor," NASA patent case, Case No. 2500

7. LMSC-A734537, <u>Summary of Laboratory Investigation</u>, by J. D. Lockhart, 15 February 1965 (U)

Appendix A
BASIC THEORY

The application of RF techniques to measure the volume of a substance in a vessel is
based on the principle that the vessel can be made to function as a cavity resonator.
The resonant frequencies will be influenced by the size of the vessel, the wall material,
the internal configuration, miscellaneous internal material and their locations, and the
quantity and properties of the substance to be measured. The variable is the amount
of the substance that dielectrically loads the cavity.

Some of the limitations are: (1) the vessel must be of conducting material and suitable
for forming a continuous electrical path; and, (2) the substance must be a nonconducting
material and, ideally, have a fairly low dielectric constant.

For a right circular cylinder, the resonant wave length for TE_{npq} and TM_{npq} modes
may be determined by the following formula (Ref. A-1)

$$\lambda = \frac{2}{\left[\left(\frac{X_{np}}{\pi a}\right)^2 + \left(\frac{q}{L}\right)^2\right]^{1/2}} \tag{1}$$

where

λ =   wave length of the resonant frequency in meters

a   =   cavity radius in meters

L   =   length of cavity in meters

X_{np} =   Pth root of J'_n (X') for TE_{npq} modes
or Pth root of J_n (X) for TM_{npq} modes

q   =   number of one-half wave lengths along the axis

The frequency is the direct relationship of velocity to the wave length and in electro-magnetic theory is

$$f = \frac{V}{\lambda} = \frac{1}{\sqrt{\mu_r \epsilon_r}} \frac{1}{\lambda} \qquad (2)$$

where

μ_r = relative permeability of the material in the cavity

ϵ_r = relative dielectric constant of the material in the cavity

For free space, the velocity equals the velocity of light

$$V = \frac{1}{\sqrt{\mu_r \epsilon_r}} = 3 \times 10^8 \text{ meters/sec}$$

By algebraic manipulation, the resonant frequency for both TE_{npq} and TM_{npq} modes may be determined by the following formula

$$f = \frac{1}{2 \pi a \sqrt{\mu_r \epsilon_r}} \sqrt{X_{np}^2 + \left(\frac{q \pi a}{L}\right)^2} \qquad (3)$$

Theoretically, an infinite number of field configurations (modes) are possible, and these can be calculated by utilizing the appropriate Bessel function root in the above formula. In pactice, however, cavity oscillators are usually designed to operate in one of the lower modes with the final choice being governed by frequency, tuning, Q, and coupling considerations. Table A-1 lists roots of $J_n'(X')$, and $J_n(X)$ for several of the lower order modes (Ref. A-2).

Table A-1
MODES FOR CYLINDRICAL CAVITIES

TE Mode	X_{np}	q	TM Mode	X_{np}	q
TE_{111}	1.841	1	TM_{010}	2.405	0
TE_{112}	1.841	2	TM_{011}	2.405	1
			TM_{012}	2.405	2
TE_{011}	3.832	1	TM_{110}	3.832	0
TE_{211}	3.054	1	TM_{111}	3.832	1

For a spherical cavity, the resonant frequencies for TE_{mnp} and TM_{mnp} modes may be determined by the following formula (Ref. A-2)

$$f = \frac{u_{np}}{2 \pi a \sqrt{\mu_r \epsilon_r}}$$ (4)

where

    a   = radius of cavity in meters

    u_{np} = Pth root of spherical $J_n(u)$ for TE_{mnp} modes or Pth root of spherical $J_n'(u')$ for TM_{mnp} modes

    μ_r = relative permeability of the material in the cavity

    ϵ_r = relative dielectric constant of the material in the cavity

As with the cylindrical modes, Table A-2 lists roots of the spherical $J_n(u)$ and $J_n'(u')$ for several of the lowest order modes.

Table A-2

MODES FOR SPHERICAL CAVITIES

TE Mode	U_{np}	TM Mode	U_{np}
TE_{011}	4.493	TM_{011}	2.744
TE_{111}	4.493	TM_{111}	2.744
TE_{021}	5.763	TM_{021}	3.870
TE_{121}	5.763	TM_{121}	3.870
		TM_{031}	4.973

For both cylindrical and spherical cavities, a change in the dielectricity of the cavity results in the change of the resonant frequency in accordance with the following formula

$$f' = \frac{f}{\sqrt{\epsilon_r}} \tag{5}$$

where

f   =   free space or empty resonant frequency

f' =   full resonant frequency

A.1 THEORETICAL EXAMPLE

A 24-in. diameter right circular cylinder by 24 in. high tank is used to illustrate the theory. For the empty tank, i.e., the tank filled with air having a dielectric constant of 1, the resonant frequency may be obtained from Eq. (3)

$$f = \frac{1}{2 \pi a \sqrt{\mu_r \epsilon_r}} \sqrt{X_{np}^2 + \left(\frac{q \pi a}{L}\right)^2}$$

A-4

Assuming, then, that the TE_{111} mode is of interest, the following is presented from Table A-1

$$X_{np} = 1.841 , \quad q = 1$$

$$f = \frac{1}{(2)(3.14)\left(\frac{12}{39.37}\right)\left(\frac{1}{3 \times 10^8}\right)} \sqrt{(1.841)^2 + \frac{(3.14)^2 (12)^2}{(24)^2}}$$

$$f = \frac{1}{.640 \times 10^{-8}} \sqrt{3.39 + 2.47}$$

$$f = \frac{\sqrt{5.86}}{.640 \times 10^{-8}}$$

$$f = \frac{2.42}{.640 \times 10^{-8}}$$

$$f = 378 \text{ MHz}$$

If the cavity was to be filled with LH_2 , LOX , or RP-1, the resonant frequency would change in accordance with Eq. (5) as follows:

$$f' = \frac{f}{\sqrt{\epsilon_r}}$$

A-5

The dielectric constant for LH_2 is 1.2; for LOX, 1.5; and for RP-1, 2.1; and the resulting resonant frequencies would be

$$f'_{LH_2} = \frac{378}{\sqrt{1.2}} = \frac{378}{1.095} = 345 \text{ MHz}$$

$$f'_{LOX} = \frac{378}{\sqrt{1.5}} = \frac{378}{1.225} = 308 \text{ MHz}$$

$$f'_{RP-1} = \frac{378}{\sqrt{2.1}} = \frac{378}{1.45} = 261 \text{ MHz}$$

The change in frequency Δf which is obtained by subtracting the filled tank frequency from the empty tank frequency, is as follows

$$\Delta f_{LH_2} = 378 - 345 = 33 \text{ MHz}$$

$$\Delta f_{LOX} = 378 - 308 = 70 \text{ MHz}$$

$$\Delta f_{RP-1} = 378 - 261 = 117 \text{ MHz}$$

A.2 PRACTICAL EXAMPLE

The following discussion presents the results of the experiments conducted during the laboratory investigation.

From the RP-1 experiments, (Fig. 3-9 shows the 24 in. diameter by 24 in. high cryogenic tank), the empty tank resonant frequency for the TE_{111} mode was measured and found to be 378 MHz. Also shown in Fig. 3-9, is the resonant frequency of the TE_{111} mode when the tank was filled with RP-1 which was 262 MHz. Figure 3-6 shows that the change in frequency from empty to full was 34 MHz for LH_2; Fig. 3-8 shows that the change for LOX was 63 MHz.

Table A-3 is a tabulation of the results of the theoretical determination and the experiments. The empty tank frequency for both the theoretical and practical experiments were within one megahertz at 378 MHz.

Table A-3

THEORETICAL VERSUS MEASURED RESONANT FREQUENCIES

Liquid	Theoretical Frequency (MHz)		Measured Frequency (MHz)	
	Resonant	Difference	Resonant	Difference
LH$_2$	345	33	344	34
LOX	308	70	315	63
RP-1	261	117	262	116

The LH$_2$ and the RP-1 results are very close. Considerable difficulty was experienced with the initial series of LOX experiments, and it is believed that an error was made in recording the data. During the second series of LOX experiments, the lower mode frequencies were not used.

A.3 MODE CONFIGURATION

To aid in the understanding of the theory of resonant cavities, a brief analysis of the electric and magnetic field configurations has been provided. To determine the fields of a right circular cavity, the wave functions must first be found. For a TE_{npq} mode, the corresponding wave function in cylindrical coordinates is as follows (Ref. A-2)

$$\psi_E = J_n \left(\frac{X'_{np} r}{a} \right) \cos(n\phi) \sin\left(\frac{q\pi}{L} z \right) \tag{6}$$

and for a TM_{npq} mode is

$$\psi_M = J_n \left(\frac{X_{np} r}{a} \right) \cos(n\phi) \cos\left(\frac{q\pi}{L} z \right) \tag{7}$$

A-7

where

$$X'_{np} = \text{Pth root of } J'_n(X')$$
$$X_{np} = \text{Pth root of } J_n(X)$$

By using these wave functions, the corresponding field configurations may be calculated from the following set of equations

$$\underline{TE_{npq} \text{ Modes}} \qquad\qquad \underline{TM_{rpq} \text{ Modes}}$$

$$E_r = -\frac{1}{r}\frac{\partial \psi_E}{\partial \phi} \qquad\qquad E_r = \frac{1}{J2\pi f \epsilon}\frac{\partial^2 \psi_M}{\partial r \partial Z}$$

$$E_\phi = \frac{\partial \psi_E}{\partial r} \qquad\qquad E_\phi = \frac{1}{J2\pi f \epsilon r}\frac{\partial^2 \psi_M}{\partial \phi \partial Z}$$

$$E_Z = 0 \qquad\qquad E_Z = \frac{1}{J2\pi f \epsilon}\left[\frac{\partial^2 \psi_M}{\partial Z^2} + 4\pi^2 f^2 \mu\epsilon\psi_M\right]$$

$$H_r = \frac{1}{J2\pi f \mu}\frac{\partial^2 \psi_E}{\partial r \partial Z} \qquad\qquad H_r = \frac{1}{r}\frac{\partial \psi_M}{\partial \phi}$$

$$H_\phi = \frac{1}{J2\pi f \mu r}\frac{\partial^2 \psi_E}{\partial \phi \partial Z} \qquad\qquad H_\phi = -\frac{\partial \psi_M}{\partial r}$$

$$H_Z = \frac{1}{J2\pi f \mu}\left[\frac{\partial^2 \psi_E}{\partial Z^2} + 4\pi^2 f^2 \mu\epsilon\psi_E\right] \qquad H_Z = 0$$

Consequently, these equations were used to find the field configurations for the modes generally encountered throughout this investigation. Plots of the fields for the TM_{01q}, TM_{11q}, and TE_{311} are shown in Figs. A-1, A-2, and A-3. Particular attention should be given to the variations in the fields around the circumference and along the length of the tank that led to the positioning of the RF loops.

The field configurations for a spherical cavity are quite difficult to determine and visualize, but the equations leading to the final result will be stated. For TE_{mnp} modes, the wave function in spherical coordinates is as follows (Ref. A-2)

$$\psi_E = \hat{J}_n \left(U_{np} \frac{r}{a} \right) P_n^m (\cos \theta) \cos m \phi$$

and for TM_{mnp} modes is

$$\psi_M = \hat{J}_n \left(U'_{n'p} \frac{r}{a} \right) P_n^m (\cos \theta) \cos m \phi$$

where

U_{np} = Pth root of spherical Bessel function $\hat{J}_n(u)$

$U'_{n'p}$ = Pth root of spherical Bessel function $\hat{J}'_n(u')$

$P_n^m(\cos \theta)$ = Legendre functions of the first kind

A-9

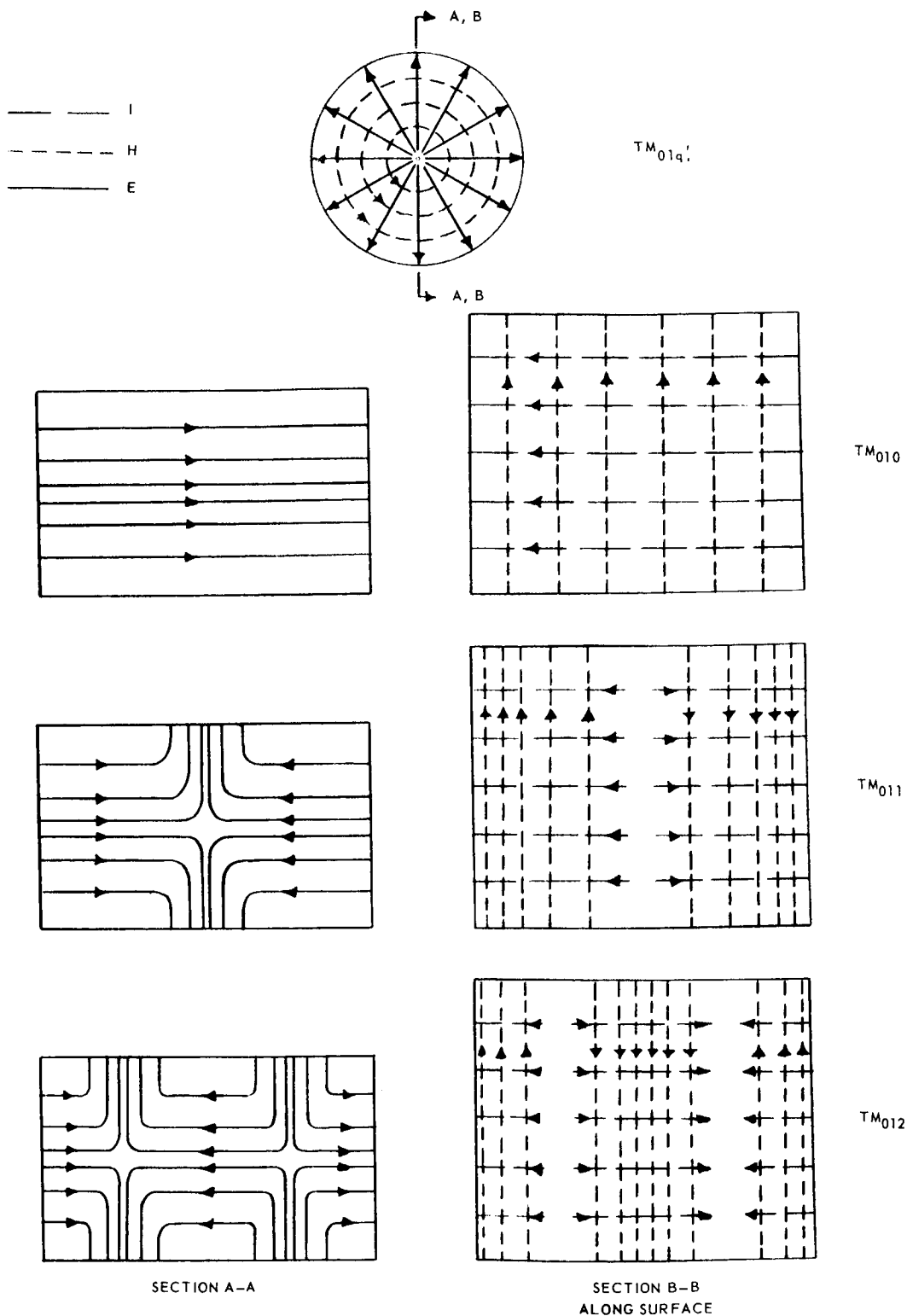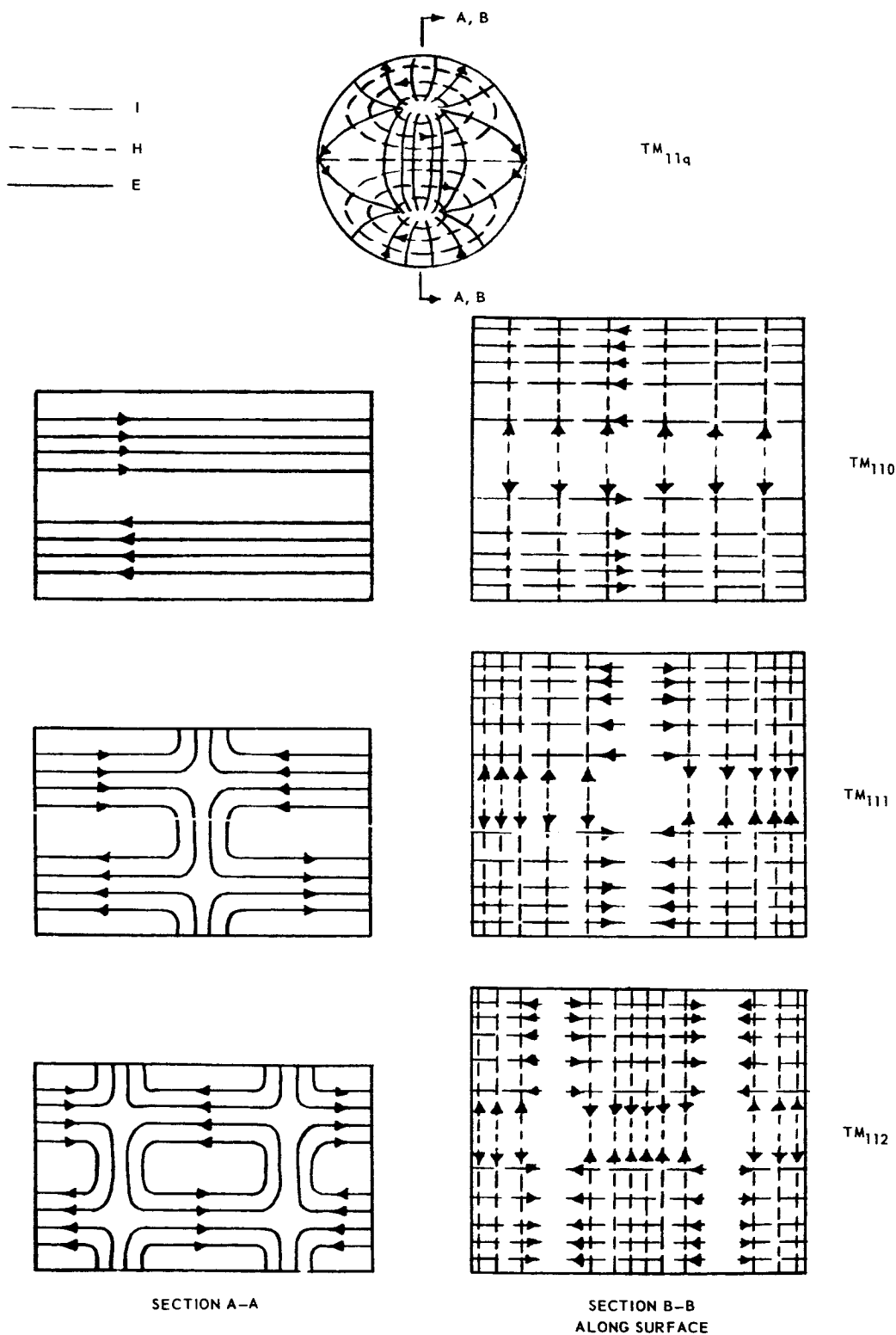Fig. A-1 Field Configuration, TM_{01q}, Right Cylinder

A-10

Fig. A-2 Field Configuration, TM_{11q} Mode, Right Cylinder
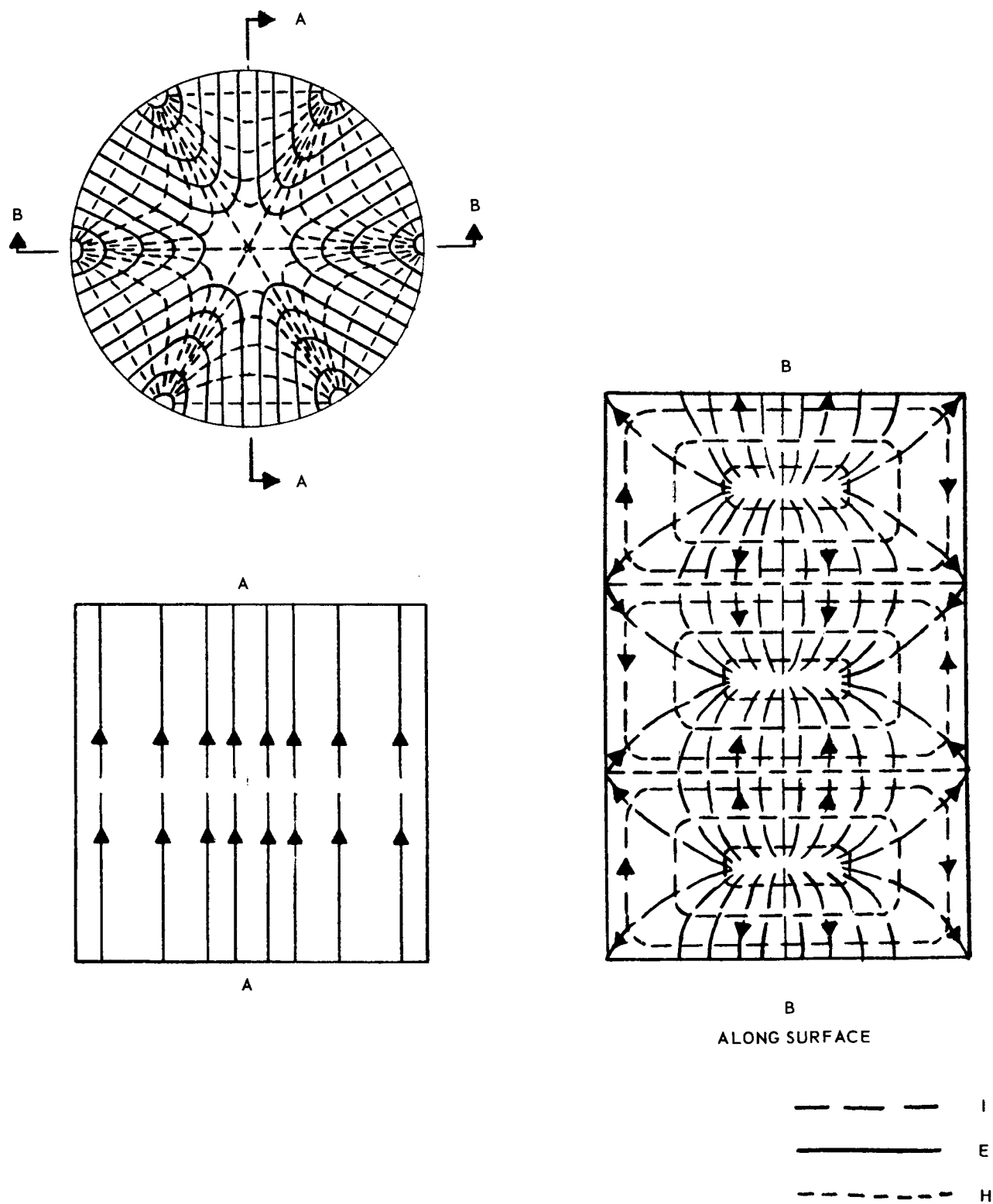
A-11

B

ALONG SURFACE

Fig. A-3 Field Configuration, TE_{311} Mode, Right Cylinder

A-12

The set of equations describing the fields are as follows

TE$_{mnp}$ Modes

TM$_{mnp}$ Modes

$$E_r = 0$$

$$E_r = \frac{1}{J2\pi f\epsilon}\left[\frac{\partial^2 \psi_M}{\partial r^2} + 4\pi^2 f^2 \mu\epsilon\, \psi_M\right]$$

$$E_\theta = \frac{-1}{r\sin\theta}\frac{\partial \psi_E}{\partial \phi}$$

$$E_\theta = \frac{1}{J2\pi f\epsilon\, r}\frac{\partial^2 \psi_M}{\partial r \partial\theta}$$

$$E_\phi = \frac{1}{r}\frac{\partial \psi_E}{\partial \theta}$$

$$E_\phi = \frac{1}{J2\pi f\epsilon\, r\sin\theta}\frac{\partial^2 \psi_M}{\partial r \partial\phi}$$

$$H_r = \frac{1}{J2\pi f\mu}\left[\frac{\partial^2 \psi_E}{\partial r^2} + 4\pi^2 f^2 \mu\epsilon\, \psi_E\right]$$

$$H_r = 0$$

$$H_\theta = \frac{1}{J2\pi f\mu r}\frac{\partial^2 \psi_E}{\partial r \partial\theta}$$

$$H_\theta = \frac{1}{r\sin\theta}\frac{\partial^2 \psi_M}{\partial \psi}$$

$$H_\phi = \frac{1}{J2\pi f\mu r\sin\theta}\frac{\partial^2 \psi_E}{\partial r \partial\phi}$$

$$H_\phi = -\frac{1}{r}\frac{\partial^2 \psi_M}{\partial \theta}$$

Plots of the fields for spherical modes develop from these equations but are not included with this brief discussion.

A.4 CITED REFERENCES

A-1   Technique of Microwave Measurements, by C. G. Montgomery, McGraw-Hill, 1947

A-2   Time Harmonic Electromagnetic Fields, by Harrington, McGraw-Hill, 1961

A.5 UNCITED REFERENCES

Fields and Waves in Modern Radio, by S. Ramo and J. R. Whinnery, Wiley 1953

Theory and Applications of Microwaves, by A. Bronwell and R. Ream, McGraw-Hill, 1947

Electronic and Radio Engineering, by F. E. Terman, McGraw-Hill, 1955

The Microwave Engineers' Handbook, Horizon House, 1964 and 1965

LOCKHEED MISSILES & SPACE COMPANY